Global Biogeochemical Cycles

FEATURE ARTICLE
10.1029/2018GB006065

Advancing Scientific Understanding of the Global Methane Budget in Support of the Paris Agreement

Anita L. Ganesan[1], Stefan Schwietzke[2], Benjamin Poulter[3], Tim Arnold[4,5], Xin Lan[6,7], Matt Rigby[8], Felix R. Vogel[9], Guido R. van der Werf[10], Greet Janssens-Maenhout[11], Hartmut Boesch[12,13], Sudhanshu Pandey[14], Alistair J. Manning[15], Robert B. Jackson[16], Euan G. Nisbet[17], and Martin R. Manning[18]

[1]School of Geographical Sciences, University of Bristol, Bristol, UK , [2]Environmental Defense Fund, Berlin, Germany , [3]Biospheric Sciences Lab, NASA Goddard Space Flight Center, Greenbelt, MD, USA , [4]National Physical Laboratory, Teddington, UK , [5]School of GeoSciences, University of Edinburgh, Edinburgh, UK , [6]Cooperative Institute for Research in Environmental Sciences, University of Colorado Boulder, Boulder, CO, USA , [7]Global Monitoring Division, National Oceanic and Atmospheric Administration, Boulder, CO, USA , [8]School of Chemistry, University of Bristol, Bristol, UK , [9]Climate Research Division, Environment and Climate Change Canada, Toronto, Ontario CA, [10]Department of Earth Sciences, Vrije Universiteit, Amsterdam, The Netherlands , [11]European Commission, Joint Research Centre, Sustainable Resources Directorate, Ispra, Italy , [12]Department of Physics and Astronomy, University of Leicester, Leicester, UK , [13]National Centre for Earth Observation NCEO, University of Leicester, Leicester, UK , [14]SRON Netherlands Institute for Space Research, Utrecht, The Netherlands , [15]Hadley Centre, Met Office, Exeter, UK , [16]Department of Earth System Science, Woods Institute for the Environment, and Precourt Institute for Energy, Stanford University, Stanford, CA, USA , [17]Department of Earth Sciences, Royal Holloway, University of London, Egham, UK , [18]Climate Change Research Institute, School of Geography Environment and Earth Sciences, Victoria University of Wellington, Wellington, New Zealand

Key Points:
- Despite rapid technological progress, major challenges still exist to diagnose the mechanisms that cause changes in atmospheric methane
- The capability must exist to determine whether emission reductions pledged as part of the Paris Agreement are actually occurring
- This study proposes improvements to methane science that could help scientists improve this capability in the coming decade

Supporting Information:
- Supporting Information S1
- Movie S1

Correspondence to:
A. L. Ganesan,
anita.ganesan@bristol.ac.uk

Citation:
Ganesan, A. L., Schwietzke, S., Poulter, B., Arnold, T., Lan, X., Rigby, M., et al. (2019). Advancing scientific understanding of the global methane budget in support of the Paris Agreement. *Global Biogeochemical Cycles*, *33*, 1475–1512. https://doi.org/10.1029/2018GB006065

Received 23 JUL 2019
Accepted 23 NOV 2019
Accepted article online 10 DEC 2019
Published online 23 DEC 2019

© 2019. The Authors.
This is an open access article under the terms of the Creative Commons Attribution License, which permits use, distribution and reproduction in any medium, provided the original work is properly cited.

Abstract The 2015 Paris Agreement of the United Nations Framework Convention on Climate Change aims to keep global average temperature increases well below 2 °C of preindustrial levels in the Year 2100. Vital to its success is achieving a decrease in the abundance of atmospheric methane (CH_4), the second most important anthropogenic greenhouse gas. If this reduction is to be achieved, individual nations must make and meet reduction goals in their nationally determined contributions, with regular and independently verifiable global stock taking. Targets for the Paris Agreement have been set, and now the capability must follow to determine whether CH_4 reductions are actually occurring. At present, however, there are significant limitations in the ability of scientists to quantify CH_4 emissions accurately at global and national scales and to diagnose what mechanisms have altered trends in atmospheric mole fractions in the past decades. For example, in 2007, mole fractions suddenly started rising globally after a decade of almost no growth. More than a decade later, scientists are still debating the mechanisms behind this increase. This study reviews the main approaches and limitations in our current capability to diagnose the drivers of changes in atmospheric CH_4 and, crucially, proposes ways to improve this capability in the coming decade. Recommendations include the following: (i) improvements to process-based models of the main sectors of CH_4 emissions—proposed developments call for the expansion of tropical wetland flux measurements, bridging remote sensing products for improved measurement of wetland area and dynamics, expanding measurements of fossil fuel emissions at the facility and regional levels, expanding country-specific data on the composition of waste sent to landfill and the types of wastewater treatment systems implemented, characterizing and representing temporal profiles of crop growing seasons, implementing parameters related to ruminant emissions such as animal feed, and improving the detection of small fires associated with agriculture and deforestation; (ii) improvements to measurements of CH_4 mole fraction and its isotopic variations—developments include greater vertical profiling at background sites, expanding networks of dense urban measurements with a greater focus on relatively poor countries, improving the precision of isotopic ratio measurements of $^{13}CH_4$, CH_3D, $^{14}CH_4$, and clumped isotopes, creating isotopic reference materials for international-scale development, and expanding spatial and temporal characterization of isotopic source signatures; and (iii) improvements to inverse modeling systems to derive emissions from atmospheric measurements—advances are proposed in the areas of hydroxyl radical quantification, in systematic uncertainty quantification through validation of chemical transport models, in the use of source tracers for estimating sector-level emissions, and in the development of time and

space resolved national inventories. These and other recommendations are proposed for the major areas of CH_4 science with the aim of improving capability in the coming decade to quantify atmospheric CH_4 budgets on the scales necessary for the success of climate policies.

Plain Language Summary Methane is the second largest contributor to climate warming from human activities since preindustrial times. Reducing human-made emissions by half is a major component of the 2015 Paris Agreement target to keep global temperature increases well below 2 °C. In parallel to the methane emission reductions pledged by individual nations, new capabilities are needed to determine independently whether these reductions are actually occurring and whether methane concentrations in the atmosphere are changing for reasons that are clearly understood. At present significant challenges limit the ability of scientists to identify the mechanisms causing changes in atmospheric methane. This study reviews current and emerging tools in methane science and proposes major advances needed in the coming decade to achieve this crucial capability. We recommend further developing the models that simulate the processes behind methane emissions, improving atmospheric measurements of methane and its major carbon and hydrogen isotopes, and advancing abilities to infer the rates of methane being emitted and removed from the atmosphere from these measurements. The improvements described here will play a major role in assessing emissions commitments as more cities, states, and countries report methane emission inventories and commit to specific emission reduction targets.

1. The Role of Atmospheric CH_4 in Achieving Global Climate Targets

Methane (CH_4) is the second most important human-made ("anthropogenic") greenhouse gas after carbon dioxide (CO_2) and accounts for at least 25% of the anthropogenic radiative forcing of warming agents since preindustrial times (including indirect effects due to atmospheric chemistry) (Etminan et al., 2016; Myhre et al., 2013). In addition to its radiative properties, CH_4 is a chemical precursor to tropospheric ozone formation, which causes air quality problems for both human and ecosystem health. Sources of CH_4 to the atmosphere are both natural and anthropogenic in origin. Current estimates of annual CH_4 emissions range from 550–740 Tg/yr, depending on the methodology, with approximately 50–60% coming from anthropogenic sources (Saunois et al., 2016).

Dry-air atmospheric CH_4 mole fraction describes the number of molecules of CH_4 in a given number of molecules of air after removal of water vapor. It is expressed in units of nanomoles per mole, which is abbreviated for simplicity as parts per billion (ppb). In the lower atmosphere, globally averaged mole fractions approached 1,860 ppb in 2018, up from 1,775 ppb in 2006 (National Oceanic and Atmospheric Administration, NOAA/ESRL, www.esrl.noaa.gov/gmd/ccgg/trends_ch4/) and approximately 710 ppb in preindustrial 1750 (Etheridge et al., 1998; Rubino et al., 2019) (Figure 1). Atmospheric CH_4 mole fractions have exhibited large fluctuations year to year, and these are observed in the high-frequency measurement record that began in 1983. Despite the fact that atmospheric observations showed these changes relatively quickly, the mechanisms driving these variations in growth rate are not always well understood. In the past few decades, there have been periods of significant differences in growth rate: a stabilization period in the 2000s during which mole fractions plateaued after a large rise in the 1980s and 1990s, and the period after 2007 during which mole fractions began rising again. The drivers of the stabilization period and of the renewed growth period are still being debated more than one decade later (Turner et al., 2019).

The 2015 Paris Agreement of the United Nations Framework Convention on Climate Change (UNFCCC) aims to limit climate warming from preindustrial levels to well below 2 °C by the Year 2100, with an aspiration of 1.5 °C. Because of its high radiative efficiency and because its lifetime in the atmosphere is only around a decade (Myhre et al., 2013; Prather et al., 2012), reductions in CH_4 emissions will need to play a significant role to quickly meet global climate targets (Mikaloff Fletcher & Schaefer, 2019). The Representative Concentration Pathways (RCPs) (van Vuuren et al., 2011) are concentration trajectories adopted by the Intergovernmental Panel on Climate Change (IPCC) for the Fifth Assessment Report to meet various anthropogenic radiative forcing scenarios up to the Year 2100. RCP2.6 is one trajectory proposed to achieve less than a 2 °C warming (Collins et al., 2013). A key component of RCP2.6 involves an approximately 30% decrease in atmospheric CH_4 mole fractions from 2005 levels by the end of this century

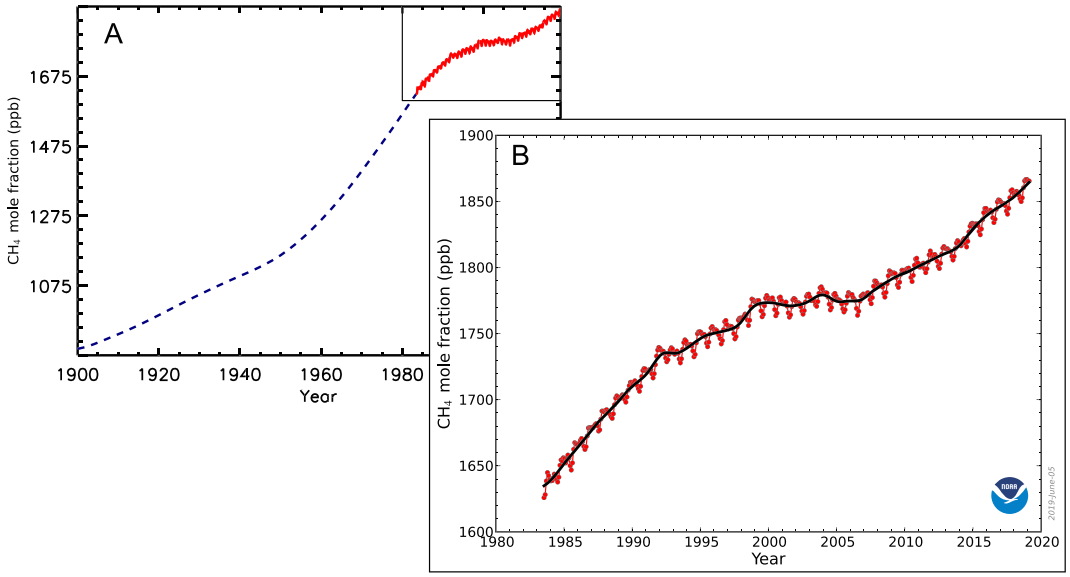


Figure 1. Globally averaged atmospheric CH_4 mole fraction (a) Prior to 1983, data are reconstructed from measurements of ice cores, firn and archived air (Etheridge et al., 1998). The boxed region corresponds to the high-frequency record. (a) High-frequency record (red) and long-term (~12-month) trend (black). (Source: Ed Dlugokencky, NOAA/ESRL, www.esrl.noaa.gov/gmd/ccgg/trends_ch4/).

(Meinshausen et al., 2011), the implication being that annual emissions, including any climate-CH_4 feedback effects, must decrease by approximately 150 Tg/yr (Nisbet et al., 2019). This decrease is equivalent to almost half of all anthropogenic CH_4 emissions today including fossil fuels, agriculture, landfills, and biomass burning.

Since the Paris Agreement, CH_4 mole fractions in the atmosphere have, however, increased above the RCP2.6 pathway (Figure 2a). In 2018, CH_4 mole fractions were more than 100 ppb higher than in RCP2.6 and were also higher than RCP4.5 (Nisbet et al., 2019). While RCP2.6 is only intended to be indicative of scenarios that keep below 2 °C, it shows a divergence in radiative forcing that has been larger for CH_4 than for CO_2 and nitrous oxide (Figure 2b, Nisbet et al., 2019). The extent to which this can be dealt with through more substantial reductions in anthropogenic CH_4 emissions or whether it will require deeper reductions in CO_2 cannot be resolved until the cause of this CH_4 increase is better understood.

The continuing importance of reducing CH_4 is seen in the newer Coupled Model Intercomparison Product 6 scenarios that are consistent with staying below 2 °C (Shared Socioeconomic Pathways, SSP1-2.6 and SSP1-1.9), and these have CH_4 mole fractions starting rapid decreases in 2020 or 2021 (Meinshausen et al., 2019) (Figure 2). Because of the unexpected rise in CH_4 mole fractions, SSP1-1.9 and SSP1-2.6 call for an even larger 45% reduction of 2020 levels by the end of the century because of the sharp decrease in CH_4 mole fraction occurring later than proposed by RCP2.6.

Achievable methods for CH_4 emission reductions have already been identified in a variety of sectors, some of them more developed and others still in the research stage. Within agriculture, preliminary research has shown how red algae and other dietary supplements can reduce methane emissions from cattle and sheep by as much as 95% (e.g., Li et al., 2018; Roque et al., 2019). Considerably more work is needed, however, to determine whether such supplements can be scaled industrywide and to confirm no change to nutrition or taste. Changes to rice cultivation are farther along, including temporary drainage regimes and cultivar selection. A recent study has shown that higher-yielding cultivars of rice can increase yield ~10% while reducing CH_4 emissions by a similar amount, potentially through increased oxygen transport through roots to the soil (Jiang et al., 2017). Within the fossil fuel sector, opportunities for mitigating emissions are already being exploited. Satellites and hyperspectral aircraft platforms are providing increasingly valuable data sets for identifying the locations of superemitters (Kort et al., 2014; Smith et al., 2017). These and other tools will increasingly help companies identify disproportionally high emitting well pads in close to real time. Natural

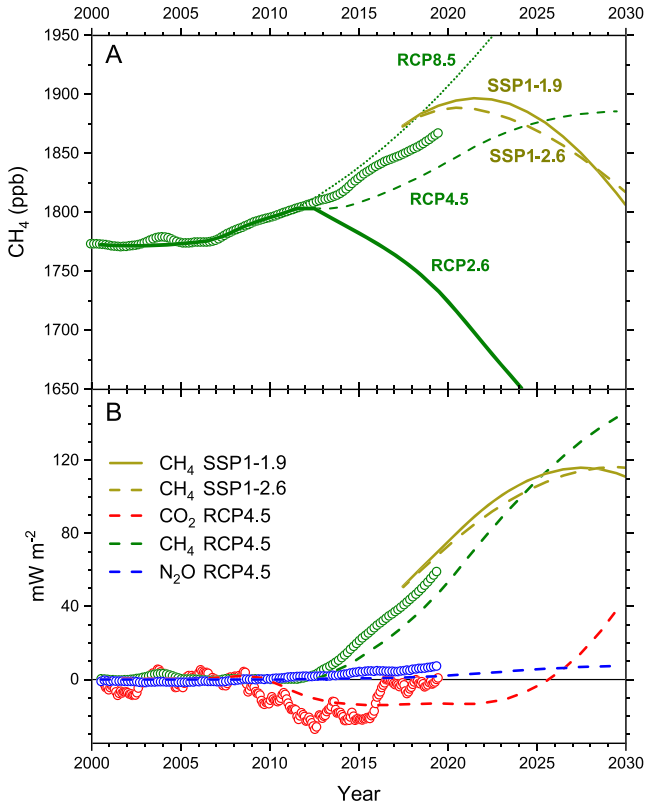


Figure 2. (a) Observed globally-averaged CH_4 mole fractions (open circles) alongside those used as the basis for climate model runs in the Fifth Assessment Report of the IPCC and which had CH_4 mole fractions adjusted from the original Representative Concentration Pathways to follow observed values to 2011 (IPCC, 2013). The two lowest scenarios, SSP1-1.9 and SSP1-2.6, being used for the Sixth Assessment Report are also shown. (b) Difference in radiative forcing (mW/m^2) for the major greenhouse gases between observations and the modified RCP2.6 scenario (open circles). Lines show differences between RCP2.6 and scenarios RCP4.5, SSP1-1.9, and SSP1-2.6 (Nisbet et al. (2019).

gas distribution networks, especially in older cities, are targets of CH_4 mitigation through gas pipeline replacement programs (Gallagher et al., 2015). Such replacement programs can take decades to complete, however, due to cost considerations and the disruptions caused (Jackson et al., 2014). Though more challenging, researchers and companies are also beginning to consider industrial CH_4 removal from the atmosphere, as a complement to the extensive work on direct air capture of atmospheric CO_2. Oxidizing CH_4 is an energy-generating reaction that could restore the atmosphere to preindustrial levels by removing ~3×10^9 t of anthropogenically derived CH_4 in the atmosphere today (Jackson et al., 2019).

The success of the Paris Agreement relies on the collective emission reductions pledged by individual nations through their nationally determined contributions. Baseline emission levels, and the reductions planned relative to the baseline, are quantified by countries using accounting-based methods. An assessment of the progress in meeting these pledges will occur through a global stocktake conducted every 5 yr. Despite the reporting requirements already in place by the UNFCCC, one of the biggest issues is that studies that have attempted to compare process-based accounting methods (referred to as "bottom-up") against emissions inferred from atmospheric measurements (referred to as "top-down") have often found substantial discrepancies (e.g., Miller et al., 2013; Saunois et al., 2016; Thompson et al., 2015). This is true both at the national scale and at the global scale and highlights the large uncertainties that exist in both types of methodologies. Without a better understanding of these discrepancies, it is difficult to know whether the national strategies to reduce emissions aimed at meeting global climate targets match the reality of what is occurring in the atmosphere.

Our current capability to understand the processes that drive changes in atmospheric CH_4 is largely based on the following (illustrated by Figure 3): bottom-up (process-based) models of emissions and top-down (inverse modeling) estimates of CH_4 emissions from atmospheric measurements. Bottom-up modeling refers to any simulation of an individual process and can be achieved with varying levels of complexity. The simplest bottom-up models will take account of the extent of an activity and multiply this activity by an emission factor (EF) (e.g., the emission per unit activity). More complex bottom-up models will simulate a process using a variety of underlying factors. Wetland models, for example, account for variations in soil temperature, moisture, and other environmental factors. These estimates are valuable for understanding underlying drivers, but uncertainties in process models, in activity data or EFs, or in not accounting for some processes, can give an incomplete or uncertain account of emissions. Top-down estimation refers to the process of indirectly quantifying emissions from measurements of atmospheric CH_4 mole fraction and other atmospheric constraints. Top-down methods can employ both global and regional (e.g., focused on a particular country) approaches. Due to the underdetermined nature (insufficient data) of the "inverse" problem, emissions using global methods are generally estimated at coarse (e.g., continental) resolution, with larger uncertainties in regions that are poorly constrained by observations. The advantage of global methods is that the full CH_4 budget (i.e., all of the individual components from emissions and removal by sources and sinks, respectively) is reconciled against the global network of atmospheric measurements. However, estimating source and sink components separately is complicated by the large uncertainties that exist in estimates of sinks. Regional methods can be applied over smaller areas where dense measurement networks exist and used to infer emissions at (sub)national scales without the limitation of sink uncertainty. However, at present, this has only been done for a few regions of the world. All three types of estimates—bottom-up, top-down global, and top-down regional—are subject to often poorly quantified random and systematic errors, making uncertainty quantification for policy purposes a challenge. This study identifies the major

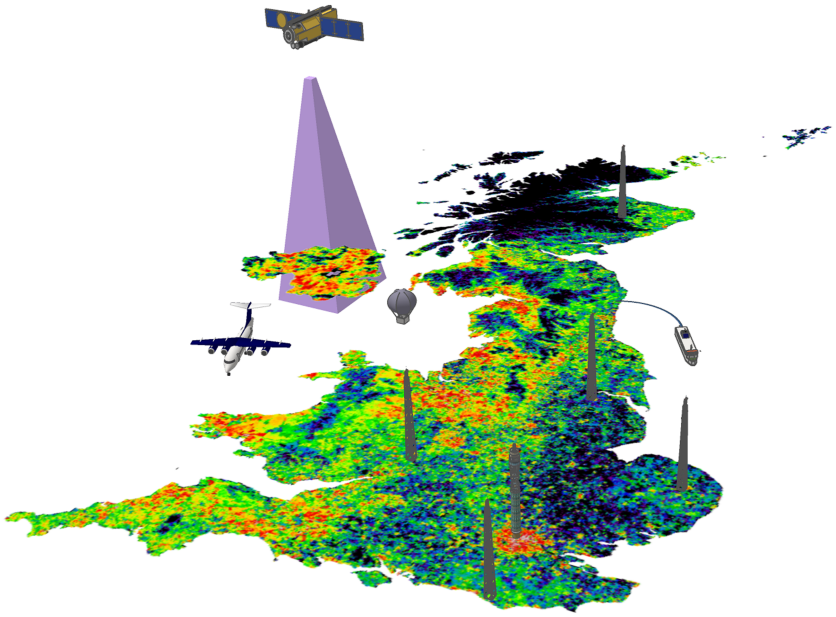


Figure 3. Schematic of bottom-up and top-down studies using the United Kingdom as an example. The bottom-up is shown by the land-based CH_4 emissions map, computed at 1km x 1km resolution by the U.K. National Atmospheric Emissions Inventory (http://naei.beis.gov.uk). Top-down estimates utilize measurements from a variety of platforms including tall towers, aircraft, ships, balloons, and satellites to infer emissions indirectly. The two are needed together to understand the drivers of changes in atmospheric CH_4 mole fraction. Emissions derived from bottom-up and top-down methods are submitted annually by the United Kingdom to the UNFCCC in its National Inventory Report (Brown et al., 2019). The United Kingdom's measurement program for quantifying national emissions is discussed in Palmer et al. (2018) and Stanley et al. (2018).

improvements that are needed in our tools and methodologies to be able to quantify global and national CH_4 emissions and understand their underlying drivers on the timescales relevant for major climate policies.

2. Measurements

2.1. Global Mole Fraction Measurement Network

Observations of atmospheric CH_4 mole fraction and their "isotopologues" (section 2.2) play a fundamental role in monitoring the global carbon cycle. The current global "background" network (Figure 4) of CH_4 mole fraction observations consists of multinational and national measurement programs (including, but not limited to, NOAA Global Greenhouse Gas Reference Network, Integrated Carbon Observation System, and Advanced Global Atmospheric Gases Experiment, Dlugokencky et al., 2009; Prinn et al., 2018, http://www.icos-ri.eu). Background measurements indicate the CH_4 mole fraction in air that has been well mixed in the global atmosphere. To ensure that measurements are of sufficient quality to meet scientific needs, programs calibrate measurements against common standards and participate in collaborative intercomparison round robins organized under the World Meteorological Organization's (WMO) Global Atmosphere Watch (WMO, 2018).

The data from the surface network are used most fundamentally to estimate global average CH_4 abundance as a function of time. This time series provides key constraints on the global CH_4 budget and year-on-year changes. Using the NOAA uncertainty quantification method as an example, the total uncertainty in annual mole fraction growth rate ranges from 0.4–1 ppb/yr (68% confidence interval), which translates to an uncertainty of approximately 1.1–2.8 Tg/yr in global budgets (assuming 1 ppb = 2.767 Tg CH_4, Fung et al., 1991). The main challenge is in separating the global budget into estimates of emissions from sources and removal by sinks because any uncertainties in the atmospheric CH_4 lifetime (discussed in section 4.1) directly translate into uncertainties in emissions.

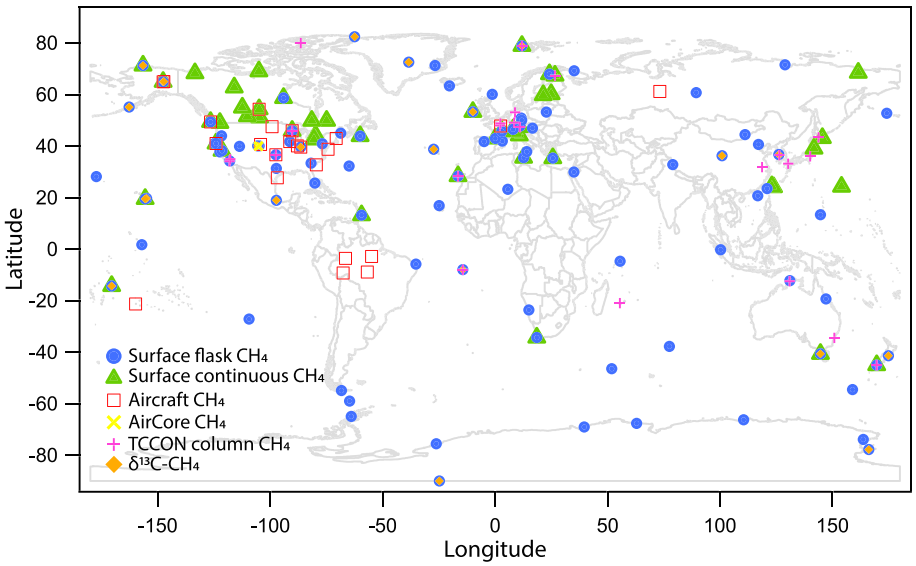


Figure 4. Publicly available background CH_4 mole fraction measurements. Sites shown have been measuring for at least 5 yr and are still in operation. Blue circles represent flasks filled with air at surface locations at approximately weekly frequency and measured at central laboratories. Green triangles represent quasi-continuous surface measurements using instruments housed on-site. Red squares designate vertical aircraft profiles made over fixed sites. Yellow crosses refer to routine vertical profiles by AirCore. Pink plus symbols indicate column measurements made by the TCCON network. Orange diamonds indicate concurrent flask measurements of the $\delta^{13}C$-CH_4 isotope ratio. Only few sites operate with colocated sampling by different measurement programs or different instruments. Data archives shown here include WMO/GAW World Data Centre for Greenhouse Gases (https://gaw.kishou.go.jp), AGAGE (https://agage.mit.edu/data/agage-data), NOAA GLOBALVIEWplus (https://www.esrl.noaa.gov/gmd/ccgg/obspack/), NIES Center for Global Environmental Research (http://db.cger.nies.go.jp/portal/geds/atmosphericAndOceanicMonitoring), NOAA AirCore (ftp://aftp.cmdl.noaa.gov/data/AirCore) and TCCON (https://tccondata.org).

The global background network is also used to quantify seasonal cycles and latitudinal gradients in CH_4 mole fraction. When combined with transport models and assumptions about sinks, data can be used to infer CH_4 emissions at, for example, continental scales. Higher-resolution mapping of the spatial and temporal distribution of atmospheric CH_4 requires better data coverage in parts of the world where there are currently significant gaps in the network. Ground-based air sampling sites are very sparse over large parts of the tropics and Siberia (e.g., Dlugokencky et al., 2011) and almost absent in interior Africa and South America (Figure 4). Pandey et al. (2019) show that although the global average CH_4 growth rate estimated by the ground network is fairly accurate, biases in estimated hemispheric or latitudinal CH_4 growth rates result from sparse sampling. The main limitations in developing new sites are in the barriers imposed by lack of political will and logistics support and in the need for long-term commitment to monitoring.

Long-term records are imperative to maintain in order to monitor changes in CH_4 over time. All measurements should either be calibrated to the scale maintained by the WMO/GAW Central Calibration Laboratory or laboratories must maintain a direct link to this scale, traceable over the entire measurement record. Measurements must be made to WMO standards and made publicly available for transparency.

The relatively long lifetime of approximately a decade means that CH_4 measured at background sites has been well mixed in the global atmosphere. Thus, these measurements are informative of emissions that have occurred over large source regions and over time. Enhancements above this well-mixed signal due to regional and local emissions are typically small in the surface background network. The challenge therefore remains in attributing the changes in atmospheric mole fraction to the underlying processes at increased spatial scales, such as national and subnational. Measurements that are representative of regional emissions and that are not influenced by very localized sources are needed to estimate emissions and their drivers at this resolution. To achieve this, some countries have implanted national measurement networks (e.g., United States and United Kingdom). The challenge is in ensuring high-quality measurements from individual groups that can be traced back to common WMO/GAW calibration scales and rigorously

intercompared with collaborating laboratories. Even with increased data density, in order to attribute changes in mole fraction to underlying processes, additional information is often required from isotopologues (section 2.2), process models (section 3), or coemitted tracers (section 4.5).

In addition to surface networks, aircraft campaigns and commercial aircraft programs provide vertical CH_4 mole fractions measurements. These vertical profiles can be used to calibrate vertical mixing in atmospheric transport models, which is critical for accurately inferring emissions from mole fraction data. Vertical profiles are also crucial for evaluating dry-air column average CH_4 (XCH_4, discussed in section 2.3) relative to the WMO mole fraction scale either by direct comparison or through the Total Column Carbon Observing Network. Current vertical profile sampling is, however, limited in both sampling frequency and spatial coverage. The NOAA North American aircraft program has a sampling frequency ranging from once per week to once every 2 months over around 15 fixed sites (Sweeney et al., 2015). Over Brazil, approximately biweekly aircraft profiles of CH_4 mole fraction are being made over four sites (Wilson et al., 2016). The CONTRAIL program makes approximately weekly CH_4 measurements on commercial flight routes between Japan and destinations in Asia, Europe, and Australia (Machida et al., 2008). The CARIBIC container is deployed at varying frequency on flights out of Germany to destinations in America, Asia, and Africa (F. Boschetti et al., 2018; Brenninkmeijer et al., 2007). The challenge that remains is in providing widespread and frequent vertical profiles economically and leveraging commercial carriers is one way to expand this type of measurement.

Vertical profiles of CH_4 have also been measured by short-term aircraft campaigns such as HIPPO (HIAPER Pole-to-Pole Observations) and ATom (Atmospheric Tomography Mission) and by the AirCore system. AirCore, typically launched to the midstratosphere on a balloon, uses a long, narrow piece of tubing that preserves a profile of air as it descends to the ground (Karion et al., 2010). Systematic sampling using the AirCore system is currently in its early development stage and has only been implemented in a few locations (Andersen et al., 2018; Engel et al., 2017; Membrive et al., 2017; Paul et al., 2016; ftp://aftp.cmdl.noaa.gov/data/AirCore). An AirCore network employed over the surface network can enable monitoring of remote locations and deliver measurements in the upper troposphere and lower stratosphere where aircraft measurements are limited.

2.2. Isotopic Ratio Measurements

The main isotopic variations (the "isotopologues") in CH_4 molecules (e.g., $^{13}CH_4$ vs. the dominant $^{12}CH_4$) have the potential to serve as important observables to understand the processes driving changes in the global CH_4 burden. This is because sources with different properties (e.g., those with biological origins versus those from burning) emit CH_4 with different ratios of the CH_4 isotopologues. Sinks, such as the chemical destruction of CH_4 in the atmosphere, also change the isotopic ratio of the atmosphere due to the different rates by which each isotopologue is chemically removed. Thus, measurements of the CH_4 isotopologue ratios provide one mechanism for attributing variations in CH_4 mole fraction to the responsible process.

Monitoring the stable isotopic composition of CH_4 has thus far been made almost exclusively through the bulk isotopic ratios $^{13}C/^{12}C$ and D/H, using isotope ratio mass spectrometry (IRMS). Standard isotopic ratios are reported using the δ notation (e.g., $\delta^{13}C\text{-}CH_4 = 1{,}000 \times [(^{13}C/^{12}C)_{sample}/(^{13}C/^{12}C)_{standard} - 1]$ with measurements linked to a common international isotopic ratio scale, either Vienna Peedee belemnite for $\delta^{13}C\text{-}CH_4$ or Vienna Standard Mean Ocean Water for $\delta D\text{-}CH_4$. Capabilities for these measurements exist at some laboratories around the world (Umezawa et al., 2018); however, very few are maintaining long-term time series.

Using single laboratory studies alone to assess long-term trends has the advantage of removing intercomparison uncertainties. The disadvantages of this approach are the potential for calibration drift within the laboratory (either due to standards or measurement methods) to go undetected and the difficulty in assimilating measurements from multiple laboratories into larger and more useful data sets. The compatibility goals, which refer to the maximum bias tolerated between measurement programs, for global monitoring of $\delta^{13}C\text{-}CH_4$ and $\delta D\text{-}CH_4$ are 0.02‰ and 1‰, respectively (WMO, 2018). Interlaboratory comparison exercises, which should be routinely performed, demonstrate that these goals are very ambitious (Umezawa et al., 2018); however, long-term data set comparisons using colocated sampling show that they can be

approached, though not attained (Nisbet et al., 2019). It is vital to maintain colocated sampling at several sites to ensure that these goals are being achieved, however very few sites currently operate in this way.

Owing to the larger abundance in the atmosphere of $^{13}CH_4$ relative to CH_3D, $\delta^{13}C\text{-}CH_4$ has been more widely measured in the atmosphere. The measurement challenge is defined by the very small observed interannual differences and latitudinal gradients. Between 2000 and 2007, the rate of change in the global background for $\delta^{13}C\text{-}CH_4$ was undetectable, followed by −0.03%/yr between 2007 and 2014 (Nisbet et al., 2016), and with an interhemispheric difference across the time series of <0.5‰ (Levin et al., 2012). With measurement precisions using IRMS for individual samples that range between 0.02‰ to 0.1‰ these small differences have only been made statistically significant through long-term single site measurements with frequent and regular sampling. For $\delta D\text{-}CH_4$, detecting trends is even more challenged by current analytical precisions and the technical capability to make measurements. Reported trends in $\delta D\text{-}CH_4$ have not been statistically significant (Fujita et al., 2018), with $+0.2 \pm 1.4$‰/yr reported between 2000 and 2006 (Rice et al., 2016). Typical analytical precisions for $\delta D\text{-}CH_4$ by IRMS are >1‰.

Interpretation of the small isotopic atmospheric variations also requires careful consideration of measurement uncertainty and any inaccuracies introduced through the propagation of standards. Despite notable efforts by laboratories for best practice and to make intercomparisons, different realizations of the international isotopic scales have resulted. A single step for improving the interlaboratory comparability of isotopic measurements is for the introduction of gaseous reference materials. Sperlich et al. (2016) have made the first effort in this regard, creating a suite of synthetic gaseous reference materials specifically for the purpose of international scale dissemination. Expansion and improvements in these efforts will be invaluable over the coming years as more laboratories gain the ability to make isotopic measurements.

The potential for measurements by laser spectrometry in the midinfrared to become a routine methodology for ambient air sampling is significant (Eyer et al., 2016; Röckmann et al., 2016) . The major benefits of laser spectrometric techniques include their potential for automation and continuous measurement, allowing deployment outside a usual laboratory setting, and their ability to measure more than one isotope system simultaneously. Measurements by laser spectroscopy have been proven in studies measuring enhanced CH_4 mole fractions near sources (Bergamaschi et al., 1998; Hoheisel et al., 2019; Santoni et al., 2012). In the analysis of ambient air samples using an inline preconcentration method, precisions of 0.1‰ and 0.5‰ for $\delta^{13}C\text{-}CH_4$ and $\delta D\text{-}CH_4$, respectively, were demonstrated, which were subsequently also shown in a field study alongside measurements by IRMS (Röckmann et al., 2016). These precisions are likely limited by the reproducibility during preconcentration, and therefore, improvements in the trapping and separation methods hold significant promise for improving the measurement precisions from ambient air samples. However, measurements by laser spectroscopy currently require large sample volumes (>5 L) to attain useful precision, whereas IRMS methods only require ambient sample volumes down to ~75 ml. Given these large sensitivity differences, optical methods will require significant advancement over the coming years if they are to compete with IRMS.

There are significant gaps in the characterization of source signatures, which are needed to interpret isotope ratio measurements. (i) Measurements from microbial and biomass burning sources are significantly sparser than for fossil sources, owing to the diffuse nature of the nonfossil samples and location of their emissions. Many regions with significant wetland emissions are very poorly sampled, especially in the dominantly C4 tropical wetlands. For example, there are no measurements from the very large C4 wetlands in South Sudan and Democratic Republic of Congo. Efforts need to be made to balance the measurements made of sources relative to their emissions strength. Despite natural wetlands and agricultural sources having the largest impact on the CH_4 budget, $\delta^{13}C\text{-}CH_4$ microbial source signature measurement numbers are underrepresented by more than 7:1 compared to fossil sources, as shown in the database compiled by Sherwood et al. (2017). (ii) Fossil fuel $\delta^{13}C\text{-}CH_4$ signatures exhibit a large range, which can be related to, for example, the type of coal being mined, the extraction method (Zazzeri et al., 2016), as well as oil and gas reservoir maturity (Sherwood et al., 2017) Better understanding the drivers of these variations provides methods for improved spatial and temporal extrapolation. In Sherwood et al. (2017), the majority of fossil samples are from North American studies, leaving a major gap in characterization of signatures of emissions from Asia (particularly China with its very large coal emissions), Middle East, Africa, and South America. (iii) Source signatures could also exhibit temporal variation due to changing emission processes. Examples of

temporal variation include changing oil and gas extraction depths within a producing basin over time (Townsend-Small et al., 2016), or wetland methanogenesis at a given location changing due to changing environmental conditions (McCalley et al., 2014). For all sources, measurements assessing temporal source signature variability are more limited than those assessing spatial variability. Studies show it may be important to implement long-term measurements quantifying temporal variation (Fisher et al., 2017; Sriskantharajah et al., 2012). The availability of relatively inexpensive off-the-shelf spectrometers could help to fill in the large gaps in source signature characterization in the coming years (Hoheisel et al., 2019).

The rate of removal of CH_3D is significantly slower than $^{12}CH_4$ leading to a significant kinetic isotope effect and an atmospheric $\delta D\text{-}CH_4$ lying well outside the global average source signature and beyond even the heaviest fossil source measurements. $\delta D\text{-}CH_4$ could therefore be of particular use in quantifying changes in OH concentration ([OH]), one of the most significant challenges in interpreting atmospheric CH_4 (section 4.1). Only few studies have used measurements of $\delta D\text{-}CH_4$ (Fujita et al., 2018; Rice et al., 2016; Tyler et al., 2007; Umezawa et al., 2012; Warwick et al., 2016) owing to their sparsity (measurements of $\delta D\text{-}CH_4$ in the NOAA network ceased some years ago, and currently, there are very few continuing long-term time series), and information on $\delta D\text{-}CH_4$ source signatures is comparatively even more limited than for $\delta^{13}C\text{-}CH_4$. Collecting representative measurements on $\delta D\text{-}CH_4$ source signatures will become important if this valuable and important constraint is to be used in model studies.

Isotopic measurements are more straightforward to interpret on regional scales rather than global scales as pollution episodes have a direct and linear impact on the observed isotopic composition, which can be related directly to the changes in mole fraction (Fisher et al., 2011; Fujita et al., 2018; Röckmann et al., 2016; Warwick et al., 2016). However, inadequate spatial and temporal coverage of measurements has meant that measurements have so far only been used to rule in or out a particular source type contribution rather to than make flux estimates (Fujita et al., 2018; Umezawa et al., 2012; Warwick et al., 2016). Deploying field instruments to measure near-continuous and high-precision $\delta^{13}C\text{-}CH_4$ and $\delta D\text{-}CH_4$ alongside mole fraction measurements will drive development in regional flux estimation over the coming years (Rigby et al., 2012; Röckmann et al., 2016).

Radiomethane (referred to in the notation $\Delta^{14}CH_4$) has potentially the strongest constraint for quantifying the fossil source of CH_4 (Lassey et al., 2007; Levin et al., 1992). The global $^{14}CH_4$ budget is balanced by three flux factors: (i) emissions of $^{14}CH_4$ from nuclear power plants and military use of nuclear propulsion, (ii) biogenic emissions whose carbon has ultimately been derived from atmospheric CO_2 (which contains $^{14}CO_2$), and (iii) fossil CH_4 which is devoid of $^{14}CH_4$. As with the stable isotope ratios, a more immediate benefit of $\Delta^{14}CH_4$ could come at the regional scale; however, in regions where nuclear sources exist, careful consideration needs to be paid to properly assess and quantify this interfering component (Graven et al., 2019; Townsend-Small et al., 2012). Coupling regional transport models to measurements of $\Delta^{14}CH_4$ would allow quantification of the fossil component of CH_4; however, the sampling methods to make this possible are only starting to be developed (Espic et al., 2019). In addition, background stations must implement routine and long-term measurements to accurately quantify the regional $\Delta^{14}CH_4$ background.

The stable isotope ratios reported in the atmosphere so far have only attempted to quantify total atomic isotope ratios, ignoring the very small differences in the multiply substituted isotopologues or "clumped" isotopes ($^{13}CH_3D$, $^{12}CH_2D_2$, $^{13}CH_2D_2$, $^{12}CHD_3$, $^{13}CHD_3$, $^{12}CD_4$, and $^{13}CD_4$). Experimental and theoretical studies have suggested enrichments in $^{13}CH_3D$ and $^{12}CH_2D_2$ due to kinetic and thermodynamic processes, and the small number of natural sample measurements to date has detected a range in clumped isotope ratios (Douglas et al., 2017; Haghnegahdar et al., 2017; Stolper et al., 2014; Stolper & Eiler, 2015; Wang et al., 2015; Whitehill et al., 2017; Young et al., 2016, 2017).

Significant developments are being made in clumped isotope measurements by both IRMS (Eiler et al., 2013; Stolper et al., 2014; Young et al., 2016) and laser spectroscopy (Ono et al., 2014); however, these methods are far from being able to measure at ambient CH_4 levels. Comparing theoretical and model calculations of clumped isotope ratios against atmospheric measurements would require CH_4 to be removed from several hundred liters of air and this feat is yet to be achieved. Similar sample volume requirements have been required for removing CH_4 from ice core samples for $\Delta^{14}CH_4$ analysis (Petrenko et al., 2008); however, the additional challenge for clumped isotopes is that the distribution among isotopologues must be

preserved during sampling. The evidence so far suggests that measuring clumped isotopes in the atmosphere is a worthwhile endeavor; however, long-term time series need to be measured and a database of source signatures compiled.

2.3. Remote Sensing of Atmospheric XCH_4

Column concentrations of trace gases can be measured by observing the absorption of radiation in the atmosphere from space. Atmospheric CH_4 absorbs radiation in the shortwave infrared (SWIR) at 1.65 and 2.3 μm and in the thermal infrared (TIR) at around 8 μm. SWIR is measured by instruments observing the backscatter of solar radiation from the Earth's surface and atmosphere, while TIR is based on measurements of thermal emissions (Jacob et al., 2016). Spaceborne observations have the advantage over ground- and aircraft-based measurements in that they provide global coverage of column concentrations at regular intervals, making observations cost effective, particularly for remote regions of the world.

Satellite observations have provided us with new insights into the CH_4 cycle. Using satellite CH_4 data, it has been possible to determine the location and strength of CH_4 emissions (Bloom et al., 2010), to diagnose the response of tropical wetland emissions to precipitation changes induced by the El Niño–Southern Oscillation (Pandey et al., 2017; Parker et al., 2018), to reevaluate the role of emissions from fires (Worden et al., 2017), and to infer trends in regional total and anthropogenic CH_4 emissions (e.g., Ganesan et al., 2017; Miller et al., 2019; Turner et al., 2015), Recent studies have also used satellites data to assess large CH_4 emission hot spots (section 2.4).

Satellites measuring absorption in the SWIR include SCIAMACHY, GOSAT, GOSAT-2, and Sentinel 5P TROPOMI and in the TIR include IMG, IASI, AIRS, TES, and CrIS. While both SWIR and TIR measure XCH_4, TIR is more sensitive to absorption in the upper troposphere and may be less appropriate for inferring surface processes (Siddans et al., 2017; Xiong et al., 2016). However, using SWIR and TIR data together in model studies may help to improve emission estimation by more accurately representing the vertical column (Jacob et al., 2016).

Both the SWIR and TIR satellites mentioned so far are passive sensors and rely on external sources of energy. Passive instruments that depend on sunlight as the source of energy are unable to measure in late fall, winter, and early spring in the high latitudes, where "shoulder-season" fluxes of CH_4 are thought to be significant part of the annual wetland CH_4 budget (Treat et al., 2018; Zona et al., 2016). Active sensors, such as MERLIN, using Lidar as the source of energy at the wavelengths that CH_4 absorbs (Ehret et al., 2017) are being planned or are in development. Active remote sensing has the potential for significantly improving measurement coverage in high-latitude regions, providing data with fine resolution along a narrow ground track that has higher likelihood of measuring backscatter from all clear-sky conditions.

The main limitation in interpreting satellite XCH_4 data is the need to quantify any biases in the data, which can vary in time and space. This is essential to ensure that data sets are consistent over time as well as between different instruments. Biases arise because it is necessary to convert raw radiances measured by the satellite into XCH_4. Two sets of retrieval algorithms are commonly used for SWIR satellites. These include a "CO_2 proxy" method and a "full-physics" method (Frankenberg, 2005; Parker et al., 2011; Streets et al., 2013). The full-physics approach attempts to model radiative transfer through the atmosphere using information on atmospheric aerosols extracted from a near-infrared O_2 band. To avoid biases from uncertainties in the treatment of aerosols and thin clouds, these retrievals are limited to regions with moderate aerosol loadings (typically with aerosol optical depth of less than 0.3). The "CO_2 proxy" method makes use of CH_4 and CO_2 absorption bands, which are in spectral proximity to each other so that aerosol effects cancel out in the retrieved CH_4:CO_2 ratio. XCH_4 can then be obtained by combining the ratio with modeled CO_2. This method results in enhanced coverage compared to full-physics methods, specifically in the tropics and the highly polluted areas of Asia. In contrast to the full-physics method where aerosols are the main reason for retrieval biases, it is primarily uncertainties in modeled CO_2 that can introduce biases in the retrieved proxy XCH_4 (Parker et al., 2015). The Total Column Carbon Observing Network of ground-based spectrometers (Wunch et al., 2011) is used to diagnose any biases in GOSAT that result from the complexity of retrieval algorithms (e.g., Buchwitz et al., 2017); however, they may be unquantified in regions not covered by the network, which operates around 30 stations worldwide. Therefore, expanded surface in situ and column measurements, potentially through the development of lower-cost instruments (e.g., Frey et al., 2019),

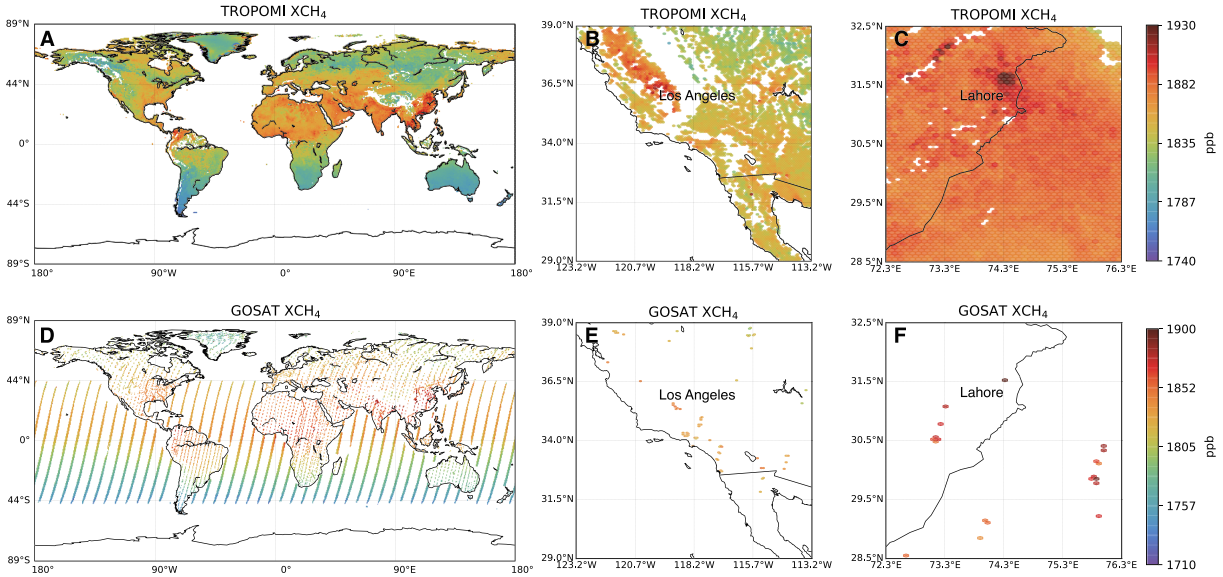


Figure 5. XCH_4 mole fractions from (a–c) TROPOMI and (d–f) GOSAT (derived using the CO_2 proxy method): (a, d) Global, (b, e) Los Angeles basin, and (c, f) Lahore, Pakistan. Values represent the annual mean of TROPOMI observations between May 2018 and May 2019 and GOSAT observations between January 2016 and January 2017. GOSAT data also include glint observations over the oceans. Background surface mole fractions differ by ~30 ppb at the midpoint of the two periods, and the color bar is shifted by the same amount so that patterns can be compared. (a–c, e, and f) TROPOMI data and regional/urban GOSAT data are plotted in 0.1° × 0.1° bins, while (d) GOSAT data are plotted globally in 0.5° × 0.5° bins to improve visibility.

and improved vertical profiling are needed to improve quantification and correction of these biases and therefore extend the utility of XCH_4 measurements for understanding surface processes. Despite any direct bias correction, all modeling studies using these data sets should attempt indirect assessment of these biases by (i) using independent calibrated data, where possible, and (ii) when using data derived from the CO_2 proxy method, investigate the systematic uncertainty in derived emissions that is imposed by the modeled CO_2 fields.

Observing System Simulation Experiments have been carried out to identify optimal sampling strategies (Sheng et al., 2018) and have identified the need for higher spatial resolution and improved spatial coverage in order for spaceborne observations to be relevant to the monitoring of international climate policies. The capability in spaceborne observation of XCH_4 is rapidly improving in spatial and temporal coverage. The TROPOMI instrument aboard Sentinel-5P (launched October 2017) represents a major step forward owing to its daily global coverage and high spatial resolution (Figure 5, Hu et al., 2018). Observations from TROPOMI will allow much better regional characterization of CH_4 emissions (Figure 5b), and their spatial resolution of ~50 km^2 (at nadir) means that large urban areas will be able to be resolved (Figure 5c). Further, due to frequent overpasses, temporal variations in emissions can be monitored, which is important for urban areas, facilities, and large-scale accidents. A further advancement in spatial resolution of space-based observations will come with the Copernicus CO_2 Monitoring Mission (CO2M), which is being developed to provide the appropriate means and capacity of assessing the effectiveness of the Paris Agreement. CO2M will consist of a constellation of identical satellite missions measuring XCO_2 and XCH_4 with 4-km^2 spatial resolution and global coverage every 3 days. With GOSAT-2/-3, Sentinel-5P and −5 and CO2M, the coming decade will provide unprecedented global monitoring capabilities of XCH_4 from space. However, these missions are all launched into Sun-synchronous low Earth orbit orbits and are aimed at providing global coverage; thus, their spatial resolution is relatively coarse and they provide no information on diurnal variations.

New satellite architectures will be needed to overcome observational limitations of these satellites and to provide synergistic observations to the global survey missions. Geostationary such as Geo-Carb and smaller satellites have the potential to provide diurnal or diel coverage of XCH_4 and pointing capabilities for point-source detection. Point-source detection maximizes the number of ground samples within a specific area whenever the satellite orbit is close to a targeted source. With GHGSat-D, the first dedicated mission for

point source detection is already in orbit which uses novel imaging technology to detect CH_4 plumes on a spatial scale of tens of meters (Varon et al., 2019). Also, the recently launched GOSAT-2 has a flexible pointing system, which will be used to target local emissions sources but the large ground footprint of GOSAT-2 with a diameter of about 10 km will limit this capability to very strong sources. Further small satellites aimed at local emissions are planned (e.g., Environmental Defense Fund's MethaneSAT) providing new capabilities for regular monitoring of localized CH_4 sources. Combining such high-resolution satellites with those that employ global and frequent coverage, such as TROPOMI, would allow for anomalies to be efficiently detected and which can be mapped in greater detail once pinpointed.

Isotopic monitoring by remote sensing methods is in its infancy and in the foreseeable future is unlikely to generate the measurement precisions required to observe isotopic differences or trends in the atmosphere. Malina et al. (2019) argue that GOSAT-2 would be able to detect $\delta^{13}C$-CH_4 changes of up to 10‰; however, these levels of detection are still inadequate for improving our understanding of flux estimates at any scale. Improvements in this technology could revolutionize the geographic coverage of isotopic measurements but are decades away.

2.4. Measurements of Oil and Gas Hot Spots

CH_4 hot spots mostly refer to spatial concentration anomalies over a background level at local or regional scale. One example is the SCIAMACHY remote sensing signal over the Four Corners region in New Mexico and Colorado, USA, where XCH_4 enhancements above regional background of 20 ppb on average were found over 2003–2009 (Kort et al., 2014). These enhancements were associated with intensive fossil fuel production in the region and confirmed with local aircraft measurements a few years later (Smith et al., 2017). It is important to note that several other high CH_4 emitting regions such as West Virginia and Pennsylvania (intensive coal mining) did not show up as hot spots in SCIAMACHY. It is likely that other factors such as regional topography at least contribute to the observation that the largest concentration hot spots are not necessarily associated with the largest emission hot spots.

A regional hot spot at the scale of 10^4–10^5 km^2 requires measurements over much larger areas ($>10^5$ km^2) to identify the anomaly from the regional background. Recently, launched satellite instruments such as TROPOMI as well as future missions (e.g., MethaneSAT) will produce more data at higher spatiotemporal resolution than current and past satellites. The new data may identify new hot spots but will also need to verify the locations, spatial extent, and magnitude of previously identified hot spots based on the much larger data sample size and signal-to-noise ratio. As discussed above, high concentrations do not necessarily imply high emission rates or even high gas production normalized emission rates ("leak rates"). In order to globally identify regions with a potential for relatively large CH_4 emission reductions, satellite measurements need to be accompanied with methods for emission rate quantification (e.g., inverse modeling driven by accurate and high-resolution meteorological inputs), databases of oil and gas production, and inventories of CH_4 sources other than fossil fuel. Given the massive data quantities at global scale, this process needs to be automated, at least at first pass, to ensure near real-time data analysis.

Aircraft are less suitable for identifying regional-scale hot spots because of the difficulty of collecting measurements over areas over 10^5 km^2 under comparable atmospheric conditions. Nevertheless, raster pattern flights have been successful in identifying local hot spots (e.g., within a natural gas producing region in Arkansas) at scales of 10^2–10^3 km^2 (Schwietzke et al., 2017). Raster flights provide precise, real-time information on spatial patterns, while mass balance flights allow for source quantification of plumes at the facility and regional scales, after simple atmospheric modeling to convert measurement data into emission estimates (Schwietzke et al., 2017). Future measurement campaigns may combine in situ measurements during raster patterns with imaging spectrometry (e.g., Thorpe et al., 2017) on the same aircraft. This approach could combine the advantages of both measurement techniques to yield instantaneous mapping of high concentrations along with the identification and quantification of point sources.

Large emission point sources occurring over relatively brief periods may also be considered hot spots. Such temporal hot spots include large-scale accidents in the oil and gas industry (e.g., Aliso Canyon natural gas storage facility in California), which can emit CH_4 for weeks to months at a rate larger than the total CH_4 emissions from the average U.S. oil and gas basin (Peischl et al., 2018). The first reported emission estimates at Aliso Canyon came from rapidly deployed light aircraft instrumented with a continuous CH_4 analyzer

that mapped the vertical 2-D concentrations immediately downwind of the gas storage facility leak. Additional downwind measurements from vehicle-based sensors (California Air Resources Board, 2016) and inverse modeling studies later confirmed the initial aircraft estimates. Some of these measurements were repeated for months to track the progress of the facility operator fixing the leak. Such tracking of temporal hot spots over time may be achieved through future satellite missions that offer the appropriate temporal and spatial resolution (section 2.3). Large-scale accidents and other equally large methane releases are also known to happen outside the United States. Examples include the bursting of a gas pipeline in Algeria (Louhibi-Bouiri & Hachemi, 2018) and venting at a compressor station in Turkmenistan (Varon et al., 2019). While the resulting emissions from the Algeria incident were based on engineering calculations (Louhibi-Bouiri & Hachemi, 2018), the Turkmenistan incident was observed from space via GHGSat-D and TROPOMI over more than 1 yr later. Such large emission events are not included in most current inventories (section 3.2).

3. Bottom-Up Modeling

We discuss below the current limitations faced in global bottom-up modeling of the major CH_4 source categories. National inventories also utilize methods to account for anthropogenic emissions and these can differ from global inventories. For submission to the UNFCCC, each country must follow the detailed guidance given in the IPCC guidelines (IPCC, 2006, 2019). The guidelines use a tiered approach in the compilation of national emissions. The simplest, Tier 1, relies on default EFs, whereas Tiers 2 and 3 allow country-specific methods, data, and models to be incorporated. These tiers require significant socioeconomic and statistical data to be available and be annually updated in a timely manner and this is a major challenge in less economically developed countries. Future improvement to national inventories would come in the form of higher tiers, which would have emissions spatially and temporally (subannually) resolved. These higher tiers would allow for detailed comparisons to be made with other independent estimates (section 4).

3.1. Wetlands and Other Natural Water Bodies

Natural water bodies emitting CH_4 are mainly comprised by wetlands, however, recent studies have highlighted local to global-scale importance of emissions from lakes (Wik, Varner, et al., 2016) including thermokarst (Walter Anthony et al., 2018), reservoirs (Deemer et al., 2016) and coastal and open ocean areas (Weber et al., 2019).

The modeling approaches used to simulate wetland CH_4 emissions are diverse and can be distinguished by how they define wetland types, quantify wetland area, and produce and transport CH_4 to the atmosphere (Xu et al., 2016). The majority of wetland models simulate CH_4 according to a general definition of vegetated wetlands and exclude emissions from rice and inland waters, which can include rivers, lakes and small ponds (Matthews & Fung, 1987). Vegetated wetlands can grow in diverse habitats (Cowardin et al., 1979), for example, along river banks (i.e., riparian zones), on mineral or organic soils, experience seasonal or permanent inundation, or have soils that have complex cycles of freezing and thawing (i.e., permafrost). In many cases, models simply assume that if soils are flooded, then anaerobic conditions are present to initiate CH_4 production.

Several global data sets of wetland area and dynamics exist (e.g., Global Inundation Extent of Multi-Satellites Observations, Surface Water Microwave Product Series, and the Land Parameter Data Record), each depending on passive microwave measurements to determine surface inundation (Du et al., 2017; Pham-Duc et al., 2017; Prigent et al., 2007). New satellite missions (e.g., Sentinel 1, SWOT) aim to provide high-resolution (<30 m), passive microwave observations that can be used to map wetlands in more detail than current technologies allow. Passive microwave observations integrate backscatter signals for vegetated wetlands and inland waters but are sensitive to the presence of surface water and thus do not capture wetlands lacking water at or above the soil surface. Optical products of vegetated wetlands using visible to near-infrared wavelengths have the advantage of inferring wetlands by mapping species composition, but these products can be uncertain or unable to provide seasonal or longer-term dynamics of hydrology (Guo et al., 2017). The high spatial resolution provided by some Cubesat technologies (1–5 m^2) could allow for mapping wetlands at very high resolution (Cooley et al., 2017). Remote sensing approaches that combine passive microwave and optical instruments should be used to leverage the capabilities of both types of observations. This advance can help in reconciling scaling and definition challenges, as one of the largest sources

of uncertainty in wetland CH_4 emission estimates is in the partitioning of fluxes between vegetated wetlands and inland waters.

More strategic observations are required to constrain the distribution of wetlands and emissions from high-latitude, lakes and ocean regions. In the permafrost regions of the high latitudes, atmospheric measurements from Alaska have been used to assess long-term trends in North Slope emissions and to determine the temperature sensitivity of these emissions (Sweeney et al., 2016). Long-term atmospheric measurements from other high-latitude regions that are not significantly impacted by anthropogenic sources and that are made alongside biogeochemical measurements are necessary to diagnose and detect any permafrost feedbacks. Including isotopic measurements at these sites, including of radiocarbon, would also be useful for robustly associating the mole fraction enhancements to emissions from permafrost rather than from other sources (K. M. Walter et al., 2006; Zimov et al., 2006). At present, atmospheric measurement stations in the high latitudes are sparse (section 2.1).

The episodic nature of emissions from lakes and coastal areas means that measurements sampling their spatial and temporal variability are required (Wik, Thornton, et al., 2016). These require long-term floating chamber measurements or oceanographic cruise measurements that can capture the variability in diffusive flux and ebullition. Utilizing atmospheric measurements could also be used constrain net fluxes from these areas provided that the impact of other sources is small. High spatial resolution remote sensing missions (i.e., from Planet or SWOT) will provide 3- to 15-m observations and could complement these in situ approaches. In the open ocean areas, more regular cruises sampling seawater CH_4 concentration are required. Most estimates of open ocean emissions have been derived from measurement composites made from measurements spanning over three decades (Bange et al., 2009), highlighting the sparsity of these measurements and the difficulty in assessing temporal changes.

The challenges in observing these heterogeneous systems can be overcome partly by expanding and combining in situ measurements with aircraft campaigns and leveraging existing and planned spaceborne missions. These observations cover a range of scales, from small footprints (10 m^2) to landscapes (10^3 m^2) to regions (10^4 m^2), which can be integrated within modeling activities. Combining measurement approaches across scales can address the heterogeneous nature of CH_4 fluxes measured by chambers, provide detailed and expansive views on CH_4 enhancements using aircraft, and can provide sustained measurements over time in the case of satellites. Process-based models can be used across these scales for parameter estimation, data assimilation, and model benchmarking activities. Data-driven "upscaling" approaches have also been developed where flux tower observations of CH_4 are interpolated using gridded fields of meteorology, soil type, and hydrologic conditions (Davidson et al., 2017; Peltola et al., 2019). However, key gaps in observation networks remain, and these networks must also consider wetland CH_4 emissions hot spots that might emerge in the future, such as in permafrost regions. A recent effort to develop a global database of flux tower measurements of CH_4 shows that only a handful of measurements of tropical wetland CH_4 emissions exist (Knox et al., 2019), despite this biome contributing >70% of global wetland CH_4 emissions (Saunois et al., 2016). Closing these coverage gaps and developing novel ways to extend the time series are needed to understand seasonal and interannual variability. Additionally, flux data sets from towers or chambers are critical for developing "response functions," whereby the response of wetland CH_4 emissions to changes in temperature or soil moisture can be accurately quantified (e.g., Turetsky et al., 2014). At present, it is not resolved whether the uncertainties in wetland emissions are mainly due to uncertainties in wetland area or from the parameterization of methanogenic responses and how these affect regional to global net CH_4 emission estimates.

Wetland models differ in how CH_4 is produced and consumed in the soil and eventually transported to the atmosphere either by diffusion, ebullition, or plant-mediated transport (M. B. Walter & Heimann, 2000). Methane emissions are typically modeled as the net production (sum of methanogenesis minus methanotrophy) by relating the better known processes like net primary production or aerobic soil decomposition that produces CO_2, to ratios of CO_2:CH_4 that have been measured in the field, typically by chambers or flux towers (Christensen et al., 1996). This calibration of carbon substrate to CH_4 production is sensitive to the footprint that CO_2 and CH_4 measurement techniques integrate over and the implementation in process-based models can lead to significant intermodel variability (Poulter et al., 2017). For example, soil chambers, flux towers, airborne eddy covariance, and atmospheric inversions have all been used to calibrate these relationships (Pickett-Heaps et al., 2011), but the observing techniques cover different spatial scales that can bias

or lead to mixed source signals in the flux. Redox states ultimately determine when and where methanogenesis (i.e., the gross flux) will take place (Grant et al., 2015; Reinhold et al., 2019), and future models should incorporate the details needed to reconcile these production and consumption processes individually. Future work must also consider the representation of permafrost in land surface models, which currently varies significantly in complexity (McGuire et al., 2018). This leads to a large uncertainty in the prediction of the magnitude of the CH_4-climate change feedback expected for the 21st century (Koven et al., 2011; Walter Anthony et al., 2018; Z. Zhang et al., 2017).

Several important processes may be missing from wetland models: (i) The production and transport of CH_4 by trees has recently been observed in forested systems in temperate and tropical biomes (Barba et al., 2019; Covey & Megonigal, 2019; Welch et al., 2019). In the tropics, for example, transport of CH_4 via tree stems accounts for a large part of the overall CH_4 budget (Pangala et al., 2017). As of yet, no wetland models include these newly identified production and transport pathways; (ii) Only some models simulate production and consumption in the soil column separately, while others only simulate the net flux (iii) New transport pathways are being identified, including the potential for dissolved CH_4 to be transported from sites of production in vegetated wetlands and emitted in adjacent inland waters (Borges et al., 2019). Including these pathways in models could the reduce double counting of emissions (Aufdenkampe et al., 2011).

3.2. Fossil Fuels

Methane emissions from fossil fuels stem largely from the extraction and processing stages when CH_4 is vented, leaked, or incompletely combusted (e.g., gas flaring where gas is generated as a side product from oil production). The main fossil fuel CH_4 inventories include data sets such as the Emissions Database for Global Atmospheric Research (EDGAR) (Janssens-Maenhout et al., 2019) and the U.S. Environmental Protection Agency (EPA). Greenhouse Gas Inventory (U.S. EPA, 2012), as well as individual studies (Höglund-Isaksson, 2017; Schwietzke et al., 2014a). The EDGAR inventory relies to a large extent on IPCC EFs (IPCC, 2006, 2019) paired with country-reported activity data. Tier 1 EFs represent the lowest level of detail and are used for countries where more detailed information is not available. Tier 2 and 3 EFs include information such as the specific geology (e.g., CH_4 intensity from coal mines) or technology used (e.g., gas distribution pipeline material). More country-level EFs are needed, which requires taking into account local operating practices and technologies. For example, coalbed CH_4 production, a common practice in Australia, includes the use of different gas production equipment than conventional or shale gas production elsewhere because of, for example, the relatively large production of water associated with the gas.

Höglund-Isaksson (2017) and Schwietzke et al. (2014a) focus specifically on the fossil fuel sector and include ethane (C_2H_6) emissions (discussed in section 4.5). These inventories share with EDGAR the gaps of partially relying on available EFs that are not necessarily representative of specific countries. Nevertheless, Höglund-Isaksson (2017) explicitly accounts for country-specific data on associated gas production along with empirical data on associated gas flaring. As a result, Höglund-Isaksson (2017) finds substantially smaller CH_4 trends from oil and gas production than EDGAR and U.S. EPA, while absolute emissions are substantially larger. The gridded emission inventory by Schwietzke et al. (2014a) was designed to test different global natural gas "leak rate" scenarios against atmospheric observations, and finds that country-level emissions vary significantly from EDGAR.

Three improvements in current inventories should be considered to enhance current knowledge of fossil fuel CH_4 emissions at the country and global levels. First, existing and future atmospheric measurements of CH_4 at the facility level (e.g., well pads and gathering stations) and regional level (e.g., oil and gas producing basin) could be used to verify and scale reported and calculated emissions in national inventories. One of the challenges with this approach is that current inventories are mostly assembled at the component level (e.g., a type of pneumatic device). Thus, component-level estimates (based on a combination of engineering calculations and component-level measurements) in the inventories may need to be aggregated to representative facilities for comparison with facility-level measurements. This is important because a recent synthesis of dozens of studies in the United States showed that inventories at the component-level substantially underestimate (by about 60%) total emissions (Alvarez et al., 2018). The reason for this underestimate is likely because component-level estimates fail to account for the so-called fat-tail in the empirical distributions in emissions that have been observed through facility-level (i.e., fence line) measurements. It has been

shown across the oil and gas supply chain that relatively few emitters (5% of the samples) account for about 50% of total emissions (Brandt et al., 2016). Accounting for fat-tail distributions in aggregated facility-level emission estimates requires development of the statistical representation of most current inventories to include central value estimates in addition to mean values.

Second, emissions from large-scale accidents (section 2.4) should be identified and included in emission inventories to avoid underestimating total emissions to the atmosphere. California's emissions inventory (California Air Resources Board, 2018) includes the Aliso Canyon accident as a "one-time event" in its inventory as a new "Other Emissions" category with the rationale that "its emissions will be fully mitigated in future years" (California Air Resources Board, 2017). The reported emission rates over time are based on a combination of aircraft measurements, remote sensing, and engineering calculations (California Air Resources Board, 2017). While such categorization provides a mechanism for including emissions from large-scale accidents, it must be noted that only accidents known by the respective governments (e.g., through mandatory reporting of such events) can be tracked this way.

Third, emissions trends derived in inventories are partly based on information about emission reduction projects, such as enhanced CH_4 capture or flaring in deep coal mines (Environmental Protection Agency, 2012). However, such information may not necessarily include data assessing whether the emission reduction projects and applied technologies actually lead to emission reductions, as shown in a recent study over China (Miller et al., 2019). Future remote sensing capabilities (section 2.3) along with campaign-style local measurements could be used to track emissions over time at wider scale, thereby providing independent estimates of global inventory trends.

3.3. Waste

In EDGAR v4.3.2 (Janssens-Maenhout et al., 2019), CH_4 emissions from waste are distinguished between landfills and waste water treatment. Both are derived from the fermentation of organically degradable material in the solid or liquid waste flow. EDGAR emissions are generally higher than those reported by countries to the UNFCCC, and its uncertainties are also relatively high.

The main uncertainties in landfill emissions stem from the composition of waste disposed to landfills and the rate of degradation of waste. A major problem in quantifying landfill emissions is in the proxy data used to calculate the amount of solid waste per capita. Detailed information on solid waste is not available for non-Annex I countries, and thus, EDGAR uses urban population with gross domestic product per capita as proxy. However, there is considerable scatter in the relationship between gross domestic product and solid waste per capita, causing the large uncertainty in landfill emissions.

The main uncertainty in wastewater emissions is caused by the lack of regional information in type of wastewater treatment system. A distinction is made between a sewer with or without city wastewater treatment, latrines (open pits and septic tanks), and raw discharge. In the absence of regional information, it is instead generally assumed that there is no wastewater treatment in relatively poor countries and that developed countries employ a certain distribution of different treatment types. This assumption is based on an assessment of which countries exhibit similar habits and infrastructures.

The CH_4 emissions from landfills and wastewater could be better characterized through expanded measurement campaigns. In developed countries, CH_4 measurements around waste plants (e.g., Sonderfeld et al., 2017, for a landfill in the United Kingdom or Yver Kwok et al., 2015, for a wastewater treatment plant in France) should be encouraged. More measurements are required to get representative data for a large fraction of landfills and wastewater treatment plants, which are expected to vary considerably amongst regions. It is also recommended to evaluate ratios of emitted CH_4 to other substances emitted by degrading waste, because data of substances such as air pollutants can have a longer history and better coverage.

Finally, the spatial distribution of any activity regarding waste or wastewater is allocated to the place of the facility, if this information is known. This information is only explicitly available over Europe through the European Pollutant Release Transfer Register. Beyond Europe, spatial distribution proxies with total population and urban population maps are used based on the assumption that waste treatment is present for the entire population in developed countries and only for the urban population in developing countries. More

data from representative regions are needed to validate these assumptions, particularly in tropical megacities, where landfill emissions are becoming more important than other sources of CH_4.

3.4. Agriculture

Emissions from agricultural soils use as activity data the total area harvested for rice cultivation (United Nations Food and Agriculture Organization, FAO, or ministerial statistics on arable land). Different ecology types (rainfed, irrigated, deep water, and upland) are considered and input from regional reports (e.g., International Rice Research Initiative statistics). The importance of accurate regional information is demonstrated as an example for China, where official statistics underestimate the total harvested area by 40% (Denier van der Gon, 1999, 2000). EFs from IPCC (2006) and from regional studies (Mitra et al., 2004; Gupta et al., 2002; Neue, 1997) also differ by ~30%. Therefore, more country-specific data, in particular on the type of rice cultivation, patterns of multiple harvesting and fertilizer usage are essential. Fertilizers usage is currently derived from trading statistics proxies, which are not verified for individual countries.

While maps of crop distributions have improved (through, e.g., the FAO spatial data sets, http://www.fao.org/geonetwork), large uncertainties are present in the temporal profiles, which need to accurately capture growing seasons. Global crop monitoring from space combining Sentinel 1 and 2 satellite data with revisit times of 10 days and spatial resolutions of 30 m has been a recent advance for assessing emissions from crops. Despite these advances, crop masks derived from satellites still require refinements in many countries, with in-country data to verify the spatial distribution of different crops.

Emissions from animals result from enteric fermentation and manure management. For enteric fermentation, EFs are formed by country-specific milk yield (dairy cattle), carcass weight (other cattle), or default regional values (other animals). In addition to needing better country-specific information on these parameters, the largest uncertainties are due to the parameters that are not typically considered in models, such as antibiotic use and feed of the animals. Emissions from manure management are also highly uncertain in the parameters related to animal weight and feed, as well as treatment (i.e., end-use of the manure), which can differ strongly by country and vary significantly over time. Due to insufficient data, it is assumed that there is no change in time in these parameters, and this likely leads to the EDGAR emission time series not reflecting the real emissions trend. For all animal emissions processes, better country- and technology-specific data are required, contrasting both developed and developing countries, where there can be a significant difference in the weight of the animal and methods of farming (such as animal feeding).

CH_4 emissions from aquaculture is now estimated to be a large global source with emissions having steadily increased over the last decade (FAO, 2018; Yuan et al., 2019). Aquaculture production is dominated by China's fish and crab ponds. Yuan et al. (2019) found a tripling of the CH_4 emissions per hectare per year when operating a fishpond instead of a rice paddy field. This finding contradicts Liu et al. (2016), which calculated EFs from aquaculture to be half as large as those from rice paddy fields. Future work needs to reconcile the contradictory estimates from this source and to have aquaculture emissions better incorporated into global inventories such as EDGAR.

3.5. Biomass Burning

Large-scale biomass burning CH_4 emissions are derived from satellites, either based on burned area and fuel load modeling or through satellite detection of active fires and fire radiative power, which are empirically converted to carbon or dry matter emissions (Kaiser et al., 2012; van der Werf et al., 2017). Those fire emissions are then multiplied with an EF that governs what fraction of the carbon or dry matter combusted is emitted as CH_4 (Akagi et al., 2011; Andreae, 2019).

Burned area has been routinely measured from National Aeronautics and Space Administration (NASA; e.g., Terra and Aqua Moderate Resolution Imaging Spectroradiometer, MODIS) satellites with almost 20 yr of high-quality coarse (500 m) resolution. Even though the coarse resolution burned area algorithms perform well over large fires, events that burn only a fraction of the satellite pixel are more difficult to detect. These are typically fires associated with agricultural burning or deforestation and estimates suggest they could increase the global amount of burned area by about 30% or more (T. Liu et al., 2019; Randerson et al., 2012; Roteta et al., 2019). European Space Agency Sentinel and NASA Landsat satellites are paving the way for moderate resolution (20–30 m) burned area detection (L. Boschetti et al., 2015; Giglio et al.,

2018; Padilla et al., 2015; Roteta et al., 2019). There is a need to integrate findings from these new medium-resolution satellite data into existing coarse resolution approaches. Some of the most frequently used coarse resolution satellite sensors (e.g., MODIS) are coming to their lifetime end and a better understanding of the complementarity of coarse and moderate approaches is necessary to maintain a consistent time series over the record.

Geostationary satellites have been used as well, mostly to monitor spatiotemporal variability in fire activity (Roberts & Wooster, 2008). Although they suffer from having a coarse spatial resolution, their superior temporal information should be used to complement existing (such as MODIS) and new (such as Sentinel-2) polar-orbiting satellite information to better understand diurnal variability in addition to the earlier mentioned role of small fires. The current suite of geostationary satellites is reasonably well positioned to monitor global fire activity (except in high latitudes). The newest generation geostationary satellites include the National Oceanic and Atmospheric Agency (NOAA) GOES-16 satellite, the Japan Meteorological Agency's Himawari-8 and Himawari-9 satellites, and the European Space Agency's Meteosat Second Generation satellite series. However, because these satellites carry different instruments and because pixel size increases with view angle, harmonization is required for a consistent data set (e.g., Hall et al., 2019).

Converting burned area to fuel consumption (amount of biomass combusted per unit area burned) relies mostly on biogeochemical modeling or the combination of field measurements extrapolated in space and time using satellite data (van der Werf et al., 2017; Veraverbeke et al., 2015; Wiedinmyer et al., 2011). However, key limitations remain. First, satellite-based Lidar systems have enabled a better quantification of standing biomass loadings and thus fuel availability and consumption, but fires in general consume mostly litter and soil carbon. While the two are related, there are no satellite-based observations of litter and soil carbon, and its variability is therefore not well studied. In general, most information on fuel consumption is derived from field studies and several regional programs are underway (e.g., NASA's Arctic—Boreal Vulnerability Experiment, the Fire Influence on Regional and Global Environments Experiment and the Western Wildfire Experiment for Cloud Chemistry, Aerosol Absorption and Nitrogen) to increase the number of measurements. Second, EFs are also mostly derived from field measurements, which include aircraft data collected from smoke plumes and on larger scales from the ratios of trace gases measured by satellites. The current body of EF measurements currently enables only a biome-level breakdown, leaving spatial and temporal variability of EFs within biomes unknown (Akagi et al., 2011; van Leeuwen et al., 2013). Tropical peat fire EFs were derived from lab studies until the first in situ measurements in 2015 indicated that the EF was actually only half of the lab-based value (Stockwell et al., 2016; Wooster et al., 2018), lowering total global biomass burning CH_4 emissions (van der Werf et al., 2017) by almost 10%. An important next step is that field experiments need to be expanded to (sub)tropical regions where fire emissions are an order of magnitude larger than those of temperate and boreal regions. The outcomes of such field experiments then need to be integrated into fire models.

3.6. Geologic Seeps

Geologic seepage is thought to be the third largest natural source of CH_4 after wetlands and freshwater systems (Etiope et al., 2019; Saunois et al., 2016). The degassing of CH_4 occurs through five main categories: gas-oil seeps, mud volcanoes, microseepage, submarine seepage, and geothermal and volcanic manifestations. Emissions from geologic seepage are difficult to distinguish from anthropogenic fossil fuel production and use due to their similar isotopic signature and colocated source origin (Petrenko et al., 2017; Schwietzke et al., 2016).

Estimates of global seepage CH_4 emissions exhibit up to a factor of 5 difference based on methodology. Estimates of 30–76 Tg/yr (Etiope et al., 2019; Saunois et al., 2016) are based on process-based modeling, statistical evaluations of experimentally determined EFs and activity data. These estimates are consistent with top-down evaluations using δ^{13}C-CH_4 and C_2H_6 (Dalsøren et al., 2018; Nicewonger et al., 2016; Schwietzke et al., 2016). In contrast, Petrenko et al. (2017) proposed a substantially lower global estimate, ranging from 0–15.4 Tg/yr based on $\Delta^{14}CH_4$ of the air trapped in Antarctic ice cores 11,000–12,000 yr ago.

Future research could help to reconcile these estimates and improve current global seepage estimates in two ways. First, mud volcanoes can be considered point sources with spatial dimensions comparable to oil and gas production/processing facilities. Their emission estimates could be empirically verified using the types of

offsite downwind measurement methodologies employed during oil and gas field campaigns over the last decade in the United States and internationally (e.g., Conley et al., 2017). Focusing on some of the largest emitters worldwide, for example, in onshore areas around the Caspian Sea could be used to validate the estimation methods used in global models (Etiope et al., 2019). Second, microseepage, the diffuse exhalation of CH_4 from the ground, not related to gas-oil seeps or mud volcanoes, is considered to be the largest geological CH_4 source globally (Etiope & Klusman, 2010). Microseepage EFs are well known, based on more than 1,500 flux measurements in 19 different petroleum provinces (Etiope et al., 2019). The largest uncertainty in microseepage global emission is in the global area where microseepage occurs (dominantly in petroleum fields, e.g., Schumacher, 1996). Positive CH_4 fluxes to the atmosphere related to microseepage are believed to occur in 57% of the global continental petroleum field area, resulting in a total potential microseepage area of about 13 million km^2 (Etiope et al., 2019). Such data need, however, to be better constrained. Microseepage can be effectively detected over wide areas using optical remote sensing techniques such as aerial photography, airborne and satellite multispectral scanner data (e.g., van der Meer et al., 2002). Such investigations, performed on different petroleum systems and sedimentary basins, can significantly improve our understanding of microseepage areal distribution.

3.7. Uptake of CH_4 by Soil

Soil methanotrophy by upland ecosystems is the only known biological sink for CH_4 and is thought to remove a similar amount as the global emissions from rice cultivation (e.g., Curry, 2007; Murguia-Flores et al., 2018; Saunois et al., 2016; Zhuang et al., 2013). Rates of upland soil methanotrophy are controlled by the concentration of CH_4 in the atmosphere and by soil temperature, soil moisture, and soil nitrogen content. Globally, the upland soil sink is expected to become stronger in the 21st century as atmospheric CH_4 mole fractions rise and soil temperatures increase, and this could partially offset any increased emissions, although nitrogen deposition can inhibit methanotrophy (Zhuang et al., 2013). Therefore, better understanding of this removal process is required when simulating future CH_4 concentration pathways.

There are large uncertainties in the spatial and temporal distribution of the upland soil CH_4 sink due to the sparsity of field measurements. There are four areas that require further measurements: (i) Measurements spanning different seasons and ecosystems of the rate of uptake are required, particularly in the Southern Hemisphere where only very few measurements currently exist (Dutaur & Verchot, 2007). The sparsity of these measurements makes it challenging to validate process-based models of soil methanotrophy. (ii) Better representation of different ecosystems in measurement of the microbial oxidation rate (Luo et al., 2013). There is considerable variability between ecosystems in this fundamental parameter that controls how much CH_4 in the soil is able to be consumed by microbes. (iii) Better ecosystem coverage of the temperature response of methanotrophy (e.g., Castro et al., 1995; del Grosso et al., 2000). (iv) Measurements to better establish the relationship between soil nitrogen content and the inhibition of soil methanotrophy (e.g., Nesbit & Breitenbeck, 1992), so that the inhibitory effect can be better accounted for in future simulations.

4. Top-Down Source and Sink Estimation at Global and Regional Scales

Atmospheric observations can be used to quantify CH_4 sources and sinks at global and regional scales, when combined with atmospheric chemical transport model (CTM) simulations, statistical "inverse" estimation methods and a priori information from inventories (section 3). Whist these methods have been used extensively in the recent literature, the results of studies by different groups can differ substantially, even when similar data sets are used (e.g., emissions for India reported by Ganesan et al. (2017) and Miller et al. (2019), which both rely primarily on GOSAT data, vary by ~70%). These differences imply that significant challenges remain in both the atmospheric model simulations and statistical frameworks used to estimate emissions. Sections 4.1 and 4.2 discuss global and regional emissions estimation and sections 4.3 and 4.4 review the CTMs and inverse methods used in these approaches. Finally, the estimation of sector-level emissions in either global or regional studies is discussed in section 4.5.

4.1. Global Estimation

Recent investigations of the CH_4 budget using global models span a range of complexity, both in the atmospheric model used, the number and type of parameters being estimated, and the statistical methods used for parameter estimation and uncertainty quantification. Models require as input a set of surface flux

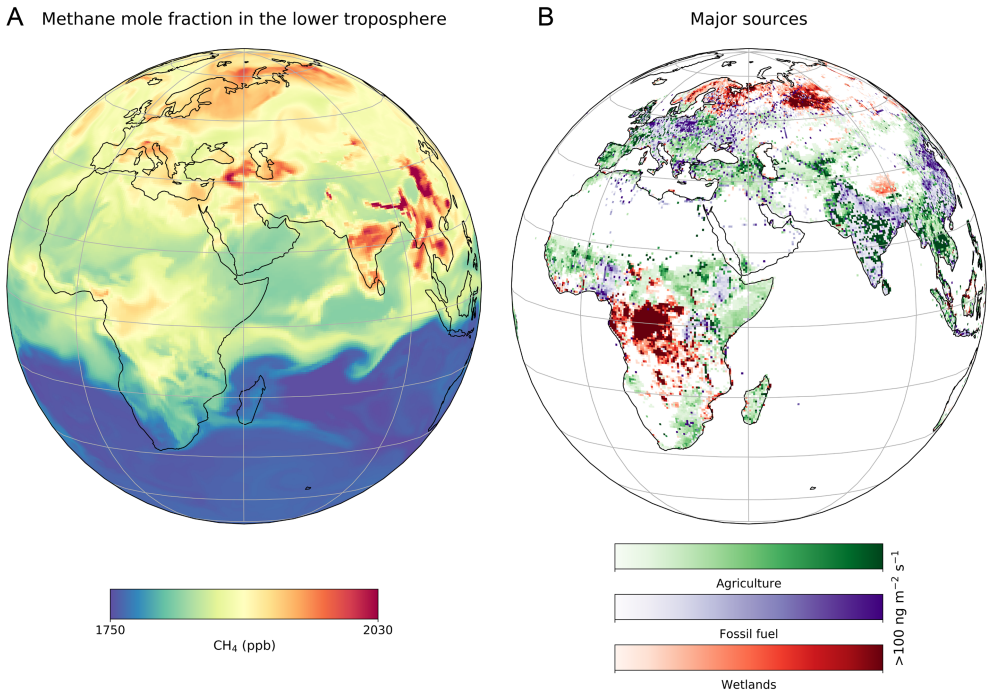


Figure 6. (a) Three-dimensional simulation of surface CH_4 mole fractions by the MOZART model (Rigby et al., 2012) driven by estimates of CH_4 emissions and removal by sinks. (b) Wetland (Bloom et al., 2017), agriculture, and fossil fuel emissions (Janssens-Maenhout et al., 2019), with the dominant source shown in each grid cell. An animation of CH_4 mole fractions is provided in the supporting information.

estimates that resolve sources and sinks at the model grid scale and, ideally, at the model integration time step. Estimation of the two-dimensional (2-D) or three-dimensional (3-D) atmospheric mole fraction field requires parameterization of atmospheric advection, turbulent transport processes (e.g., boundary layer turbulence and convection), CH_4 losses via reaction with OH, and losses in the stratosphere. Sources and sinks of CH_4 are then estimated by comparison of the model mole fraction fields with global measurement data sets (such as those discussed in section 2) through the use of a statistical inverse modeling framework.

4.1.1. Global Atmospheric Chemical Transport Modeling

The simplest global models are one-dimensional or 2-D, where the atmosphere is separated into some number of vertical and/or zonal mean boxes (Cunnold et al., 2002; Rigby et al., 2008; Turner et al., 2017). These models can only be used to estimate global or zonal average sources and sinks and can suffer from biases due to the lack of resolved 3-D meteorology (Naus et al., 2019). However, because of their computational efficiency, box models can be run for a very large range of input parameter values. Therefore, the benefit brought about by the use of box models lies in the ability to explore a wide range of important but uncertain parameters in the global CH_4 budget, such as [OH], or isotopic source signatures (e.g., Rigby et al., 2017; Turner et al., 2017

Global models in 3-D additionally separate the atmosphere into longitudinally resolved boxes and simulate atmospheric transport either off-line, using archived meteorological analyses (e.g., Fung et al., 1991; Hein et al., 1997; Patra et al., 2011; Figure 6), or online, at the same time as the atmospheric physical state is being estimated, based on the assimilation of meteorological observations (e.g., Patra et al., 2016). Compared to box models, 3-D models allow surface fluxes to be resolved at a range of scales; some studies have estimated emissions at continental scales (e.g., Bruhwiler et al., 2014; Chen & Prinn, 2006; Mikaloff Fletcher et al., 2004b; Miller et al., 2019), while others have estimated grid-scale fluxes, albeit by typically assuming spatial correlations between grid cells to make the problem less underdetermined (e.g., Bergamaschi et al., 2013; Bousquet et al., 2011; Houweling et al., 1999). Many studies attempt to estimate emissions from multiple sectors, making use of the differing spatial or temporal distribution of individual sources (e.g., Chen and Prinn (2006), section 3) or by using $\delta^{13}C\text{-}CH_4$ or other tracer observations (e.g., Helmig et al., 2016; McNorton et al., 2018; Mikaloff Fletcher et al., 2004a, 2004b), section 4.5).

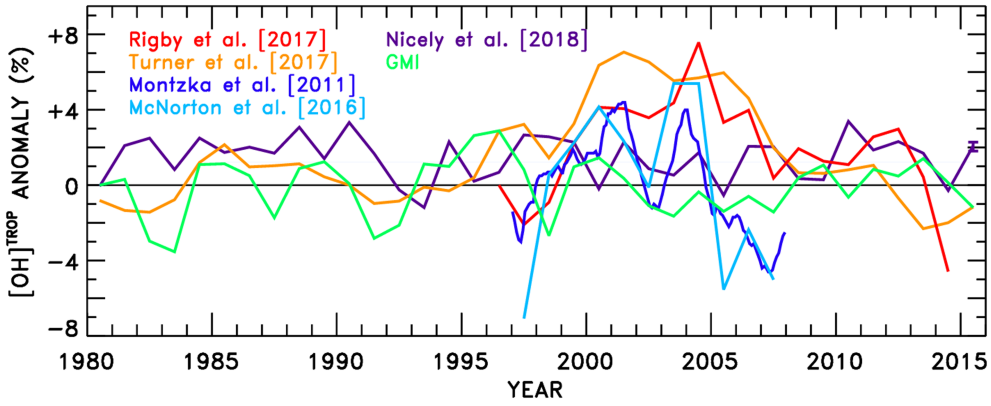


Figure 7. Anomalies of [OH] in the troposphere estimated using different approaches, including methyl chloroform based estimates and photochemical models. Anomalies are presented to indicate the magnitude of interannual variability in [OH]. (Source: Julie Nicely, Nicely et al., 2018).

To make effective use of the rapidly growing global monitoring system, 3-D models will be required, rather than box models. However, it must be noted that, even when driven by common emissions and loss fields, global 3-D CTMs are known to vary in their simulations of atmospheric CH_4 mole fractions and CH_4 loss rates (e.g., Palmer et al., 2018; Patra et al., 2011). Differences in CH_4 simulations are caused by differences in key transport phenomena, such as interhemispheric and stratosphere-troposphere exchange rates, which are themselves likely to be driven by factors such as model resolution and parameterizations of unresolved features such as convection or turbulence. Furthermore, global models, which are usually run at resolutions on the order of 1° longitude and latitude or more, can suffer from severe "representation" or "mismatch" errors, caused by the need to represent point measurements in a coarsely gridded model atmosphere (e.g., Chen & Prinn, 2006). Therefore, these models require improvements in their resolution and physical parameterizations, and new methods are needed for the robust evaluation of model performance (section 4.3). Finally, in order to fully estimate uncertainties, it is important that future 3-D model estimation frameworks include systematic and nonlinear uncertainties that, so far, only box model studies have been able to rigorously explore (section 4.4).

4.1.2. Global Hydroxyl Radical Concentration Estimation

Because it is the largest single term in the global atmospheric CH_4 budget, perhaps the most important challenge for modeling CH_4 at the global scale is the quantification of the OH sink. Estimates of [OH] made using different approaches vary significantly in both absolute [OH] as well as the size of year-to-year variations (Figure 7). While observations of methyl chloroform (CH_3CCl_3, MCF) trends have been widely used for this purpose, it is known that uncertainties in its emissions can lead to uncertainties in the derived [OH], similar to, or larger than, the inferred [OH] variability (Rigby et al., 2017; Turner et al., 2017). In the coming years, estimation of [OH] using MCF will become more uncertain as its atmospheric mole fraction declines (Prinn et al., 2018). While some recent MCF, budget-based studies have suggested that [OH] changes could be a major contributor to recent methane growth rate variability, albeit with very large uncertainty (Rigby et al., 2017; Turner et al., 2017), atmospheric photochemical models do not tend to find evidence for strong variability in global [OH] (e.g., Figure 7, Nicely et al., 2018). However, photochemical models disagree substantially in their predictions of the average global [OH] (Voulgarakis et al., 2013). Given these considerations, a primary challenge is to find new, more accurate, methods for inferring global [OH]. There are several areas of research that may lead to stronger constraints, which include developments in atmospheric photochemical model predictions, improved "budget" methods, in which [OH] is inferred using observations of some reduced gases along with estimates of their emissions, and "proxy" methods that use observations of gases whose production is linked to [OH]. Whichever methods advance our understanding of [OH] magnitude and variability, uncertainties will remain, and it is vital for the uncertainties due to [OH] to be included in inverse modeling systems (section 4.4).

Improvements in atmospheric photochemical models will require developments in model parameterizations (e.g., incorporation of new reactions or kinetics into chemical mechanisms), atmospheric physical state

estimates, and emissions inventories (i.e., for reactive gases which participate in the formation of OH). Recent studies have quantified sensitivities of global model [OH] to various inputs and parameterizations, which may help modelers better understand how global [OH] simulations could be improved in future (López-Comí et al., 2016; Nicely et al., 2017; Ryan et al., 2018). Alternatively, more comprehensive observations of key tropospheric gases (e.g., O_3 and H_2O) may allow estimation of [OH] variability using relatively simplified chemical schemes (e.g., Nicely et al., 2018).

In terms of indirect inference of [OH] by estimation of the loss rate of trace gases, new approaches are needed that can provide a stronger constraint than is currently possible from the widely used MCF method. (i) It has been proposed that observations of multiple reduced gases with atmospheric lifetimes of a few years (e.g., some HCFCs or HFCs) may improve such estimates, particularly if emissions can be inferred simultaneously with losses, by considering factors such as the observed interhemispheric gradient (e.g., Huang & Prinn, 2002; Liang et al., 2017). Ideally, a compound, or compounds, would be found where all global emissions could conceivably be monitored, for example, in the case of a gas that is only manufactured by a small number of producers that would be willing to make their atmospheric emissions known. However, such a "tracer of opportunity" has not yet been identified. (ii) [OH] can be inferred using observations of ^{14}CO, which is produced in the upper atmosphere and has a lifetime with respect to OH of 2–3 months (Manning et al., 2005). Stronger constraints on [OH] from ^{14}CO observations would likely require a more extensive global monitoring network, as ^{14}CO is strongly influenced by regional [OH], and the current network is more sensitive to high latitudes than the tropics, where the majority of OH is produced (Krol et al., 2008). Furthermore, model representations of stratosphere-troposphere exchange will require improvement, to ensure accurate transport from the upper atmosphere, where ^{14}CO is produced, to surface observation sites. (iii) CH_4 data themselves can potentially be used to infer [OH] in addition to other terms in the global CH_4 budget, provided that there is high enough spatial density and global coverage in the measurements (Maasakkers et al., 2019; Y. Zhang et al., 2018). Such an approach relies on the fact that, compared to observations of lower abundance compounds such as MCF, dense observations of CH_4 are possible from space. (iv) Potentially, the most accurate budget-based approach would involve the intentional release and global observation of a tracer compound that reacts primarily with OH. Such an approach has been proposed at urban or regional scales (Davenport & Singh, 1987; Prinn, 1985; White et al., 2014) but whether such a method could be feasibly scaled to monitor global [OH] over multiyear timescales is not clear. Such an experiment would likely involve very large costs (which would need to be compared to other costly activities such as satellite missions), international cooperation, partnerships with industry (who would need to manufacture large quantities of tracer), and technological advances to develop sensitive detectors.

To complement such budget-based approaches, complementary [OH] "proxy" estimates may also be possible. It has recently been proposed that, due to the close relationship between formaldehyde (HCHO) production and [OH] in the remote atmosphere (i.e., above the ocean), remotely sensed HCHO fields could provide a method by which to map [OH] (Wolfe et al., 2019). Further validation and additional satellite data sets may be required to extend this method to the estimation of long-term [OH] trends.

4.2. Regional Estimation

Inversions to estimate emissions for individual regions are distinct from global inversions in several important aspects. First, boundary conditions are required, unlike their global counterparts, because air resides in regional domains for at most a few weeks. Therefore, CH_4 loss due to OH typically can be neglected and uncertainties in the sinks are not limitations in regional inversions. In addition, on the timescales of the simulations, uncertainties in the ability to model complex stratospheric-tropospheric exchange processes are mitigated. The limited geographical extent of regional models, and therefore the reduced computational cost, allows for emissions to be estimated at much finer scales (order tens to hundreds of kilometers) compared to global inversions (order thousands of kilometers), provided the density of measurements exist (Figure 3).

The potential success of an inverse modeling approach for national estimation of CH_4 emissions is fundamentally linked to several key factors: the density and frequency of CH_4 mole fraction and isotopic ratio measurements, access to high-resolution (kilometer-scale) three-dimensional meteorological data, the ability to model atmospheric dispersion, information on the spatial and temporal variability in emission sources,

understanding the topography in the areas surrounding measurement stations, and the ability to differentiate between natural and anthropogenic emissions within a country. The latter point is important for policy since countries account for their anthropogenic emissions and national-scale inverse modeling estimates are most useful if they can provide an independent constraint on the anthropogenic contribution. The importance of each of these factors varies from country to country but each needs to be considered when assessing the national emission estimates from inverse modeling.

An observation is most sensitive to its surrounding emissions and its sensitivity decreases rapidly as the distances increase. A network of tall (~100 m) tower observations at subdaily resolution spaced every ~300 km is potentially sufficient to define an annual national CH_4 emission total, although the network must be designed with the consideration of prevailing meteorology. Critically, these measurements must not be influenced by local emissions that lie within a few model grid boxes from the site, as these processes will not be able to be resolved by the model.

The comparison of reported national CH_4 emission estimates with those from inverse modeling in some cases show some marked differences and can be used to identify sources of discrepancy. Reported U.K. CH_4 emissions in the early 1990s are a factor of 2 higher than those estimated through inverse modeling for reasons that are not well understood (Brown et al., 2019). Top-down estimates in the United States and EU are larger than reported (Bergamaschi et al., 2018; Turner et al., 2015), whereas top-down emissions in China are lower than inventories (Miller et al., 2019; Thompson et al., 2015), highlighting that differences are region specific and must be evaluated for each country.

Provided that there is adequate measurement and modeling capability in place, the main limitation in the top-down regional estimation approach is in the sizable systematic uncertainties in the modeling systems. The range of choices for the meteorological drivers, the atmospheric transport model, and the inversion methodology have been shown to result in estimates for national-scale emissions that differ significantly using similar measurement data sets (Bergamaschi et al., 2018; Ganesan et al., 2017; Miller et al., 2019). Therefore, to make top-down estimates more useful for policy makers, the challenge is to understand why these differences occur (sections 4.3 and 4.4) and ultimately to improve the accuracy of emissions estimation.

4.3. Atmospheric CTM Improvements

The disagreements between model predictions of atmospheric CH_4 mole fractions that result from errors in CTM transport are systematic uncertainties that would result in inaccurate (biased) inference of emissions in inverse modeling studies at both global and regional scales. Some improvements in atmospheric model transport may occur naturally as the meteorological observing and forecasting system evolves. Increased model resolution, brought about by developments in high-performance computing, may yield improved CH_4 simulations, for example, by reducing model-measurement representation errors or allowing atmospheric transport processes which were previously parameterized to be resolved. However, it is likely that model parameterizations themselves need to be modified and tested (e.g., Krol et al., 2018).

By whatever means advances in model physics occur (which is beyond the scope of this paper), it is critical that methods exist to test CTM transport. Model intercomparisons (e.g., Krol et al., 2018; Patra et al., 2011) and model parameter sensitivity studies using, for example, Gaussian process emulation (e.g., Harvey et al., 2018) are likely to help target where developments are needed. However, they do not indicate whether model transport is accurate. Tests of model transport require knowledge of the exact magnitude and time of release of some gas, which is measured with sufficient spatial density and over appropriate timescales to test relevant model transport processes. There have thus far been very few long-range intentional release tracer experiments (e.g., Ryall & Maryon, 1998) that have attempted to quantify the accuracy of CTMs. In future, additional intentional release experiments will be needed, particularly when attempting to estimate emissions that are important for policy. Measurements of radon (^{222}Rn) may provide constraints on model transport, based on knowledge of its emissions from the Earth's crust (Jacob & Prather, 1990). However, recent studies have highlighted the need for further information on the influence of factors such as soil moisture on its emissions (Karstens et al., 2015). Alternatively, it may be possible to identify a "tracer of opportunity," where some industrially produced inert gas is known to be released from some well-defined locations, by producers or users who are willing to share high-quality release rate estimates. In either case, the well characterized surface emission would have to be sufficiently large to be observable at scales of 500–1,000 km for

evaluation of regional dispersion processes and potentially between hemispheres for global model evaluation. Background concentrations would need to be well known, and in the case of an intentional release, the impact on climate, ozone depletion, and human health would need to be small. If such an experiment existed, individual CTMs and their associated underpinning meteorology could be assessed and characterized and ultimately improved.

Improvements in regional and global CH_4 simulations will also occur as a result of developments to each of the bottom-up data sets discussed in section 3 because they are used as inputs to atmospheric models. It is important that these data sets are spatially resolved, ideally at a resolution greater than or equal to the atmospheric model. Equally importantly, they should also be resolved by time at the highest resolution possible. Many top-down estimates currently assume that emissions are constant over weekly to monthly periods. Higher-frequency variability in emissions, unless well represented in bottom-up models, can lead to significant, unaccounted-for, error in top-down estimates. Therefore, in addition to the totals currently reported by individual nations to the UNFCCC, emission inventories broken down by sector, on regular grids, and time-resolved should be considered best practice by all countries.

4.4. Inverse Methods and Uncertainty Quantification

The inference of CH_4 sources and/or sinks using measurements of atmospheric mole fractions and coemitted species requires a statistical inverse modeling framework. These frameworks account for the varying "sensitivity" of each measurement to parameters of interest (e.g., emissions) and attempt to quantify the influence of measurement and model uncertainties on the derived quantities. Given the underdetermined nature of the inversion problem for CH_4, a Bayesian approach is usually followed, in which a priori estimates of sources or sinks (e.g., inventories described in section 3) are adjusted to improve the agreement between the data and models. To better understand the top-down CH_4 budget, there are a number of areas where improvements are needed: quantification of uncertainties, including systematic and nonlinear effects, and algorithms that can utilize high-dimensional data to estimate high-dimensional outputs.

Traditional Bayesian methods require an estimate of probability density functions (PDFs), which describe the uncertainty in the a priori constraints and the expected level of agreement between the data and the model. Very often, because of their helpful mathematical properties, these PDFs are assumed to follow specified Gaussian distributions. However, there are known to be two major problems with this approach. First, the a priori uncertainty and model-measurement uncertainty are often very poorly quantified, making robust a posteriori uncertainty quantification challenging. Second, Gaussian PDFs can lead to unphysical solutions (e.g., negative emissions). To address these limitations, recent developments have used Markov chain Monte Carlo approaches (e.g., Ganesan et al., 2014; Jeong et al., 2016; Miller et al., 2014; Rigby et al., 2011). These methods allow PDFs of any form to be used to constrain the inversion (e.g., the lognormal distribution, which is not defined below 0) and, when applied in hierarchical Bayesian frameworks, can allow the magnitude of uncertainties to be themselves uncertain. The limitation of Markov chain Monte Carlo methods is that, because they require the a posteriori PDF to be approximated through sampling, they become computationally expensive, and sometimes prohibitively so, when applied to high-dimensional problems and when estimating spatiotemporal uncertainties.

The above developments in inverse methods have focused primarily on the treatment of random uncertainties. However, it is possible that systematic effects, such as model parametric errors, dominate top-down CH_4 uncertainty budgets. These effects may be particularly important where uncertain parameters are nonlinearly related to atmospheric observations (e.g., uncertainty in isotopic source signatures, or [OH]). Recent studies have investigated such uncertainties in simple box models (Naus et al., 2019; Rigby et al., 2017). However, methods are needed that can account for systematic, nonlinear uncertainties in inversions using more complex and computationally expensive 3-D global and regional models with high-dimensional outputs.

As data density has increased, there has been a push toward inverse methods that can efficiently use high-dimensional data to estimate high-dimensional parameter spaces. The most common in use are adjoined CTMs, in which the sensitivity of the model outputs to various inputs is simulated directly by code that complements the forward model (e.g., Houweling et al., 1999) or ensemble methods that approximate these sensitivities (e.g., Peters et al. (2005). As remote sensing further increases the amount of data available for

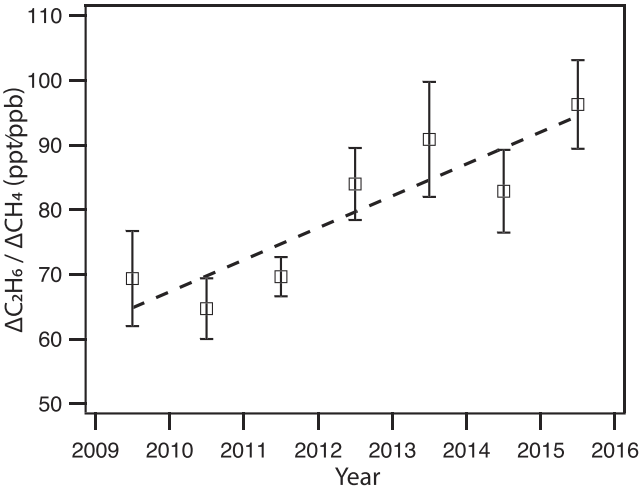


Figure 8. Ratios of mole fraction enhancement (defined as the deviation from background) in C_2H_6 to CH_4 derived from surface flask measurements at Southern Great Plains, Oklahoma (SGP-s). These enhancement ratios are equivalent to oil and gas emission ratios when the enhancements are largely due to emissions from oil and gas sources, as is the case at SGP-s. (Source: Lan et al., 2019).

top-down source and sink estimation at finer spatial and temporal scales (section 2.3), such methods are likely to become increasingly important. However, at present, these frameworks rely heavily on Gaussian assumptions, are sensitive to poorly quantified uncertainties, often neglect spatiotemporal correlations in uncertainties, and do not routinely incorporate systematic uncertainties. Therefore, a major challenge for the coming years will be to develop high-dimensional inverse modeling systems, which allow for robust uncertainty quantification, as described in the previous paragraphs.

A further area for development that may yield new insights for CH_4 is the direct estimation of process model parameters using atmospheric data (e.g., as described by Houweling et al., 2017). Such an approach combines flux and atmospheric models into the same estimation framework, so that flux model parameters can be constrained using the data. Such an approach has been explored for CO_2 (Koffi et al., 2013; Peylin et al., 2016) but not yet for CH_4. The potential advantage of such a system is that, in principle, process-level understanding can be gained, without the need to propagate information via the estimation of a high-dimensional flux field. However, the technical challenge in coupling together different models, and ingesting disparate data types (e.g., mole fraction and flux measurements) is substantial.

4.5. Sector Estimation Using Tracers

Because CH_4 mole fraction measurements are not source specific, top-down emissions estimation at all scales (global, national, and urban) often rely on bottom-up inventory trends and spatial patterns for source sector attribution (Bruhwiler et al., 2014; Houweling et al., 2017; Schwietzke et al., 2016, section 3). In order for sectoral estimation to not rely on bottom-up spatial separation, inversions would require additional information, often in the form of source specific tracers or CH_4 isotopic ratios.

Global $\delta^{13}C$-CH_4 measurements have been interpreted as part of many studies of global CH_4 (Bousquet et al., 2006; McNorton et al., 2018; Nisbet et al., 2016, 2019; Rice et al., 2016; Rigby et al., 2017; Schaefer et al., 2016; Schwietzke et al., 2016; Turner et al., 2017; Worden et al., 2017). It has been shown that incorporation of $\delta^{13}C$-CH_4 and/or δD-CH_4 measurements into regional and global inverse modeling frameworks provides some additional sector-level constraint, compared to mole-fraction-only inversions (Rigby et al., 2012). However, interpretation in these studies is complicated by the fact that source signatures are highly uncertain or variable (Schwietzke et al., 2016; Sherwood et al., 2017). Ganesan et al. (2018) shows that incomplete accounting of variations in source signatures, such as spatial variability, results in significant biases when used to interpret atmospheric measurements (source signature characterization is discussed in section 2.2). Furthermore, it must be noted that the well-mixed isotopic signal is also slow to reach steady state compared to the relatively rapid change in CH_4 mole fraction for a given change in any sources or sinks. Tans (1997) shows that it takes the order of a century for $\delta^{13}C$-CH_4 to equilibrate fully in the atmosphere. Thus, use of $\delta^{13}C$-CH_4 to diagnose flux changes on the global scale requires longer time series analysis and appropriate spin-up in global atmospheric modeling studies.

Source tracers have been used to estimate a variety of CH_4 sectors by assuming that the ratio between emitted CH_4 and the tracer is well characterized. To illustrate the challenges with this method, the example of the fossil fuel sector through measurement of atmospheric C_2H_6, is discussed. The main limitations are that (i) the emitted C_2H_6:CH_4 ratio is highly variable (up to order of magnitude) from well to well (oil/gas), mine to mine (coal), and to some extent across country-level averages (Sherwood et al., 2017). More data are needed at this scale, particularly for the Middle East, Europe, and Africa (Sherwood et al., 2017). (ii) The C_2H_6:CH_4 ratio of produced gas can vary substantially over time scales of years and perhaps decades as shown in Lan et al. (2019) and Figure 8. C_2H_6:CH_4 source ratios from oil/gas production are largely a function of the "wetness" of the produced gas (i.e., the ratio of coproduced oil and gas) (Dalsøren et al., 2018; Helmig et al., 2016; Höglund-Isaksson, 2017; Kort et al., 2016; Schwietzke et al., 2014a). Considering that gas production roughly doubled over the past three decades while oil production increased by only

half that rate (U.S. Energy Information Administration, 2016), the C_2H_6:CH_4 source ratios of combined oil/gas should not be expected to remain the same. (iii) The C_2H_6:CH_4 ratio downstream of oil/gas production and processing (i.e., pipeline transmission, local distribution, and end-use) can vary over time due to changing market demands of hydrocarbons (Schwietzke et al., 2014b). Long-term observations of aircraft vertical profiles downwind of U.S. oil and gas production regions have recently confirmed this trend (Lan et al., 2019). Monitoring these trends is important, for example, through local measurements or by making international data on C_2H_6 production publicly available.

Lan et al. (2019) show that incorrect U.S. oil and gas emission trends can be derived if the variability in C_2H_6:CH_4 ratios are not accounted for. Global CH_4 emission trends (e.g., Helmig et al., 2016) also acknowledge the discrepancy in estimated CH_4 trend magnitude and timing when using C_2H_6:CH_4 ratios, CH_4 inversions and/or isotope data. The three factors discussed above indicate that more widespread long-term and region-specific C_2H_6:CH_4 source ratio measurements would be required.

Despite the difficulties in reconciling estimates using different methods, the United States is comparatively well monitored for both CH_4, CH_4 isotopic ratios, C_2H_6:CH_4 source ratios and atmospheric C_2H_6 data. Other regions of the world with growing contributions from fossil fuel (e.g., Asia and Africa) will require a step change in the number of measurements made to make use of this type of methodology.

5. Urban Emissions Quantification

The most important anthropogenic CH_4 sources at urban scale are typically the natural gas distribution infrastructure and the waste sector (e.g., Nangini et al. (2019). Beyond the policy and scientific interest, natural gas is also considered a safety issue as previous leakages have caused fatal explosions and displaced thousands of residents (Conley et al., 2016).

The bottom-up methodologies used to quantify urban CH_4 emissions are not all consistent and can thus not always be easily compared across cities. Furthermore, studies that compared reported emissions for urbanized regions with estimates from local and scientific inventories (e.g., EDGAR) sometimes find significant inconsistencies for CH_4 (e.g., Chandra et al., 2019; Lowry et al., 2001; Ren et al., 2018; Vogel et al., 2012; Wunch et al., 2009). Cities with routine reporting are usually situated in Organisation for Economic Co-operation and Development countries and limited data are available from, for example, African, South American, and Asian (with the exception of Chinese) cities. As infrastructure can strongly differ regionally, this limits the ability to assess urban CH_4 globally using bottom-up techniques. Important efforts are underway to harmonize bottom-up techniques and standards for urban areas by establishing tools such as the Greenhouse Gas Protocol (https://ghgprotocol.org) and implementing common reporting platforms like the UNFCCC's NAZCA (https://climateaction.unfccc.int/). Adopting UNFCCC methodologies into reporting standards will be crucial to also increase consistency with national bottom-up efforts.

Because uncertainties in inventory approaches are larger on smaller scales (due to the complexities of spatially and temporally disaggregating emissions), the urban scale is of particular interest for top-down studies (e.g., within the WMO Integrated Global Greenhouse Gas Information System; IG^{3}IS, https://ig3is.wmo.int/en). Top-down studies on urban CH_4 emissions also show a bias toward cities in Organisation for Economic Co-operation and Development countries rather than developing countries. Many of these studies rely on small monitoring networks of one to six measurement stations, which can quantify the overall emissions of a city or metropolitan area but does not allow emissions to be resolved at the neighborhood scale. The larger local enhancements at urban scales (over regional and global scales) in atmospheric CH_4 mole fraction might allow use of lower-cost medium precision sensors as long as they can be shown not to introduce systematic biases in observations. The improved observational density could then allow more spatially explicit emission estimates to be derived. A complete observing system would include a dense network of lower-cost in situ sensors combined with a network of classical instruments. These include measurements of isotopic ratio and coemitted species, recently developed ground-based remote sensing instruments (e.g., Frey et al., 2019) and data from satellite-based instruments that are deployed in an urban targeting mode (as planned for by, e.g., GOSAT-2).

Large uncertainties can result in urban top-down studies due to the difficulty in resolving fine-scale processes. Very high resolution (i.e., less than a kilometer) meteorological data are needed in urban areas

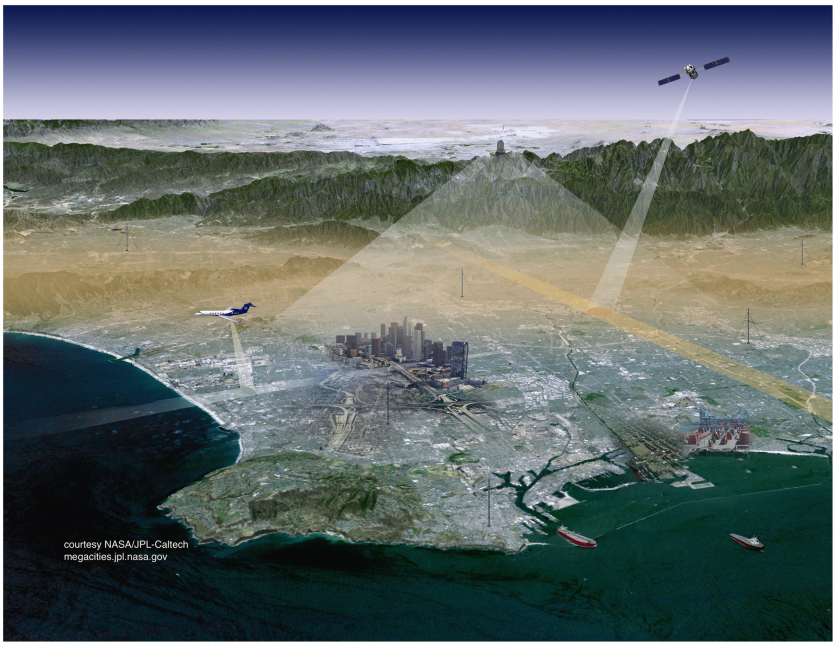


Figure 9. Concept of an urban greenhouse gas observation network for the Los Angeles metropolitan area, which includes ground-based in situ measurements, vehicle-based surveys as well as remote sensing from satellite, aircrafts and fixed sites. (Source: JPL/Caltech Megacities team, Hutyra et al., 2014).

that include, for example, town-energy balance modules to account for urban heat island effects or turbulence introduced by traffic or buildings. These are promising but are computationally expensive. A recent comparison of urban-scale models for air quality found that current state of the art transport models still displays important differences and need to be harmonized (Thunis et al., 2016). Such a fully integrated system has yet to be deployed, but efforts such as the Jet Propulsion Laboratory Megacities project in Los Angeles (Figure 9) and other IG^{3}IS demonstration cities are leading such efforts.

Besides quantifying urban CH_4 emissions using fixed sites, XCH_4, aircraft data and inverse modeling studies, measurements from simpler vehicle-based platforms have been hugely successful in identifying the importance of natural gas infrastructure in different cities (e.g., Lamb et al., 2016; McKain et al., 2015; Phillips et al., 2013). Such surveys often do not rely on exact quantification of CH_4 emission rates from each source location in the city but can use more empirical methods to translate concentration enhancements into emission rate estimates (e.g., von Fischer et al., 2017; Weller et al., 2018). Using this approach, it is possible to quickly rank sources into categories, which then allow more efficient repair schedules and targeted mitigation efforts. Mobile surveys in U.S. cities frequently found fat-tail distributions (i.e., that CH_4 emissions of the city are dominated by a few localized sources), which allows significant emission reductions at limited cost when effective partnerships with public utilities are established (Hopkins et al., 2016). To be able to track the success of interventions, a long-term strategy for implementing observations is needed, but only few regions/cities have started using, for example, the public transit system as a routinely operating mobile platform (Lin et al., 2018). Deployment of unmanned aerial vehicles is also a key advancement as it significantly reduces cost and unmanned aerial vehicle platforms are becoming more readily available (e.g., Andersen et al., 2018; Brownlow et al., 2016). Novel high-altitude platforms would also offer the additional ability for longer term observations over urban areas from a fixed point at approximately 20–50 km above ground level (Gonzalo et al., 2018).

The ability to provide useful information to stakeholders hinges on the ability to link CH_4 emission drivers (e.g., age of infrastructure, population density, and climatic conditions) to the observed atmospheric variations. Advancing research at urban scale can leverage many of the developments in the aforementioned sections, but due to the scale, some issues are specifically challenging. Urban areas will always strongly differ, for example, in size, population density, economic power, available technical skill, political will, and

ambitions. Therefore, bespoke solutions seem necessary rather than a one size fits all approach to understanding urban CH_4.

6. Extending the Impact of CH_4 Science: Communication and Cooperation

The advances described above could improve the extent to which CH_4 sources and sinks can be quantified, but additional efforts are needed to maximize impact in order to help reach the Paris Agreement targets. Although scientists are already contributing to efforts to make data and interpretations available closer to real time and at spatial resolutions that are more relevant to policy makers, such for as individual cities, more can be done to make science useful and accessible.

The Global Carbon Project (www.globalcarbonproject.org) integrates knowledge of sources and sinks for CH_4, CO_2, and nitrous oxide from natural and anthropogenic sources. As part of its annual or biennial releases for greenhouse gas budgets (e.g., Saunois et al., 2016) it teams with professional communicators to help present data as infographics (e.g., www.globalcarbonatlas.org), hone the language and presentation of updates and take-home messages, tailor information for specific countries, and make data more useable and available through its web portals. Similarly, WMO IG^{3}IS attempts to provide stakeholders with emissions information in as timely a fashion as possible. Its priorities include reducing uncertainties in national emission inventories, supporting the Paris Agreement's global stock take for greenhouse gases, and encouraging the implementation of national top-down emissions quantification programs.

National-scale top-down flux estimation can allow for useful benchmarking of inventories. and is considered best practice by the IPCC (2019). It is therefore critical that good dialogue and common goal setting occur between all aspects of the CH_4 science discussed here, which includes those measuring CH_4, inventory compilers and inverse modelers. One such way for ensuring good dialogue is through common funding sources, whereby measurements, the national inventory and top-down estimation, are funded by the same agency, providing a vital route of communication.

Understanding the roles that emissions, sinks, and the uptake of mitigation/removal technologies play in altering trends in atmospheric CH_4 mole fractions will require enhanced measurement and modeling systems. The improvements that are described here will play a key role in helping to assess emissions commitments as more cities, states, and countries report CH_4 emission inventories and commit to mitigation targets. Scientists working on implementing these advances should make their data publicly available and should synthesize their data into forms accessible for use by other researchers. Such best practices will advance progress in this highly connected field. Where possible, scientists should also engage policy makers and other stakeholders early and often. Such cooperation will make it more likely that CH_4 science makes the world a better place.

Acknowledgments
We would like to thank those that strive to maintain long-term records of atmospheric CH_4 around the world and those that perform the meticulous measurements that make CH_4 science possible. We thank Daniel Hoare for the high-resolution U.K. CH_4 emissions map, and we thank Giuseppe Etiope and David Lyon for discussions. A. L. G was supported by U.K. Natural Environment Research Council (NERC) Independent Research Fellowship (NE/L010992/1). B. P. acknowledges support from the NASA Terrestrial Ecology Program. R. B. J and B. P. acknowledge support from the Gordon and Betty Moore Foundation (GBMF5439). A. G., M. R., and E. N. acknowledge funding from the NERC MOYA project (NE/N016548/1 and NE/N016211/1). S. P. acknowledges funding by the Dutch Technology Foundation STW of the Netherlands Organisation for Scientific Research (GALES, 15597). The generation of the SRON GOSAT and TROPOMI XCH_4 data shown here is funded by Copernicus Climate Change Service and ESA's Climate change initiative. Sentinel-5 Precursor satellite is part of the EU Copernicus program, and the TROPOMI instrument is commissioned by Netherlands Space Office (NSO) and ESA. Data shown in Figure 4: WMO/GAW World Data Centre for Greenhouse Gases (https://gaw.kishou.go.jp), NOAA GLOBALVIEWplus (https://www.esrl.noaa.gov/gmd/ccgg/obspack/), NIES Center for Global Environmental Research (http://db.cger.nies.go.jp/portal/geds/atmosphericAndOceanicMonitoring), and NOAA AirCore (ftp://aftp.cmdl.noaa.gov/data/AirCore). Data shown in Figure 5: ESA TROPOMI Level 2 XCH_4 (version RPRO 1.2.0) (https://doi.org/10.5270/S5P-3p6lnwd) and ESA CCI GOSAT SRPR XCH_4 version 2.3.8 (ftp://ftp.sron.nl/pub/pub/RemoTeC/C3S/CH4_GOS_SRPR/).

References

Akagi, S. K., Yokelson, R. J., Wiedinmyer, C., Alvarado, M. J., Reid, J. S., Karl, T., et al. (2011). Emission factors for open and domestic biomass burning for use in atmospheric models. *Atmospheric Chemistry and Physics*, *11*(9), 4039–4072. https://doi.org/10.5194/acp-11-4039-2011

Alvarez, R. A., Zavala-Araiza, D., Lyon, D. R., Allen, D. T., Barkley, Z. R., Brandt, A. R., et al. (2018). Assessment of methane emissions from the U.S. oil and gas supply chain. *Science*, eaar7204. https://doi.org/10.1126/science.aar7204

Andersen, T., Scheeren, B., Peters, W., & Chen, H. (2018). A UAV-based active AirCore system for measurements of greenhouse gases. *Atmospheric Measurement Techniques*, *11*(5), 2683–2699. https://doi.org/10.5194/amt-11-2683-2018

Andreae, M. O. (2019). Emission of trace gases and aerosols from biomass burning—An updated assessment. *Atmospheric Chemistry and Physics*, *19*(13), 8523–8546. https://doi.org/10.5194/acp-19-8523-2019

Aufdenkampe, A. K., Mayorga, E., Raymond, P. A., Melack, J. M., Doney, S. C., Alin, S. R., et al. (2011). Riverine coupling of biogeochemical cycles between land, oceans, and atmosphere. *Frontiers in Ecology and Evolution*, *9*(1), 53–60. https://doi.org/10.1890/100014

Bange, H. W., Bell, T. G., Cornejo, M., Freing, A., Uher, G., Upstill-Goddard, R. C., & Zhang, G. (2009). MEMENTO: A proposal to develop a database of marine nitrous oxide and methane measurements. *Environmental Chemistry*, *6*(3), 195. https://doi.org/10.1071/EN09033

Barba, J., Bradford, M. A., Brewer, P. E., Bruhn, D., Covey, K., van Haren, J., et al. (2019). Methane emissions from tree stems: A new frontier in the global carbon cycle. *The New Phytologist*, *222*(1), 18–28. https://doi.org/doi:10.1111/nph.15582

Bergamaschi, P., Houweling, S., Segers, A., Krol, M., Frankenberg, C., Scheepmaker, R. A., et al. (2013). Atmospheric CH_4 in the first decade of the 21st century: Inverse modeling analysis using SCIAMACHY satellite retrievals and NOAA surface measurements. *Journal of Geophysical Research: Atmospheres*, *118*, 7350–7369. https://doi.org/10.1002/jgrd.50480

Bergamaschi, P., Karstens, U., Manning, A. J., Saunois, M., Tsuruta, A., Berchet, A., et al. (2018). Inverse modelling of European CH_4 emissions during 2006–2012 using different inverse models and reassessed atmospheric observations. *Atmospheric Chemistry and Physics*, *18*(2), 901–920. https://doi.org/10.5194/acp-18-901-2018

Bergamaschi, P., Lubina, C., Königstedt, R., Fischer, H., Veltkamp, A. C., & Zwaagstra, O. (1998). Stable isotopic signatures ($\delta^{13}C$, δD) of methane from European landfill sites. *Journal of Geophysical Research*, *103*(D7), 8251–8265. https://doi.org/10.1029/98JD00105

Bloom, A. A., Bowman, K. W., Lee, M., Turner, A. J., Schroeder, R., Worden, J. R., et al. (2017). A global wetland methane emissions and uncertainty dataset for atmospheric chemical transport models (WetCHARTs version 1.0). *Geoscientific Model Development*, *10*, 2141–2156. https://doi.org/10.5194/gmd-10-2141-2017>

Bloom, A. A., Palmer, P. I., Fraser, A., Reay, D. S., & Frankenberg, C. (2010). Large-scale controls of methanogenesis inferred from methane and gravity spaceborne data. *Science*, *327*(5963), 322–325. https://doi.org/10.1126/science.1175176

Borges, A. V., Darchambeau, F., Lambert, T., Morana, C., Allen, G. H., Tambwe, E., et al. (2019). Variations in dissolved greenhouse gases (CO_2, CH_4, N_2O) in the Congo River network overwhelmingly driven by fluvial-wetland connectivity. *Biogeosciences*, *16*(19), 3801–3834. https://doi.org/10.5194/bg-16-3801-2019

Boschetti, F., Thouret, V., Maenhout, G. J., Totsche, K. U., Marshall, J., & Gerbig, C. (2018). Multi-species inversion and IAGOS airborne data for a better constraint of continental-scale fluxes. *Atmospheric Chemistry and Physics*, *18*(13), 9225–9241. https://doi.org/10.5194/acp-18-9225-2018

Boschetti, L., Roy, D. P., Justice, C. O., & Humber, M. L. (2015). MODIS–Landsat fusion for large area 30 m burned area mapping. *Remote Sensing of Environment*, *161*, 27–42. https://doi.org/10.1016/j.rse.2015.01.022

Bousquet, P., Ciais, P., Miller, J. B., Dlugokencky, E. J., Hauglustaine, D. A., Prigent, C., et al. (2006). Contribution of anthropogenic and natural sources to atmospheric methane variability. *Nature*, *443*(7110), 439–443. https://doi.org/10.1038/nature05132

Bousquet, P., Ringeval, B., Pison, I., Dlugokencky, E. J., Brunke, E.-G., Carouge, C., et al. (2011). Source attribution of the changes in atmospheric methane for 2006–2008. *Atmospheric Chemistry and Physics*, *11*(8), 3689–3700. https://doi.org/10.5194/acp-11-3689-2011

Brandt, A. R., Heath, G. A., & Cooley, D. (2016). Methane leaks from natural gas systems follow extreme distributions. *Environmental Science & Technology*, *50*(22), 12512–12520. https://doi.org/10.1021/acs.est.6b04303

Brenninkmeijer, C. A. M., Crutzen, P., Boumard, F., Dauer, T., Dix, B., Ebinghaus, R., et al. (2007). Civil Aircraft for the regular investigation of the atmosphere based on an instrumented container: The new CARIBIC system. *Atmospheric Chemistry and Physics*, *24*, 4953–4976.

Brown, P., Broomfield, M., Cardenas, L., Choudrie, S., Jones, L., Karagianni, E., et al. (2019). UK Greenhouse Gas Inventory, 1990 to 2017: Annual Report for Submission under the Framework Convention on Climate Change (No. UK NIR 2019 (Issue 2)). UK: Department for Business, Energy and Industrial Strategy.

Brownlow, R., Lowry, D., Thomas, R. M., Fisher, R. E., France, J. L., Cain, M., et al. (2016). Methane mole fraction and $\delta^{13}C$ above and below the trade wind inversion at Ascension Island in air sampled by aerial robotics. *Geophysical Research Letters*, *43*, 11,893–11,902. https://doi.org/10.1002/2016GL071155

Bruhwiler, L. M., Dlugokencky, E., Masarie, K., Ishizawa, M., Andrews, A., Miller, J., et al. (2014). CarbonTracker-CH_4: An assimilation system for estimating emissions of atmospheric methane. *Atmospheric Chemistry and Physics*, *14*(16), 8269–8293. https://doi.org/10.5194/acp-14-8269-2014

Buchwitz, M., Reuter, M., Schneising, O., Hewson, W., Detmers, R. G., Boesch, H., et al. (2017). Global satellite observations of column-averaged carbon dioxide and methane: The GHG-CCI XCO_2 and XCH_4 CRDP3 data set. *Remote Sensing of Environment*, *203*, 276–295. https://doi.org/10.1016/j.rse.2016.12.027

California Air Resources Board. (2016). California Air Resources Board 2016. Determination of Total Methane Emissions from the Aliso Canyon Natural Gas Leak Incident. Retrieved from https://ww3.arb.ca.gov/research/aliso_canyon/aliso_canyon_methane_emissions-arb_final.pdf

California Air Resources Board. (2017). California's 2000-2015 Greenhouse Gas Emissions Inventory 2017 Edition. Supplement to the Technical Support Document. https://www.arb.ca.gov/cc/inventory/pubs/reports/2000_2015/ghg_inventory_00-15_method_update_document.pdf.

California Air Resources Board. (2018). California Greenhouse Gas Emissions for 2000 to 2016. Trends of Emissions and Other Indicators. https://www.arb.ca.gov/cc/inventory/pubs/reports/2000_2016/ghg_inventory_trends_00-16.pdf.

Castro, M. S., Steudler, P. A., Melillo, J. M., Aber, J. D., & Bowden, R. D. (1995). Factors controlling atmospheric methane consumption by temperate forest soils. *Global Biogeochemical Cycles*, *9*(1), 1–10. https://doi.org/10.1029/94GB02651

Chandra, N., Venkataramani, S., Lal, S., Patra, P. K., Ramonet, M., Lin, X., & Sharma, S. K. (2019). Observational evidence of high methane emissions over a city in western India. *Atmospheric Environment*, *202*, 41–52. https://doi.org/10.1016/j.atmosenv.2019.01.007

Chen, Y.-H., & Prinn, R. G. (2006). Estimation of atmospheric methane emissions between 1996 and 2001 using a three-dimensional global chemical transport model. *Journal of Geophysical Research*, *111*, D10307. https://doi.org/10.1029/2005JD006058

Christensen, T. R., Prentice, I. C., Kaplan, J. O., Haxeltine, A., & Sitch, S. (1996). Methane flux from northern wetlands and tundra: An ecosystem source modelling approach. *Tellus*, *48B*, 652–661.

Collins, M., Knutti, R., Arblaster, J., Dufresne, J.-L., Fichefet, T., Friedlingstein, P., et al. (2013). Long-term Climate Change: Projections, Commitments and Irreversibility. In T. F. Stocker et al. (Eds.), *Climate Change 2013: The Physical Science Basis. Contribution of Working Group I to the Fifth Assessment Report of the Intergovernmental Panel on Climate Change*. Cambridge, United Kingdom and New York, NY, USA: Cambridge University Press.

Conley, S., Faloona, I., Mehrotra, S., Suard, M., Lenschow, D. H., Sweeney, C., et al. (2017). Application of Gauss's theorem to quantify localized surface emissions from airborne measurements of wind and trace gases. *Atmospheric Measurement Techniques*, *10*(9), 3345–3358. https://doi.org/10.5194/amt-10-3345-2017

Conley, S., Franco, G., Faloona, I., Blake, D. R., Peischl, J., & Ryerson, T. B. (2016). Methane emissions from the 2015 Aliso Canyon blowout in Los Angeles, CA. *Science*, *351*(6279), 1317–1320. https://doi.org/10.1126/science.aaf2348

Cooley, W. S., Smith, C. L., Stepan, L., & Mascaro, J. (2017). Tracking dynamic northern surface water changes with high-frequency planet CubeSat imagery. *Remote Sensing*, *9*(12). https://doi.org/10.3390/rs9121306

Covey, K. R., & Megonigal, J. P. (2019). Methane production and emissions in trees and forests. *New Phytologist*, *222*(1), 35–51. https://doi.org/doi:10.1111/nph.15624

Cowardin, L. M., Carter, V., Golet, F. C., & LaRoe, E. T. (1979). Classification of wetlands and deepwater habitats of the United States (Technical Report). U.S. Department of the Interior, U.S. Fish and Wildlife Service. Retrieved from. https://tamug-ir.tdl.org/handle/1969.3/20139

Cunnold, D. M., Steele, L. P., Fraser, P. J., Simmonds, P. G., Prinn, R. G., Weiss, R. F., et al. (2002). In situ measurements of atmospheric methane at GAGE/AGAGE sites during 1985–2000 and resulting source inferences. *Journal of Geophysical Research*, *107*(D14), 4225. https://doi.org/10.1029/2001JD001226

Curry, C. L. (2007). Modeling the soil consumption of atmospheric methane at the global scale. *Global Biogeochemical Cycles*, *21*(4), GB4012. https://doi.org/10.1029/2006GB002818

Dalsøren, S. B., Myhre, G., Hodnebrog, O., Myhre, C. L., Stohl, A., Pisso, I., et al. (2018). Discrepancy between simulated and observed ethane and propane levels explained by underestimated fossil emissions/704/106/35/824/704/172/169/824/119 article. *Nature Geoscience*, *11*(3), 178–184. https://doi.org/10.1038/s41561-018-0073-0

Davenport, J. E., & Singh, H. B. (1987). Systematic development of reactive tracer technology to determine hydroxyl radical concentrations in the troposphere. *Atmospheric Environment (1967)*, *21*(9), 1969–1981. https://doi.org/10.1016/0004-6981(87)90158-2

Davidson, J. S., Santos, J. M., Sloan, L. V., Reuss-Schmidt, K., Phoenix, K. G., Oechel, C. W., & Zona, D. (2017). Upscaling CH_4 fluxes using high-resolution imagery in Arctic tundra ecosystems. *Remote Sensing*, *9*(12). https://doi.org/10.3390/rs9121227

Deemer, B. R., Harrison, J. A., Li, S., Beaulieu, J. J., DelSontro, T., Barros, N., et al. (2016). Greenhouse gas emissions from reservoir water surfaces: A new global synthesis. *BioScience*, *66*(11), 949–964. https://doi.org/10.1093/biosci/biw117

del Grosso, S. J., Parton, W. J., Mosier, A. R., Ojima, D. S., Potter, C. S., Borken, W., et al. (2000). General CH_4 oxidation model and comparisons of CH_4 Oxidation in natural and managed systems. *Global Biogeochemical Cycles*, *14*(4), 999–1019. https://doi.org/10.1029/1999GB001226

Denier van der Gon, H. (1999). Changes in CH_4 emission from rice fields from 1960 to 1990s: 2. The declining use of organic inputs in rice farming. *Global Biogeochemical Cycles*, *13*(4), 1053–1062. https://doi.org/10.1029/1999GB900048

Denier van der Gon, H. (2000). Changes in CH_4 emission from rice fields from 1960 to 1990s: 1. Impacts of modern rice technology. *Global Biogeochemical Cycles*, *14*(1), 61–72. https://doi.org/10.1029/1999GB900096

Dlugokencky, E. J., Bruhwiler, L., White, J. W. C., Emmons, L. K., Novelli, P. C., Montzka, S. A., et al. (2009). Observational constraints on recent increases in the atmospheric CH_4 burden. *Geophysical Research Letters*, *36*, L18803. https://doi.org/10.1029/2009GL039780

Dlugokencky, E. J., Nisbet, E. G., Fisher, R., & Lowry, D. (2011). Global atmospheric methane: Budget, changes and dangers. *Philosophical Transactions of the Royal Society A: Mathematical, Physical and Engineering Sciences*, *369*, 2058–2072. https://doi.org/10.1098/rsta.2010.0341

Douglas, P. M. J., Stolper, D. A., Eiler, J. M., Sessions, A. L., Lawson, M., Shuai, Y., et al. (2017). Methane clumped isotopes: Progress and potential for a new isotopic tracer. *Organic Geochemistry*, *113*, 262–282. https://doi.org/10.1016/j.orggeochem.2017.07.016

Du, J., Kimball, J. S., Jones, L. A., Kim, Y., Glassy, J., & Watts, J. D. (2017). A global satellite environmental data record derived from AMSR-E and AMSR2 microwave Earth observations. *Earth System Science Data*, *9*(2), 791–808. https://doi.org/10.5194/essd-9-791-2017

Dutaur, L., & Verchot, L. V. (2007). A global inventory of the soil CH_4 sink. *Global Biogeochemical Cycles*, *21*, GB4013. https://doi.org/10.1029/2006GB002734

Ehret, G., Bousquet, P., Pierangelo, C., Alpers, M., Millet, B., Abshire, J. B., et al. (2017). MERLIN: A French-German Space Lidar Mission dedicated to atmospheric methane. *Remote Sensing*, *9*(10), 1052. https://doi.org/10.3390/rs9101052

Eiler, J. M., Clog, M., Magyar, P., Piasecki, A., Sessions, A., Stolper, D., et al. (2013). A high-resolution gas-source isotope ratio mass spectrometer. *International Journal of Mass Spectrometry*, *335*, 45–56. https://doi.org/10.1016/j.ijms.2012.10.014

Engel, A., Bönisch, H., Ullrich, M., Sitals, R., Membrive, O., Danis, F., & Crevoisier, C. (2017). Mean age of stratospheric air derived from AirCore observations. *Atmospheric Chemistry and Physics*, *17*(11), 6825–6838. https://doi.org/10.5194/acp-17-6825-2017

Environmental Protection Agency. (2012). Global Methane International Coal Mine Methane Projects Database. Retrieved from http://www2.ergweb.com/cmm/projects/ProjectFindResultsAll.aspx?mode=new

Espic, C., Liechti, M., Battaglia, M., Paul, D., Röckmann, T., & Szidat, S. (2019). Compound-specific radiocarbon analysis of atmospheric methane: A new preconcentration and purification setup. *Radiocarbon*, *61*(5), 1461–1476. https://doi.org/10.1017/RDC.2019.76

Etheridge, D. M., Steele, L. P., Francey, R. J., & Langenfelds, R. L. (1998). Atmospheric methane between 1000 A.D. and present: Evidence of anthropogenic emissions and climatic variability. *Journal of Geophysical Research*, *103*(D13), 15979–15993. https://doi.org/10.1029/98JD00923

Etiope, G., Ciotoli, G., Schwietzke, S., & Schoell, M. (2019). Gridded maps of geological methane emissions and their isotopic signature. *Earth System Science Data*, *11*, 1–22. https://doi.org/10.5194/essd-11-1-2019

Etiope, G., & Klusman, R. W. (2010). Microseepage in drylands: Flux and implications in the global atmospheric source/sink budget of methane. *Global and Planetary Change*, *72*(4), 265–274. https://doi.org/10.1016/j.gloplacha.2010.01.002

Etminan, M., Myhre, G., Highwood, E. J., & Shine, K. P. (2016). Radiative forcing of carbon dioxide, methane, and nitrous oxide: A significant revision of the methane radiative forcing. *Geophysical Research Letters*, *43*, 12,614–12,623. https://doi.org/10.1002/2016GL071930

Eyer, S., Tuzson, B., Popa, M. E., van der Veen, C., Röckmann, T., Rothe, M., et al. (2016). Real-time analysis of $\delta^{13}C$- and δD-CH_4 in ambient air with laser spectroscopy: Method development and first intercomparison results. *Atmospheric Measurement Techniques*, *9*(1), 263–280. https://doi.org/10.5194/amt-9-263-2016

Fisher, R. E., France, J. L., Lowry, D., Lanoisellé, M., Brownlow, R., Pyle, J. A., et al. (2017). Measurement of the ^{13}C isotopic signature of methane emissions from northern European wetlands. *Global Biogeochemical Cycles*, *31*, 605–623. https://doi.org/10.1002/2016GB005504

Fisher, R. E., Sriskantharajah, S., Lowry, D., Lanoisellé, M., Fowler, C. M. R., James, R. H., et al. (2011). Arctic methane sources: Isotopic evidence for atmospheric inputs. *Geophysical Research Letters*, *38*, L21803. https://doi.org/10.1029/2011GL049319

Food and Agriculture Organization. (2018). The State of World Fisheries and Aquaculture 2018—Meeting the sustainable development goals. Rome.

Frankenberg, C. (2005). Assessing methane emissions from global space-borne observations. *Science*, *308*(5724), 1010–1014. https://doi.org/10.1126/science.1106644

Frey, M., Sha, M. K., Hase, F., Kiel, M., Blumenstock, T., Harig, R., et al. (2019). Building the COllaborative Carbon Column Observing Network (COCCON): Long-term stability and ensemble performance of the EM27/SUN Fourier transform spectrometer. *Atmospheric Measurement Techniques*, *12*(3), 1513–1530. https://doi.org/10.5194/amt-12-1513-2019

Fujita, R., Morimoto, S., Umezawa, T., Ishijima, K., Patra, P. K., Worthy, D. E. J., et al. (2018). Temporal variations of the mole fraction, carbon, and hydrogen isotope ratios of atmospheric methane in the Hudson Bay Lowlands, Canada. *Journal of Geophysical Research: Atmospheres*, *123*, 4695–4711. https://doi.org/10.1002/2017JD027972

Fung, I., John, J., Lerner, J., Matthews, E., Prather, M., Steele, L. P., & Fraser, P. J. (1991). Three-dimensional model synthesis of the global methane cycle. *Journal of Geophysical Research*, *96*(D7), 13033–13065. https://doi.org/10.1029/91JD01247

Gallagher, M. E., Down, A., Ackley, R. C., Zhao, K., Phillips, N., & Jackson, R. B. (2015). Natural gas pipeline replacement programs reduce methane leaks and improve consumer safety. *Environmental Science & Technology Letters*, *2*(10), 286–291. https://doi.org/10.1021/acs.estlett.5b00213

Ganesan, A. L., Rigby, M., Lunt, M. F., Parker, R. J., Boesch, H., Goulding, N., et al. (2017). Atmospheric observations show accurate reporting and little growth in India's methane emissions. *Nature Communications*, *8*(1), 836. https://doi.org/10.1038/s41467-017-00994-7

Ganesan, A. L., Rigby, M., Zammit-Mangion, A., Manning, A. J., Prinn, R. G., Fraser, P. J., et al. (2014). Characterization of uncertainties in atmospheric trace gas inversions using hierarchical Bayesian methods. *Atmospheric Chemistry and Physics*, *14*(8), 3855–3864. https://doi.org/10.5194/acp-14-3855-2014

Ganesan, A. L., Stell, A. C., Gedney, N., Comyn-Platt, E., Hayman, G., Rigby, M., et al. (2018). Spatially resolved isotopic source signatures of wetland methane emissions. *Geophysical Research Letters*, *45*, 3737–3745. https://doi.org/10.1002/2018GL077536

Giglio, L., Boschetti, L., Roy, D. P., Humber, M. L., & Justice, C. O. (2018). The collection 6 MODIS burned area mapping algorithm and product. *Remote Sensing of Environment*, *217*, 72–85. https://doi.org/10.1016/j.rse.2018.08.005

Gonzalo, J., López, D., Domínguez, D., García, A., & Escapa, A. (2018). On the capabilities and limitations of high altitude pseudo-satellites. *Progress in Aerospace Sciences*, *98*, 37–56. https://doi.org/10.1016/j.paerosci.2018.03.006

Grant, R. F., Humphreys, E. R., & Lafleur, P. (2015). Ecosystem CO_2 and CH_4 exchange in a mixed tundra and a fen within a hydrologically diverse Arctic landscape: 1. Modeling versus measurements. *Journal of Geophysical Research: Biogeosciences*, *120*, 1366–1387. https://doi.org/10.1002/2014JG002888

Graven, H., Hocking, T., & Zazzeri, G. (2019). Detection of fossil and biogenic methane at regional scales using atmospheric radiocarbon. *Earth's Future*, *7*, 283–299. https://doi.org/10.1029/2018EF001064

Guo, M., Li, J., Sheng, C., Xu, J., & Wu, L. (2017). A review of wetland remote sensing. *Sensors (Basel, Switzerland)*, *17*(4). https://doi.org/10.3390/s17040777

Gupta, P. K., Sharma, C., Bhattacharya, S., & Mitra, A. P. (2002). Scientific basis for establishing country greenhouse gas estimates for rice-based agriculture: An Indian case study. *Nutrient Cycling in Agroecosystems*, *64*(1), 19–31. https://doi.org/10.1023/A:1021117029359

Haghnegahdar, M. A., Schauble, E. A., & Young, E. D. (2017). A model for $^{12}CH_2D_2$ and $^{13}CH_3D$ as complementary tracers for the budget of atmospheric CH_4. *Global Biogeochemical Cycles*, *31*, 1387–1407. https://doi.org/10.1002/2017GB005655

Hall, J. V., Zhang, R., Schroeder, W., Huang, C., & Giglio, L. (2019). Validation of GOES-16 ABI and MSG SEVIRI active fire products. *International Journal of Applied Earth Observation and Geoinformation*, *83*, 101928. https://doi.org/10.1016/j.jag.2019.101928

Harvey, N. J., Huntley, N., Dacre, H. F., Goldstein, M., Thomson, D., & Webster, H. (2018). Multi-level emulation of a volcanic ash transport and dispersion model to quantify sensitivity to uncertain parameters. *Natural Hazards and Earth System Sciences*, *18*(1), 41–63. https://doi.org/10.5194/nhess-18-41-2018

Hein, R., Crutzen, P. J., & Heimann, M. (1997). An inverse modeling approach to investigate the global atmospheric methane cycle. *Global Biogeochemical Cycles*, *11*(1), 43–76.

Helmig, D., Rossabi, S., Hueber, J., Tans, P., Montzka, S. A., Masarie, K., et al. (2016). Reversal of global atmospheric ethane and propane trends largely due to US oil and natural gas production. *Nature Geoscience*, *9*(7), 490–495. https://doi.org/10.1038/ngeo2721

Höglund-Isaksson, L. (2017). Bottom-up simulations of methane and ethane emissions from global oil and gas systems 1980 to 2012. *Environmental Research Letters*, *12*(2), 024007. https://doi.org/10.1088/1748-9326/aa583e

Hoheisel, A., Yeman, C., Dinger, F., Eckhardt, H., & Schmidt, M. (2019). An improved method for mobile characterisation of $\delta^{13}CH_4$ source signatures and its application in Germany. *Atmospheric Measurement Techniques*, *12*(2), 1123–1139. https://doi.org/10.5194/amt-12-1123-2019

Hopkins, F. M., Ehleringer, J. R., Bush, S. E., Duren, R. M., Miller, C. E., Lai, C.-T., et al. (2016). Mitigation of methane emissions in cities: How new measurements and partnerships can contribute to emissions reduction strategies. *Earth's Future*, *4*, 408–425. https://doi.org/10.1002/2016EF000381

Houweling, S., Bergamaschi, P., Chevallier, F., Heimann, M., Kaminski, T., Krol, M., et al. (2017). Global inverse modeling of CH_4 sources and sinks: An overview of methods. *Atmospheric Chemistry and Physics*, *17*(1), 235–256. https://doi.org/10.5194/acp-17-235-2017

Houweling, S., Kaminski, T., Dentener, F., Lelieveld, J., & Heimann, M. (1999). Inverse modeling of methane sources and sinks using the adjoint of a global transport model. *Journal of Geophysical Research*, *104*(D21), 26137–26160. https://doi.org/10.1029/1999JD900428

Hu, H., Landgraf, J., Detmers, R., Borsdorff, T., Aan de Brugh, J., Aben, I., et al. (2018). Toward global mapping of methane with TROPOMI: First results and intersatellite comparison to GOSAT. *Geophysical Research Letters*, *45*, 3682–3689. https://doi.org/10.1002/2018GL077259

Huang, J., & Prinn, R. G. (2002). Critical evaluation of emissions of potential new gases for OH estimation. *Journal of Geophysical Research*, *107*(D24), 4784. https://doi.org/10.1029/2002JD002394

Hutyra, L. R., Duren, R., Gurney, K. R., Grimm, N., Kort, E. A., Larson, E., & Shrestha, G. (2014). Urbanization and the carbon cycle: Current capabilities and research outlook from the natural sciences perspective. *Earth's Future*, *2*, 473–495. https://doi.org/10.1002/2014EF000255

IPCC (2006). In H. S. Eggleston, L. Buendia, K. Miwa, T. Ngara, & K. Tanabe (Eds.), *2006 IPCC Guidelines for National Greenhouse Gas Inventories*, Prepared by the National Greenhouse Gas Inventories Programme. Japan: IGES.

IPCC (2013). IPCC, 2013: Annex II: Climate System Scenario Tables [Prather, M., G. Flato, P. Friedlingstein, C. Jones, J.-F. Lamarque, H. Liao and P. Rasch (eds.)]. In T. F. Stocker et al. (Eds.), *Climate Change 2013: The physical science basis. Contribution of Working Group I to the Fifth Assessment Report of the Intergovernmental Panel on Climate Change*. Cambridge, United Kingdom and New York, NY, USA: Cambridge University Press.

IPCC. (2019). 2019 Refinement to the 2006 IPCC Guidelines for National Greenhouse Gas Inventories, accepted.

Jackson, R. B., Solomon, E. I., Canadell, J. G., Cargnello, M., & Field, C. B. (2019). Methane removal and atmospheric restoration. *Nature Sustainability*, *2*(6), 436. https://doi.org/10.1038/s41893-019-0299-x

Jackson, R. B., Vengosh, A., Carey, J. W., Davies, R. J., Darrah, T. H., O'Sullivan, F., & Pétron, G. (2014). The environmental costs and benefits of fracking. *Annual Review of Environment and Resources*, *39*(1), 327–362. https://doi.org/10.1146/annurev-environ-031113-144051

Jacob, D. J., & Prather, M. J. (1990). Radon-222 as a test of convective transport in a general circulation model. *Tellus B*, *42*(1), 118–134. https://doi.org/10.1034/j.1600-0889.1990.00012.x

Jacob, D. J., Turner, A. J., Maasakkers, J. D., Sheng, J., Sun, K., Liu, X., et al. (2016). Satellite observations of atmospheric methane and their value for quantifying methane emissions. *Atmospheric Chemistry and Physics*, *16*(22), 14371–14396. https://doi.org/10.5194/acp-16-14371-2016

Janssens-Maenhout, G., Crippa, M., Guizzardi, D., Muntean, M., Schaaf, E., Dentener, F., et al. (2019). EDGAR v4.3.2 Global Atlas of the three major greenhouse gas emissions for the period 1970–2012. *Earth System Science Data*, *11*(3), 959–1002. https://doi.org/10.5194/essd-11-959-2019

Jeong, S., Newman, S., Zhang, J., Andrews, A. E., Bianco, L., Bagley, J., et al. (2016). Estimating methane emissions in California's urban and rural regions using multitower observations. *Journal of Geophysical Research: Atmospheres*, *121*, 13,031–13,049. https://doi.org/10.1002/2016JD025404

Jiang, Y., van Groenigen, K. J., Huang, S., Hungate, B. A., van Kessel, C., Hu, S., et al. (2017). Higher yields and lower methane emissions with new rice cultivars. *Global Change Biology*, *23*(11), 4728–4738. https://doi.org/10.1111/gcb.13737

Kaiser, J. W., Heil, A., Andreae, M. O., Benedetti, A., Chubarova, N., Jones, L., et al. (2012). Biomass burning emissions estimated with a global fire assimilation system based on observed fire radiative power. *Biogeosciences*, *9*(1), 527–554. https://doi.org/10.5194/bg-9-527-2012

Karion, A., Sweeney, C., Tans, P., & Newberger, T. (2010). AirCore: An innovative atmospheric sampling system. *Journal of Atmospheric and Oceanic Technology*, *27*(11), 1839–1853. https://doi.org/10.1175/2010JTECHA1448.1

Karstens, U., Schwingshackl, C., Schmithüsen, D., & Levin, I. (2015). A process-based ^{222}radon flux map for Europe and its comparison to long-term observations. *Atmospheric Chemistry and Physics*, *15*(22), 12845–12865. https://doi.org/10.5194/acp-15-12845-2015

Knox, S. H., Jackson, R. B., Poulter, B., McNicol, G., Fluet-Chouinard, E., Zhang, Z., et al. (2019). FLUXNET-CH_4 synthesis activity: Objectives, observations, and future directions. *Bulletin of the American Meteorological Society*. https://doi.org/10.1175/BAMS-D-18-0268.1

Koffi, E. N., Rayner, P. J., Scholze, M., Chevallier, F., & Kaminski, T. (2013). Quantifying the constraint of biospheric process parameters by CO_2 concentration and flux measurement networks through a carbon cycle data assimilation system. *Atmospheric Chemistry and Physics*, *13*(21), 10555–10572. https://doi.org/10.5194/acp-13-10555-2013

Kort, E. A., Frankenberg, C., Costigan, K. R., Lindenmaier, R., Dubey, M. K., & Wunch, D. (2014). Four corners: The largest US methane anomaly viewed from space. *Geophysical Research Letters*, *41*, 6898–6903. https://doi.org/10.1002/2014GL061503

Kort, E. A., Smith, M. L., Murray, L. T., Gvakharia, A., Brandt, A. R., Peischl, J., et al. (2016). Fugitive emissions from the Bakken shale illustrate role of shale production in global ethane shift: Ethane emissions from the Bakken Shale. *Geophysical Research Letters*, *43*, 4617–4623. https://doi.org/10.1002/2016GL068703

Koven, C. D., Ringeval, B., Friedlingstein, P., Ciais, P., Cadule, P., Khvorostyanov, D., et al. (2011). Permafrost carbon-climate feedbacks accelerate global warming. *Proceedings of the National Academy of Sciences*, *108*(36), 14769–14774. https://doi.org/10.1073/pnas.1103910108

Krol, M., de Bruine, M., Killaars, L., Ouwersloot, H., Pozzer, A., Yin, Y., et al. (2018). Age of air as a diagnostic for transport timescales in global models. *Geoscientific Model Development*, *11*(8), 3109–3130. https://doi.org/10.5194/gmd-11-3109-2018

Krol, M., Meirink, J. F., Bergamaschi, P., Mak, J. E., Lowe, D., Jöckel, P., et al. (2008). What can ^{14}CO measurements tell us about OH? *Atmospheric Chemistry and Physics*, *8*(16), 5033–5044. https://doi.org/10.5194/acp-8-5033-2008

Lamb, B. K., Cambaliza, M. O. L., Davis, K. J., Edburg, S. L., Ferrara, T. W., Floerchinger, C., et al. (2016). Direct and indirect measurements and modeling of methane emissions in Indianapolis, Indiana. *Environmental Science & Technology*, *50*(16), 8910–8917. https://doi.org/10.1021/acs.est.6b01198

Lan, X., Tans, P., Sweeney, C., Andrews, A., Dlugokencky, E., Schwietzke, S., et al. (2019). Long-term measurements show little evidence for large increases in total U.S. methane emissions over the past decade. *Geophysical Research Letters*, *46*, 4991–4999. https://doi.org/10.1029/2018GL081731

Lassey, K. R., Etheridge, D. M., Lowe, D. C., Smith, A. M., & Ferretti, D. F. (2007). Centennial evolution of the atmospheric methane budget: What do the carbon isotopes tell us? *Atmospheric Chemistry and Physics*, *21*.

Levin, I., Bösinger, R., Bonani, G., Francey, R. J., Kromer, B., Münnich, K. O., et al. (1992). Radiocarbon in atmospheric carbon dioxide and methane: Global distribution and trends. In R. E. Taylor, A. Long, & R. S. Kra (Eds.), *Radiocarbon After Four Decades* (pp. 503–518). New York: Springer.

Levin, I., Veidt, C., Vaughn, B. H., Brailsford, G., Bromley, T., Heinz, R., et al. (2012). No inter-hemispheric $\delta^{13}CH_4$ trend observed. *Nature*, *486*(7404), E3–E4. https://doi.org/10.1038/nature11175

Li, X., Norman, H. C., Kinley, R. D., Laurence, M., Wilmot, M., Bender, H., et al. (2018). Asparagopsis taxiformis decreases enteric methane production from sheep. *Animal Production Science*, *58*(4), 681–688. https://doi.org/10.1071/AN15883

Liang, Q., Chipperfield, M. P., Fleming, E. L., Abraham, N. L., Braesicke, P., Burkholder, J. B., et al. (2017). Deriving global OH abundance and atmospheric lifetimes for long-lived gases: A search for CH_3CCl_3 alternatives. *Journal of Geophysical Research: Atmospheres*, *122*, 11,914–11,933. https://doi.org/10.1002/2017JD026926

Lin, J. C., Mitchell, L., Crosman, E., Mendoza, D. L., Buchert, M., Bares, R., et al. (2018). CO_2 and carbon emissions from cities: Linkages to air quality, socioeconomic activity, and stakeholders in the Salt Lake City urban area. *Bulletin of the American Meteorological Society*, *99*(11), 2325–2339. https://doi.org/10.1175/BAMS-D-17-0037.1

Liu, S., Hu, Z., Wu, S., Li, S., Li, Z., & Zou, J. (2016). Methane and nitrous oxide emissions reduced following conversion of rice paddies to inland crab–fish aquaculture in Southeast China. *Environmental Science & Technology*, *50*(2), 633–642. https://doi.org/10.1021/acs.est.5b04343

Liu, T., Marlier, M. E., Karambelas, A., Jain, M., Singh, S., Singh, M. K., et al. (2019). Missing emissions from post-monsoon agricultural fires in northwestern India: Regional limitations of MODIS burned area and active fire products. *Environmental Research Communications*, *1*(1), 011007. https://doi.org/10.1088/2515-7620/ab056c

López-Comí, L., Morgenstern, O., Zeng, G., Masters, S. L., Querel, R. R., & Nedoluha, G. E. (2016). Assessing the sensitivity of the hydroxyl radical to model biases in composition and temperature using a single-column photochemical model for Lauder, New Zealand. *Atmospheric Chemistry and Physics*, *16*(22), 14599–14619. https://doi.org/10.5194/acp-16-14599-2016

Louhibi-Bouiri, M., & Hachemi, M. (2018). Methane emissions from the Algerian natural gas pipelines transportation: Exploring process to reduce environmental consequences. *Energy & Environment*. https://doi.org/10.1177/0958305X18772423

Lowry, D., Holmes, C. W., Rata, N. D., O'Brien, P., & Nisbet, E. G. (2001). London methane emissions: Use of diurnal changes in concentration and $\delta^{13}C$ to identify urban sources and verify inventories. *Journal of Geophysical Research*, *106*(D7), 7427–7448. https://doi.org/10.1029/2000JD900601

Luo, G. J., Kiese, R., Wolf, B., & Butterbach-Bahl, K. (2013). Effects of soil temperature and moisture on methane uptake and nitrous oxide emissions across three different ecosystem types. *Biogeosciences*, *10*(5), 3205–3219. https://doi.org/10.5194/bg-10-3205-2013

Maasakkers, J. D., Jacob, D. J., Sulprizio, M. P., Scarpelli, T. R., Nesser, H., Sheng, J.-X., et al. (2019). Global distribution of methane emissions, emission trends, and OH concentrations and trends inferred from an inversion of GOSAT satellite data for 2010–2015. *Atmospheric Chemistry and Physics*, *19*(11), 7859–7881. https://doi.org/10.5194/acp-19-7859-2019

Machida, T., Matsueda, H., Sawa, Y., Nakagawa, Y., Hirotani, K., Kondo, N., et al. (2008). Worldwide measurements of atmospheric CO_2 and other trace gas species using commercial airlines. *Journal of Atmospheric and Oceanic Technology*, *25*(10), 1744–1754. https://doi.org/10.1175/2008JTECHA1082.1

Malina, E., Hu, H., Landgraf, J., & Veihelmann, B. (2019). A study of synthetic $^{13}CH_4$ retrievals from TROPOMI and Sentinel 5/UVNS Part 1: Non scattering atmosphere. *Atmospheric Measurement Techniques Discussions*, 1–36. https://doi.org/10.5194/amt-2018-450

Manning, M. R., Lowe, D. C., Moss, R. C., Bodeker, G. E., & Allan, W. (2005). Short-term variations in the oxidizing power of the atmosphere. *Nature*, *436*(7053), 1001. https://doi.org/10.1038/nature03900

Matthews, E., & Fung, I. (1987). Methane emission from natural wetlands: Global distribution, area, and environmental characteristics of sources. *Global Biogeochemical Cycles*, *1*(1), 61–86. https://doi.org/10.1029/GB001i001p00061

McCalley, C. K., Woodcroft, B. J., Hodgkins, S. B., Wehr, R. A., Kim, E.-H., Mondav, R., et al. (2014). Methane dynamics regulated by microbial community response to permafrost thaw. *Nature*, *514*(7523), 478–481. https://doi.org/10.1038/nature13798

McGuire, A. D., Lawrence, D. M., Koven, C., Clein, J. S., Burke, E., Chen, G., et al. (2018). Dependence of the evolution of carbon dynamics in the northern permafrost region on the trajectory of climate change. *Proceedings of the National Academy of Sciences*, *115*(15), 3882–3887. https://doi.org/10.1073/pnas.1719903115

McKain, K., Down, A., Raciti, S. M., Budney, J., Hutyra, L. R., Floerchinger, C., et al. (2015). Methane emissions from natural gas infrastructure and use in the urban region of Boston, Massachusetts. *Proceedings of the National Academy of Sciences*, *112*(7), 1941–1946. https://doi.org/10.1073/pnas.1416261112

McNorton, J., Wilson, C., Gloor, M., Parker, R. J., Boesch, H., Feng, W., et al. (2018). Attribution of recent increases in atmospheric methane through 3-D inverse modelling. *Atmospheric Chemistry and Physics*, *18*(24), 18149–18168. https://doi.org/10.5194/acp-18-18149-2018

Meinshausen, M., Nicholls, Z., Lewis, J., Gidden, M. J., Vogel, E., Freund, M., et al. (2019). The SSP greenhouse gas concentrations and their extensions to 2500 (preprint). *Climate and Earth System Modeling*. https://doi.org/10.5194/gmd-2019-222

Meinshausen, M., Smith, S. J., Calvin, K., Daniel, J. S., Kainuma, M. L. T., Lamarque, J.-F., et al. (2011). The RCP greenhouse gas concentrations and their extensions from 1765 to 2300. *Climatic Change*, *109*(1-2), 213–241. https://doi.org/10.1007/s10584-011-0156-z

Membrive, O., Crevoisier, C., Sweeney, C., Danis, F., Hertzog, A., Engel, A., et al. (2017). AirCore-HR: A high-resolution column sampling to enhance the vertical description of CH_4 and CO_2. *Atmospheric Measurement Techniques*, *10*(6), 2163–2181. https://doi.org/10.5194/amt-10-2163-2017

Mikaloff Fletcher, S. E., & Schaefer, H. (2019). Rising methane: A new climate challenge. *Science*, *364*(6444), 932–933. https://doi.org/10.1126/science.aax1828

Mikaloff Fletcher, S. E., Tans, P. P., Bruhwiler, L. M., Miller, J. B., & Heimann, M. (2004a). CH4 sources estimated from atmospheric observations of CH_4 and its $^{13}C/^{12}C$ isotopic ratios: 1. Inverse modeling of source processes. *Global Biogeochemical Cycles*, *18*, GB4004. https://doi.org/10.1029/2004GB002223

Mikaloff Fletcher, S. E., Tans, P. P., Bruhwiler, L. M., Miller, J. B., & Heimann, M. (2004b). CH4 sources estimated from atmospheric observations of CH_4 and its $^{13}C/^{12}C$ isotopic ratios: 2. Inverse modeling of CH_4 fluxes from geographical regions. *Global Biogeochemical Cycles*, *18*, GB4005. https://doi.org/10.1029/2004GB002224

Miller, S. M., Michalak, A. M., Detmers, R. G., Hasekamp, O. P., Bruhwiler, L. M., & Schwietzke, S. (2019). China's coal mine methane regulations have not curbed growing emissions. *Nature Communications*, *10*(1). https://doi.org/10.1038/s41467-018-07891-7

Miller, S. M., Michalak, A. M., & Levi, P. J. (2014). Atmospheric inverse modeling with known physical bounds: An example from trace gas emissions. *Geoscientific Model Development*, *7*(1), 303–315. https://doi.org/10.5194/gmd-7-303-2014

Miller, S. M., Wofsy, S. C., Michalak, A. M., Kort, E. A., Andrews, A. E., Biraud, S. C., et al. (2013). Anthropogenic emissions of methane in the United States. *Proceedings of the National Academy of Sciences*, *110*(50), 20018–20022. https://doi.org/10.1073/pnas.1314392110

Mitra, A. P., Sharma, S., Bhattacharya, S., Garg, A., Devotta, S., & Sen, K. (Eds.) (2004). Climate change and India: Uncertainty reduction in greenhouse gas inventory estimates. Hyderabad (IN): Universities Press.

Murguia-Flores, F., Arndt, S., Ganesan, A. L., Murray-Tortarolo, G., & Hornibrook, E. R. C. (2018). Soil Methanotrophy Model (MeMo v1.0): A process-based model to quantify global uptake of atmospheric methane by soil. *Geoscientific Model Development*, *11*(6), 2009–2032. https://doi.org/10.5194/gmd-11-2009-2018

Myhre, G., Shindell, D., Bréon, F.-M., Collins, W., Fuglestvedt, J., Huang, J., et al. (2013). Anthropogenic and natural radiative forcing. In T. F. Stocker et al. (Eds.), *Climate change 2013: The Physical Science Basis. Contribution of Working Group I to the Fifth Assessment Report of the Intergovernmental Panel on Climate Change*. Cambridge, United Kingdom and New York, NY, USA: Cambridge University Press.

Nangini, C., Peregon, A., Ciais, P., Weddige, U., Vogel, F., Wang, J., et al. (2019). A global dataset of CO_2 emissions and ancillary data related to emissions for 343 cities. *Scientific Data*, *6*(1), 180280. https://doi.org/10.1038/sdata.2018.280

Naus, S., Montzka, S. A., Pandey, S., Basu, S., Dlugokencky, E. J., & Krol, M. (2019). Constraints and biases in a tropospheric two-box model of OH. *Atmospheric Chemistry and Physics*, *19*(1), 407–424. https://doi.org/10.5194/acp-19-407-2019

Nesbit, S. P., & Breitenbeck, G. A. (1992). A laboratory study of factors influencing methane uptake by soils. *Agriculture, Ecosystems & Environment*, *41*(1), 39–54. https://doi.org/10.1016/0167-8809(92)90178-E

Neue, H. U. (1997). Fluxes of methane from rice fields and potential for mitigation. *Soil Use and Management*, *13*(s4), 258–267. https://doi.org/10.1111/j.1475-2743.1997.tb00597.x

Nicely, J. M., Canty, T. P., Manyin, M., Oman, L. D., Salawitch, R. J., Steenrod, S. D., et al. (2018). Changes in global tropospheric OH expected as a result of climate change over the last several decades. *Journal of Geophysical Research: Atmospheres*, *123*, 10,774–10,795. https://doi.org/10.1029/2018JD028388

Nicely, J. M., Salawitch, R. J., Canty, T., Anderson, D. C., Arnold, S. R., Chipperfield, M. P., et al. (2017). Quantifying the causes of differences in tropospheric OH within global models. *Journal of Geophysical Research: Atmospheres*, *122*, 1983–2007. https://doi.org/10.1002/2016JD026239

Nicewonger, M. R., Verhulst, K. R., Aydin, M., & Saltzman, E. S. (2016). Preindustrial atmospheric ethane levels inferred from polar ice cores: A constraint on the geologic sources of atmospheric ethane and methane. *Geophysical Research Letters*, *43*, 214–221. https://doi.org/10.1002/2015GL066854

Nisbet, E. G., Dlugokencky, E. J., Manning, M. R., Lowry, D., Fisher, R. E., France, J. L., et al. (2016). Rising atmospheric methane: 2007–2014 growth and isotopic shift. *Global Biogeochemical Cycles*, *30*, 1356–1370. https://doi.org/10.1002/2016GB005406

Nisbet, E. G., Manning, M. R., Dlugokencky, E. J., Fisher, R. E., Lowry, D., Michel, S. E., et al. (2019). Very strong atmospheric methane growth in the 4 years 2014–2017: Implications for the Paris Agreement. *Global Biogeochemical Cycles*, *33*, 318–342. https://doi.org/10.1029/2018GB006009

Ono, S., Wang, D. T., Gruen, D. S., Sherwood Lollar, B., Zahniser, M. S., McManus, B. J., & Nelson, D. D. (2014). Measurement of a Doubly Substituted Methane Isotopologue, 13CH3D, by Tunable Infrared Laser Direct Absorption Spectroscopy. *Analytical Chemistry*, *86*, 6487–6494. https://doi.org/10.1021/ac5010579

Padilla, M., Stehman, S. V., Ramo, R., Corti, D., Hantson, S., Oliva, P., et al. (2015). Comparing the accuracies of remote sensing global burned area products using stratified random sampling and estimation. *Remote Sensing of Environment*, *160*, 114–121. https://doi.org/10.1016/j.rse.2015.01.005

Palmer, P. I., O'Doherty, S., Allen, G., Bower, K., Bösch, H., Chipperfield, M. P., et al. (2018). A measurement-based verification framework for UK greenhouse gas emissions: An overview of the Greenhouse gAs Uk and Global Emissions (GAUGE) project. *Atmospheric Chemistry and Physics*, *18*(16), 11753–11777. https://doi.org/10.5194/acp-18-11753-2018

Pandey, S., Houweling, S., Krol, M., Aben, I., Monteil, G., Nechita-Banda, N., et al. (2017). Enhanced methane emissions from tropical wetlands during the 2011 La Niña. *Scientific Reports*, *7*(1), 45759. https://doi.org/10.1038/srep45759

Pandey, S., Houweling, S., Krol, M., Aben, I., Nechita-Banda, N., Thoning, K., et al. (2019). Influence of atmospheric transport on estimates of variability in the global methane burden. *Geophysical Research Letters*, *46*, 2302–2311. https://doi.org/10.1029/2018GL081092

Pangala, S. R., Enrich-Prast, A., Basso, L. S., Peixoto, R. B., Bastviken, D., Hornibrook, E. R. C., et al. (2017). Large emissions from floodplain trees close the Amazon methane budget. *Nature*, *552*(7684), 230–234. https://doi.org/10.1038/nature24639, https://www.nature.com/articles/nature24639#supplementary-information

Parker, R. J., Boesch, H., Byckling, K., Webb, A. J., Palmer, P. I., Feng, L., et al. (2015). Assessing 5 years of GOSAT Proxy XCH_4 data and associated uncertainties. *Atmospheric Measurement Techniques*, *8*(11), 4785–4801. https://doi.org/10.5194/amt-8-4785-2015

Parker, R. J., Boesch, H., Cogan, A., Fraser, A., Feng, L., Palmer, P. I., et al. (2011). Methane observations from the greenhouse gases observing SATellite: Comparison to ground-based TCCON data and model calculations. *Geophysical Research Letters*, *38*, L15807. https://doi.org/10.1029/2011GL047871

Parker, R. J., Boesch, H., McNorton, J., Comyn-Platt, E., Gloor, M., Wilson, C., et al. (2018). Evaluating year-to-year anomalies in tropical wetland methane emissions using satellite CH_4 observations. *Remote Sensing of Environment*, *211*, 261–275. https://doi.org/10.1016/j.rse.2018.02.011

Patra, P. K., Houweling, S., Krol, M., Bousquet, P., Belikov, D., Bergmann, D., et al. (2011). TransCom model simulations of CH_4 and related species: Linking transport, surface flux and chemical loss with CH_4 variability in the troposphere and lower stratosphere. *Atmospheric Chemistry and Physics*, *11*(24), 12813–12837. https://doi.org/10.5194/acp-11-12813-2011

Patra, P. K., Saeki, T., Dlugokencky, E. J., Ishijima, K., Umezawa, T., Ito, A., et al. (2016). Regional methane emission estimation based on observed atmospheric concentrations (2002–2012). *Journal of the Meteorological Society of Japan. Series II*, *94*(1), 91–113. https://doi.org/10.2151/jmsj.2016-006

Paul, D., Chen, H., Been, H. A., Kivi, R., & Meijer, H. A. J. (2016). Radiocarbon analysis of stratospheric CO_2 retrieved from AirCore sampling. *Atmospheric Measurement Techniques*, *9*(10), 4997–5006. https://doi.org/10.5194/amt-9-4997-2016

Peischl, J., Eilerman, S. J., Neuman, J. A., Aikin, K. C., de Gouw, J., Gilman, J. B., et al. (2018). Quantifying methane and ethane emissions to the atmosphere from central and western U.S. oil and natural gas production regions. *Journal of Geophysical Research: Atmospheres*, *123*, 7725–7740. https://doi.org/10.1029/2018JD028622

Peltola, O., Vesala, T., Gao, Y., Räty, O., Alekseychik, P., Aurela, M., et al. (2019). Monthly gridded data product of northern wetland methane emissions based on upscaling eddy covariance observations. *Earth System Science Data Discussions*, *2019*, 1–50. https://doi.org/10.5194/essd-2019-28

Peters, W., Miller, J. B., Whitaker, J., Denning, A. S., Hirsch, A., Krol, M. C., et al. (2005). An ensemble data assimilation system to estimate CO_2 surface fluxes from atmospheric trace gas observations. *Journal of Geophysical Research*, *110*, D24304. https://doi.org/10.1029/2005JD006157

Petrenko, V. V., Smith, A. M., Brailsford, G., Riedel, K., Hua, Q., Lowe, D., et al. (2008). A New Method for Analyzing 14C of Methane in Ancient Air Extracted from Glacial Ice. *Radiocarbon*, *50*, 53–73. https://doi.org/10.1017/S0033822200043368

Petrenko, V. V., Smith, A. M., Schaefer, H., Riedel, K., Brook, E., Baggenstos, D., et al. (2017). Minimal geological methane emissions during the Younger Dryas–Preboreal abrupt warming event. *Nature*, *548*(7668), 443–446. https://doi.org/10.1038/nature23316

Peylin, P., Bacour, C., MacBean, N., Leonard, S., Rayner, P., Kuppel, S., et al. (2016). A new stepwise carbon cycle data assimilation system using multiple data streams to constrain the simulated land surface carbon cycle. *Geoscientific Model Development*, *9*(9), 3321–3346. https://doi.org/10.5194/gmd-9-3321-2016

Pham-Duc, B., Prigent, C., Aires, F., & Papa, F. (2017). Comparisons of global terrestrial surface water datasets over 15 years. *Journal of Hydrometerology*, *18*(4), 993–1007. https://doi.org/10.1175/JHM-D-16-0206.1

Phillips, N. G., Ackley, R., Crosson, E. R., Down, A., Hutyra, L. R., Brondfield, M., et al. (2013). Mapping urban pipeline leaks: Methane leaks across Boston. *Environmental Pollution*, *173*, 1–4. https://doi.org/10.1016/j.envpol.2012.11.003

Pickett-Heaps, C. A., Jacob, D. J., Wecht, K. J., Kort, E. A., Wofsy, S. C., Diskin, G. S., et al. (2011). Magnitude and seasonality of wetland methane emissions from the Hudson Bay Lowlands (Canada). *Atmospheric Chemistry and Physics*, *11*(8), 3773–3779. https://doi.org/10.5194/acp-11-3773-2011

Poulter, B., Bousquet, P., Canadell, J. G., Ciais, P., Peregon, A., Saunois, M., et al. (2017). Global wetland contribution to 2000–2012 atmospheric methane growth rate dynamics. *Environmental Research Letters*, *12*, 094013. https://doi.org/10.1088/1748-9326/aa8391

Prather, M. J., Holmes, C. D., & Hsu, J. (2012). Reactive greenhouse gas scenarios: Systematic exploration of uncertainties and the role of atmospheric chemistry. *Geophysical Research Letters*, *39*, L09803. https://doi.org/10.1029/2012GL051440

Prigent, C., Papa, F., Aires, F., Rossow, W. B., & Matthews, E. (2007). Global inundation dynamics inferred from multiple satellite observations, 1993–2000. *Journal of Geophysical Research*, *112*, D12107. https://doi.org/10.1029/2006JD007847

Prinn, R. G. (1985). On the feasibility of quantitative analysis of atmospheric OH by titration. *Geophysical Research Letters*, *12*(9), 597–600. https://doi.org/10.1029/GL012i009p00597

Prinn, R. G., Weiss, R. F., Arduini, J., Arnold, T., DeWitt, H. L., Fraser, P. J., et al. (2018). History of chemically and radiatively important atmospheric gases from the Advanced Global Atmospheric Gases Experiment (AGAGE). *Earth System Science Data*, *10*(2), 985–1018. https://doi.org/10.5194/essd-10-985-2018

Randerson, J. T., Chen, Y., van der Werf, G. R., Rogers, B. M., & Morton, D. C. (2012). Global burned area and biomass burning emissions from small fires. *Journal of Geophysical Research*, *117*, G04012. https://doi.org/10.1029/2012JG002128

Reinhold, A. M., Poole, G. C., Izurieta, C., Helton, A. M., & Bernhardt, E. S. (2019). Constraint-based simulation of multiple interactive elemental cycles in biogeochemical systems. *Ecological Informatics*, *50*, 102–121. https://doi.org/10.1016/j.ecoinf.2018.12.008

Ren, X., Salmon, O. E., Hansford, J. R., Ahn, D., Hall, D., Benish, S. E., et al. (2018). Methane emissions from the Baltimore-Washington area based on airborne observations: Comparison to emissions inventories. *Journal of Geophysical Research: Atmospheres*, *123*, 8869–8882. https://doi.org/10.1029/2018JD028851

Rice, A. L., Butenhoff, C. L., Teama, D. G., Röger, F. H., Khalil, M. A. K., & Rasmussen, R. A. (2016). Atmospheric methane isotopic record favors fossil sources flat in 1980s and 1990s with recent increase. *Proceedings of the National Academy of Sciences*, *113*(39), 10791–10796. https://doi.org/10.1073/pnas.1522923113

Rigby, M., Manning, A. J., & Prinn, R. G. (2011). Inversion of long-lived trace gas emissions using combined Eulerian and Lagrangian chemical transport models. *Atmospheric Chemistry and Physics*, *11*(18), 9887–9898. https://doi.org/10.5194/acp-11-9887-2011

Rigby, M., Manning, A. J., & Prinn, R. G. (2012). The value of high-frequency, high-precision methane isotopologue measurements for source and sink estimation. *Journal of Geophysical Research*, *117*, D12312. https://doi.org/10.1029/2011JD017384

Rigby, M., Montzka, S. A., Prinn, R. G., White, J. W. C., Young, D., O'Doherty, S., et al. (2017). Role of atmospheric oxidation in recent methane growth. *Proceedings of the National Academy of Sciences*, *114*(21), 5373–5377. https://doi.org/10.1073/pnas.1616426114

Rigby, M., Prinn, R. G., Fraser, P. J., Simmonds, P. G., Langenfelds, R. L., Huang, J., et al. (2008). Renewed growth of atmospheric methane. *Geophysical Research Letters*, *35*, L22805. https://doi.org/10.1029/2008GL036037

Roberts, G. J., & Wooster, M. J. (2008). Fire detection and fire characterization over Africa using Meteosat SEVIRI. *IEEE Transactions on Geoscience and Remote Sensing*, *46*(4), 1200–1218. https://doi.org/10.1109/TGRS.2008.915751

Röckmann, T., Eyer, S., van der Veen, C., Popa, M. E., Tuzson, B., Monteil, G., et al. (2016). In situ observations of the isotopic composition of methane at the Cabauw tall tower site. *Atmospheric Chemistry and Physics*, *16*(16), 10469–10487. https://doi.org/10.5194/acp-16-10469-2016

Roque, B. M., Brooke, C. G., Ladau, J., Polley, T., Marsh, L. J., Najafi, N., et al. (2019). Effect of the macroalgae Asparagopsis taxiformis on methane production and rumen microbiome assemblage. *Animal Microbiome*, *1*(1), 3. https://doi.org/10.1186/s42523-019-0004-4

Roteta, E., Bastarrika, A., Padilla, M., Storm, T., & Chuvieco, E. (2019). Development of a Sentinel-2 burned area algorithm: Generation of a small fire database for sub-Saharan Africa. *Remote Sensing of Environment*, *222*, 1–17. https://doi.org/10.1016/j.rse.2018.12.011

Rubino, M., Etheridge, D. M., Thornton, D. P., Howden, R., Allison, C. E., Francey, R. J., et al. (2019). Revised records of atmospheric trace gases CO_2, CH_4, N_2O, and $\delta^{13}C$-CO_2 over the last 2000 years from Law Dome, Antarctica. *Earth System Science Data*, *11*(2), 473–492. https://doi.org/10.5194/essd-11-473-2019

Ryall, D. B., & Maryon, R. H. (1998). Validation of the UK Met. Office's name model against the ETEX dataset. *Atmospheric Environment*, *32*(24), 4265–4276. https://doi.org/10.1016/S1352-2310(98)00177-0

Ryan, E., Wild, O., Voulgarakis, A., & Lee, L. (2018). Fast sensitivity analysis methods for computationally expensive models with multi-dimensional output. *Geoscientific Model Development*, *11*(8), 3131–3146. https://doi.org/10.5194/gmd-11-3131-2018

Santoni, G. W., Lee, B. H., Goodrich, J. P., Varner, R. K., Crill, P. M., McManus, J. B., et al. (2012). Mass fluxes and isofluxes of methane (CH_4) at a New Hampshire fen measured by a continuous wave quantum cascade laser spectrometer. *Journal of Geophysical Research*, *117*, D10301. https://doi.org/10.1029/2011JD016960

Saunois, M., Bousquet, P., Poulter, B., Peregon, A., Ciais, P., Canadell, J. G., et al. (2016). The global methane budget 2000–2012. *Earth System Science Data*, *8*(2), 697–751. https://doi.org/10.5194/essd-8-697-2016

Schaefer, H., Fletcher, S. E. M., Veidt, C., Lassey, K. R., Brailsford, G. W., Bromley, T. M., et al. (2016). A 21st-century shift from fossil-fuel to biogenic methane emissions indicated by $^{13}CH_4$. *Science*, *352*(6281), 80–84. https://doi.org/10.1126/science.aad2705

Schumacher, D. (1996). Hydrocarbon-Induced Alteration of Soils and Sediments. In D. Schumacher, & M. A. Abrams (Eds.), *Hydrocarbon migration and its near-surface expression*, *AAPG Memoir* (Vol. 66, pp. 71–89). Tulsa: PennWell Publishing.

Schwietzke, S., Griffin, W. M., Matthews, H. S., & Bruhwiler, L. M. P. (2014a). Global Bottom-Up Fossil Fuel Fugitive Methane and Ethane Emissions Inventory for Atmospheric Modeling. *ACS Sustainable Chemistry & Engineering*, *2*(8), 1992–2001. https://doi.org/10.1021/sc500163h

Schwietzke, S., Griffin, W. M., Matthews, H. S., & Bruhwiler, L. M. P. (2014b). Natural gas fugitive emissions rates constrained by global atmospheric methane and ethane. *Environmental Science & Technology*, *48*(14), 7714–7722. https://doi.org/10.1021/es501204c

Schwietzke, S., Pétron, G., Conley, S., Pickering, C., Mielke-Maday, I., Dlugokencky, E. J., et al. (2017). Improved mechanistic understanding of natural gas methane emissions from spatially resolved aircraft measurements. *Environmental Science & Technology*, *51*(12), 7286–7294. https://doi.org/10.1021/acs.est.7b01810

Schwietzke, S., Sherwood, O. A., Bruhwiler, L. M. P., Miller, J. B., Etiope, G., Dlugokencky, E. J., et al. (2016). Upward revision of global fossil fuel methane emissions based on isotope database. *Nature*, *538*(7623), 88–91. https://doi.org/10.1038/nature19797

Sheng, J.-X., Jacob, D. J., Turner, A. J., Maasakkers, J. D., Sulprizio, M. P., Bloom, A. A., et al. (2018). High-resolution inversion of methane emissions in the Southeast US using SEAC^{4}RS aircraft observations of atmospheric methane: Anthropogenic and wetland sources. *Atmospheric Chemistry and Physics*, *18*(9), 6483–6491. https://doi.org/10.5194/acp-18-6483-2018

Sherwood, O. A., Schwietzke, S., Arling, V. A., & Etiope, G. (2017). Global inventory of gas geochemistry data from fossil fuel, microbial and burning sources, version 2017. *Earth System Science Data*, *9*(2), 639–656. https://doi.org/10.5194/essd-9-639-2017

Siddans, R., Knappett, D., Kerridge, B., Waterfall, A., Hurley, J., Latter, B., et al. (2017). Global height-resolved methane retrievals from the Infrared Atmospheric Sounding Interferometer (IASI) on MetOp. *Atmospheric Measurement Techniques*, *10*(11), 4135–4164. https://doi.org/10.5194/amt-10-4135-2017

Smith, M. L., Gvakharia, A., Kort, E. A., Sweeney, C., Conley, S. A., Faloona, I., et al. (2017). Airborne quantification of methane emissions over the Four Corners Region. *Environmental Science & Technology*, *51*(10), 5832–5837. https://doi.org/10.1021/acs.est.6b06107

Sonderfeld, H., Bösch, H., Jeanjean, A. P. R., Riddick, S. N., Allen, G., Ars, S., et al. (2017). CH_4 emission estimates from an active landfill site inferred from a combined approach of CFD modelling and in situ FTIR measurements. *Atmospheric Measurement Techniques*, *10*(10), 3931–3946. https://doi.org/10.5194/amt-10-3931-2017

Sperlich, P., Uitslag, N. A. M., Richter, J. M., Rothe, M., Geilmann, H., van der Veen, C., et al. (2016). Development and evaluation of a suite of isotope reference gases for methane in air. *Atmospheric Measurement Techniques*, *9*(8), 3717–3737. https://doi.org/10.5194/amt-9-3717-2016

Sriskantharajah, S., Fisher, R. E., Lowry, D., Aalto, T., Hatakka, J., Aurela, M., et al. (2012). Stable carbon isotope signatures of methane from a Finnish subarctic wetland. *Tellus Series B: Chemical and Physical Meteorology*, *64*(1), 18818. https://doi.org/10.3402/tellusb.v64i0.18818

Stanley, K. M., Grant, A., O'Doherty, S., Young, D., Manning, A. J., Stavert, A. R., et al. (2018). Greenhouse gas measurements from a UK network of tall towers: Technical description and first results. *Atmospheric Measurement Techniques*, *11*(3), 1437–1458. https://doi.org/10.5194/amt-11-1437-2018

Stockwell, C. E., Jayarathne, T., Cochrane, M. A., Ryan, K. C., Putra, E. I., Saharjo, B. H., et al. (2016). Field measurements of trace gases and aerosols emitted by peat fires in Central Kalimantan, Indonesia, during the 2015 El Niño. *Atmospheric Chemistry and Physics*, *16*(18), 11711–11732. https://doi.org/10.5194/acp-16-11711-2016

Stolper, D. A., & Eiler, J. M. (2015). The kinetics of solid-state isotope-exchange reactions for clumped isotopes: A study of inorganic calcites and apatites from natural and experimental samples. *American Journal of Science*, *315*(5), 363–411. https://doi.org/10.2475/05.2015.01

Stolper, D. A., Sessions, A. L., Ferreira, A. A., Santos Neto, E. V., Schimmelmann, A., Shusta, S. S., et al. (2014). Combined ^{13}C–D and D–D clumping in methane: Methods and preliminary results. *Geochimica et Cosmochimica Acta*, *126*, 169–191. https://doi.org/10.1016/j.gca.2013.10.045

Streets, D. G., Canty, T., Carmichael, G. R., de Foy, B., Dickerson, R. R., Duncan, B. N., et al. (2013). Emissions estimation from satellite retrievals: A review of current capability. *Atmospheric Environment*, *77*, 1011–1042. https://doi.org/10.1016/j.atmosenv.2013.05.051

Sweeney, C., Dlugokencky, E., Miller, C. E., Wofsy, S., Karion, A., Dinardo, S., et al. (2016). No significant increase in long-term CH_4 emissions on North Slope of Alaska despite significant increase in air temperature. *Geophysical Research Letters*, *43*, 6604–6611. https://doi.org/10.1002/2016GL069292

Sweeney, C., Karion, A., Wolter, S., Newberger, T., Guenther, D., Higgs, J. A., et al. (2015). Seasonal climatology of CO_2 across North America from aircraft measurements in the NOAA/ESRL Global Greenhouse Gas Reference Network. *Journal of Geophysical Research: Atmospheres*, *120*, 5155–5190. https://doi.org/10.1002/2014JD022591

Tans, P. P. (1997). A note on isotopic ratios and the global atmospheric methane budget. *Global Biogeochemical Cycles*, *11*(1), 77–81. https://doi.org/10.1029/96GB03940

Thompson, R. L., Stohl, A., Zhou, L. X., Dlugokencky, E., Fukuyama, Y., Tohjima, Y., et al. (2015). Methane emissions in East Asia for 2000-2011 estimated using an atmospheric Bayesian inversion. *Journal of Geophysical Research: Atmospheres*, *120*, 4352–4369. https://doi.org/10.1002/2014JD022394

Thorpe, A. K., Frankenberg, C., Thompson, D. R., Duren, R. M., Aubrey, A. D., Bue, B. D., et al. (2017). Airborne DOAS retrievals of methane, carbon dioxide, and water vapor concentrations at high spatial resolution: Application to AVIRIS-NG. *Atmospheric Measurement Techniques*, *10*(10), 3833–3850. https://doi.org/10.5194/amt-10-3833-2017

Thunis, P., Miranda, A., Baldasano, J. M., Blond, N., Douros, J., Graff, A., et al. (2016). Overview of current regional and local scale air quality modelling practices: Assessment and planning tools in the EU. *Environmental Science & Policy*, *65*, 13–21. https://doi.org/10.1016/j.envsci.2016.03.013

Townsend-Small, A., Botner, E. C., Jimenez, K. L., Schroeder, J. R., Blake, N. J., Meinardi, S., et al. (2016). Using stable isotopes of hydrogen to quantify biogenic and thermogenic atmospheric methane sources: A case study from the Colorado Front Range: Hydrogen Isotopes in the Front Range. *Geophysical Research Letters*, *43*, 11,462–11,471. https://doi.org/10.1002/2016GL071438

Townsend-Small, A., Tyler, S. C., Pataki, D. E., Xu, X., & Christensen, L. E. (2012). Isotopic measurements of atmospheric methane in Los Angeles, California, USA: Influence of "fugitive" fossil fuel emissions. *Journal of Geophysical Research*, *117*, D07308. https://doi.org/10.1029/2011JD016826

Treat, C. C., Bloom, A. A., & Marushchak, M. E. (2018). Nongrowing season methane emissions—A significant component of annual emissions across northern ecosystems. *Global Change Biology*, *24*(8), 3331–3343. https://doi.org/doi:10.1111/gcb.14137

Turetsky, M. R., Kotowska, A., Bubier, J., Dise, N. B., Crill, P., Hornibrook, E. R. C., et al. (2014). A synthesis of methane emissions from 71 northern, temperate, and subtropical wetlands. *Global Change Biology*, *20*(7), 2183–2197. https://doi.org/10.1111/gcb.12580

Turner, A. J., Frankenberg, C., & Kort, E. A. (2019). Interpreting contemporary trends in atmospheric methane. *Proceedings of the National Academy of Sciences*, 201814297. https://doi.org/10.1073/pnas.1814297116

Turner, A. J., Frankenberg, C., Wennberg, P. O., & Jacob, D. J. (2017). Ambiguity in the causes for decadal trends in atmospheric methane and hydroxyl. *Proceedings of the National Academy of Sciences*, *114*(21), 5367–5372. https://doi.org/10.1073/pnas.1616020114

Turner, A. J., Jacob, D. J., Wecht, K. J., Maasakkers, J. D., Lundgren, E., Andrews, A. E., et al. (2015). Estimating global and North American methane emissions with high spatial resolution using GOSAT satellite data. *Atmospheric Chemistry and Physics*, *15*(12), 7049–7069. https://doi.org/10.5194/acp-15-7049-2015

Tyler, S. C., Rice, A. L., & Ajie, H. O. (2007). Stable isotope ratios in atmospheric CH_4: Implications for seasonal sources and sinks. *Journal of Geophysical Research*, *112*, D03303. https://doi.org/10.1029/2006JD007231

U.S. Energy Information Administration. (2016). International Energy Statistics. US Energy Information Administration (EIA).

U.S. Environmental Protection Agency. (2012). Global anthropogenic non-CO_2 greenhouse gas emissions: 1990-2030. Washington, D.C.

Umezawa, T., Brenninkmeijer, C. A. M., Röckmann, T., van der Veen, C., Tyler, S. C., Fujita, R., et al. (2018). Interlaboratory comparison of δ^{13}C and δD measurements of atmospheric CH_4 for combined use of data sets from different laboratories. *Atmospheric Measurement Techniques*, *11*(2), 1207–1231. https://doi.org/10.5194/amt-11-1207-2018

Umezawa, T., Machida, T., Ishijima, K., Matsueda, H., Sawa, Y., Patra, P. K., et al. (2012). Carbon and hydrogen isotopic ratios of atmospheric methane in the upper troposphere over the Western Pacific. *Atmospheric Chemistry and Physics*, *12*(17), 8095–8113. https://doi.org/10.5194/acp-12-8095-2012

van der Meer, F., van Dijk, P., van der Werff, H., & Yang, H. (2002). Remote sensing and petroleum seepage: A review and case study. *Terra Nova*, *14*(1), 1–17. https://doi.org/10.1046/j.1365-3121.2002.00390.x

van der Werf, G. R., Randerson, J. T., Giglio, L., van Leeuwen, T. T., Chen, Y., Rogers, B. M., et al. (2017). Global fire emissions estimates during 1997–2016. *Earth System Science Data*, *9*(2), 697–720. https://doi.org/10.5194/essd-9-697-2017

van Leeuwen, T. T., Peters, W., Krol, M. C., & van der Werf, G. R. (2013). Dynamic biomass burning emission factors and their impact on atmospheric CO mixing ratios. *Journal of Geophysical Research: Atmospheres*, *118*, 6797–6815. https://doi.org/10.1002/jgrd.50478

van Vuuren, D. P., Edmonds, J., Kainuma, M., Riahi, K., Thomson, A., Hibbard, K., et al. (2011). The representative concentration pathways: An overview. *Climatic Change*, *109*(1-2), 5–31. https://doi.org/10.1007/s10584-011-0148-z

Varon, D. J., McKeever, J., Jervis, D., Maasakkers, J. D., Pandey, S., Houweling, S., et al. (2019). Satellite discovery of anomalously large methane point sources from oil/gas production. *Geophysical Research Letters*, *46*. https://doi.org/10.1029/2019GL083798

Veraverbeke, S., Rogers, B. M., & Randerson, J. T. (2015). Daily burned area and carbon emissions from boreal fires in Alaska. *Biogeosciences*, *12*(11), 3579–3601. https://doi.org/10.5194/bg-12-3579-2015

Vogel, F. R., Ishizawa, M., Chan, E., Chan, D., Hammer, S., Levin, I., & Worthy, D. E. J. (2012). Regional non-CO_2 greenhouse gas fluxes inferred from atmospheric measurements in Ontario, Canada. *Journal of Integrative Environmental Sciences*, *9*(sup1), 41–55. https://doi.org/10.1080/1943815X.2012.691884

von Fischer, J. C., Cooley, D., Chamberlain, S., Gaylord, A., Griebenow, C. J., Hamburg, S. P., et al. (2017). Rapid, vehicle-based identification of location and magnitude of urban natural gas pipeline leaks. *Environmental Science & Technology*, *51*(7), 4091–4099. https://doi.org/10.1021/acs.est.6b06095

Voulgarakis, A., Naik, V., Lamarque, J.-F., Shindell, D. T., Young, P. J., Prather, M. J., et al. (2013). Analysis of present day and future OH and methane lifetime in the ACCMIP simulations. *Atmospheric Chemistry and Physics*, *13*(5), 2563–2587. https://doi.org/10.5194/acp-13-2563-2013

Walter Anthony, K., Schneider von Deimling, T., Nitze, I., Frolking, S., Emond, A., Daanen, R., et al. (2018). 21st-century modeled permafrost carbon emissions accelerated by abrupt thaw beneath lakes. *Nature Communications*, *9*(1), 3262. https://doi.org/10.1038/s41467-018-05738-9

Walter, K. M., Zimov, S. A., Chanton, J. P., Verbyla, D., & Chapin, F. S. (2006). Methane bubbling from Siberian thaw lakes as a positive feedback to climate warming. *Nature*, *443*(7107), 71–75. https://doi.org/10.1038/nature05040

Walter, M. B., & Heimann, M. (2000). A process-based climate-sensitive model to derive methane emissions from natural wetlands: Application to five wetland sites, sensitivity to model parameters, and climate. *Global Biogeochemical Cycles*, *14*(3), 745–765.

Wang, D. T., Gruen, D. S., Lollar, B. S., Hinrichs, K.-U., Stewart, L. C., Holden, J. F., et al. (2015). Nonequilibrium clumped isotope signals in microbial methane. *Science*, *348*(6233), 428–431. https://doi.org/10.1126/science.aaa4326

Warwick, N. J., Cain, M. L., Fisher, R., France, J. L., Lowry, D., Michel, S. E., et al. (2016). Using δ^{13}C-CH_4 and δD-CH_4 to constrain Arctic methane emissions. *Atmospheric Chemistry and Physics*, *16*(23), 14891–14908. https://doi.org/10.5194/acp-16-14891-2016

Weber, T., Wiseman, N. A., & Kock, A. (2019). Global ocean methane emissions dominated by shallow coastal waters. *Nature Communications*, *10*(1), 4584. https://doi.org/10.1038/s41467-019-12541-7

Welch, B., Gauci, V., & Sayer, E. J. (2019). Tree stem bases are sources of CH4 and N_2O in a tropical forest on upland soil during the dry to wet season transition. *Global Change Biology*, *25*(1), 361–372. https://doi.org/doi:10.1111/gcb.14498

Weller, Z. D., Roscioli, J. R., Daube, W. C., Lamb, B. K., Ferrara, T. W., Brewer, P. E., & von Fischer, J. C. (2018). Vehicle-based methane surveys for finding natural gas leaks and estimating their size: Validation and uncertainty. *Environmental Science & Technology*, *52*(20), 11922–11930. https://doi.org/10.1021/acs.est.8b03135

White, I. R., Martin, D., Petersson, K. F., Henshaw, S. J., Nickless, G., Lloyd-Jones, G. C., et al. (2014). A feasibility study of the use of reactive tracers to determine outdoor daytime OH radical concentrations within the urban environment. *Atmospheric Science Letters*, *15*(3), 178–185. https://doi.org/10.1002/asl2.487

Whitehill, A. R., Joelsson, L. M. T., Schmidt, J. A., Wang, D. T., Johnson, M. S., & Ono, S. (2017). Clumped isotope effects during OH and Cl oxidation of methane. *Geochimica et Cosmochimica Acta*, *196*, 307–325. https://doi.org/10.1016/j.gca.2016.09.012

Wiedinmyer, C., Akagi, S. K., Yokelson, R. J., Emmons, L. K., Al-Saadi, J. A., Orlando, J. J., & Soja, A. J. (2011). The Fire INventory from NCAR (FINN): A high resolution global model to estimate the emissions from open burning. *Geoscientific Model Development*, *4*(3), 625–641. https://doi.org/10.5194/gmd-4-625-2011

Wik, M., Thornton, B. F., Bastviken, D., Uhlbäck, J., & Crill, P. M. (2016). Biased sampling of methane release from northern lakes: A problem for extrapolation. *Geophysical Research Letters*, *43*, 1256–1262. https://doi.org/10.1002/2015GL066501

Wik, M., Varner, R. K., Anthony, K. W., MacIntyre, S., & Bastviken, D. (2016). Climate-sensitive northern lakes and ponds are critical components of methane release. *Nature Geoscience*, *9*(2), 99–105. https://doi.org/10.1038/ngeo2578

Wilson, C., Gloor, M., Gatti, L. V., Miller, J. B., Monks, S. A., McNorton, J., et al. (2016). Contribution of regional sources to atmospheric methane over the Amazon Basin in 2010 and 2011. *Global Biogeochemical Cycles*, *30*, 400–420. https://doi.org/10.1002/2015GB005300

WMO. (2018). 19th WMO/IAEA Meeting on Carbon Dioxide, Other Greenhouse Gases and Related Measurement Techniques (GGMT-2017) (No. 242).

Wolfe, G. M., Nicely, J. M., Clair, J. M. S., Hanisco, T. F., Liao, J., Oman, L. D., et al. (2019). Mapping hydroxyl variability throughout the global remote troposphere via synthesis of airborne and satellite formaldehyde observations. *Proceedings of the National Academy of Sciences*, *116*(23), 11171–11180. https://doi.org/10.1073/pnas.1821661116

Wooster, M., Gaveau, D., Salim, M., Zhang, T., Xu, W., Green, D., et al. (2018). New tropical peatland gas and particulate emissions factors indicate 2015 Indonesian fires released far more particulate matter (but less methane) than current inventories imply. *Remote Sensing*, *10*(4), 495. https://doi.org/10.3390/rs10040495

Worden, J. R., Bloom, A. A., Pandey, S., Jiang, Z., Worden, H. M., Walker, T. W., et al. (2017). Reduced biomass burning emissions reconcile conflicting estimates of the post-2006 atmospheric methane budget. *Nature Communications*, *8*(1), 2227. https://doi.org/10.1038/s41467-017-02246-0

Wunch, D., Wennberg, P. O., Toon, G. C., Keppel-Aleks, G., & Yavin, Y. G. (2009). Emissions of greenhouse gases from a North American megacity. *Geophysical Research Letters*, *36*, L15810. https://doi.org/10.1029/2009GL039825

Wunch, D., Toon, G. C., Blavier, J.-F. L., Washenfelder, R. A., Notholt, J., Connor, B. J., et al. (2011). The total carbon column observing network. *Philosophical Transactions of the Royal Society A - Mathematical Physical and Engineering Sciences*, *369*(1943), 2087–2112. https://doi.org/10.1098/rsta.2010.0240

Xiong, X., Han, Y., Liu, Q., & Weng, F. (2016). Comparison of atmospheric methane retrievals from AIRS and IASI. *IEEE Journal of Selected Topics in Applied Earth Observations and Remote Sensing*, *9*(7), 3297–3303. https://doi.org/10.1109/JSTARS.2016.2588279

Xu, X., Riley, W. J., Koven, C. D., Billesbach, D. P., Chang, R. Y.-W., Commane, R., et al. (2016). A multi-scale comparison of modeled and observed seasonal methane emissions in northern wetlands. *Biogeosciences (Online)*, *13*(17), 5043–5056. https://doi.org/10.5194/bg-13-5043-2016

Young, E. D., Kohl, I. E., Lollar, B. S., Etiope, G., Rumble, D., Li, S., et al. (2017). The relative abundances of resolved $^{12}CH_2D_2$ and $^{13}CH_3D$ and mechanisms controlling isotopic bond ordering in abiotic and biotic methane gases. *Geochimica et Cosmochimica Acta*, *203*, 235–264. https://doi.org/10.1016/j.gca.2016.12.041

Young, E. D., Rumble, D., Freedman, P., & Mills, M. (2016). A large-radius high-mass-resolution multiple-collector isotope ratio mass spectrometer for analysis of rare isotopologues of O_2, N_2, CH_4 and other gases. *International Journal of Mass Spectrometry*, *401*, 1–10. https://doi.org/10.1016/j.ijms.2016.01.006

Yuan, J., Xiang, J., Liu, D., Kang, H., He, T., Kim, S., et al. (2019). Rapid growth in greenhouse gas emissions from the adoption of industrial-scale aquaculture. *Nature Climate Change*, *9*(4), 318–322. https://doi.org/10.1038/s41558-019-0425-9

Yver Kwok, C. E., Müller, D., Caldow, C., Lebègue, B., Mønster, J. G., Rella, C. W., et al. (2015). Methane emission estimates using chamber and tracer release experiments for a municipal waste water treatment plant. *Atmospheric Measurement Techniques*, *8*(7), 2853–2867. https://doi.org/10.5194/amt-8-2853-2015

Zazzeri, G., Lowry, D., Fisher, R. E., France, J. L., Lanoisellé, M., Kelly, B. F. J., et al. (2016). Carbon isotopic signature of coal-derived methane emissions to the atmosphere: From coalification to alteration. *Atmospheric Chemistry and Physics*, *16*(21), 13669–13680. https://doi.org/10.5194/acp-16-13669-2016

Zhang, Y., Jacob, D. J., Maasakkers, J. D., Sulprizio, M. P., Sheng, J.-X., Gautam, R., & Worden, J. (2018). Monitoring global tropospheric OH concentrations using satellite observations of atmospheric methane. *Atmospheric Chemistry and Physics*, *18*(21), 15959–15973. https://doi.org/10.5194/acp-18-15959-2018

Zhang, Z., Zimmermann, N. E., Stenke, A., Li, X., Hodson, E. L., Zhu, G., et al. (2017). Emerging role of wetland methane emissions in driving 21st century climate change. *Proceedings of the National Academy of Sciences*, *114*(36), 9647–9652. https://doi.org/10.1073/pnas.1618765114

Zhuang, Q., Chen, M., Xu, K., Tang, J., Saikawa, E., Lu, Y., et al. (2013). Response of global soil consumption of atmospheric methane to changes in atmospheric climate and nitrogen deposition. *Global Biogeochemical Cycles*, *27*, 650–663. https://doi.org/10.1002/gbc.20057

Zimov, S. A., Schuur, E. A. G., & Chappin, F. S. III (2006). Permafrost and the global carbon budget. *Science*, *312*(5780), 1612–1613. https://doi.org/10.1126/science.1128908

Zona, D., Gioli, B., Commane, R., Lindaas, J., Wofsy, S. C., Miller, C. E., et al. (2016). Cold season emissions dominate the Arctic tundra methane budget. *Proceedings of the National Academy of Sciences*, *113*(1), 40–45. https://doi.org/10.1073/pnas.1516017113